HERIOT-WATT UNIVERSITY

Exponential Time Differencing Methods and Asymptotic Behaviour of Solutions of Problems in Ground Water Flow

Aisha M. Alqahtani

June 15, 2015

SUBMITTED FOR THE DEGREE OF
DOCTOR OF PHILOSOPHY IN MATHEMATICS
ON COMPLETION OF RESEARCH IN THE
DEPARTMENT OF MATHEMATICS,
SCHOOL OF MATHEMATICAL AND COMPUTER SCIENCES.

Abstract

We start this thesis with a numerical study of the convergence of the exponential time differencing (ETD) schemes and the semi-implicit Euler method for the Allen-Cahn equation and a reaction-convection-diffusion equation and also compare the accuracy and efficiency of these methods.

Next, we solve the nonlinear convection-diffusion (green roof) model numerically using the ETD method and central difference approximation. This numerical solution is investigated for three different initial values for the saturation.

Finally, we study travelling wave solutions and self-similar solutions for the green roof, in particular, for the two limiting cases of being close to a saturated region and a dry region. Travelling waves, in the form of fronts, are found for most realistic limiting values of saturation; travelling waves are also investigated for some limiting versions of the model. Self-similar solutions, valid for high or for low saturations, are additionally investigated.

Dedication

To my parents, with love.

Acknowledgements

I believe every successful research journey happens because of the help and support we get from huge hearts around us. I was fortunate to be surrounded by many people who positively marked my journey in many ways.

First and foremost I am deeply grateful to my supervisor Professor Andrew Lacy for his great support, guidance, advice, encouragement and unlimited help. There is nothing in PhD student's life greater than having a very compassionate, knowledgeable and understanding advisor; great morals that Professor Lacy encompass.

I must also convey my gratitude to some other people who contributed positively to this journey. Thanks go to Professor Dugald Duncan for his help following my progress reports during my study, and finally all the staff within the Department of Mathematics at Heriot- Watt University for their help and support with all the research, teaching and learning as well as administrative activities I needed during my study there. Their support is highly appreciated.

Importantly I offer my special thanks and appreciation to my immediate family; my husband (Mubarak), my son (Aziz) and my daughter (Ola) for the joy and love they brought into my life as well as to this journey. My sincere thanks go to my extended family; my mother, brothers and sisters for their continued prayers and wishes during the long period of this journey.

Contents

List of Figures

Chapter 1

Introduction

1.1 Literature Review on Green Roof

A green roof (or living roof) can be defined as a roof of a building with a vegetative and a growing medium cover on top of a waterproof membrane. This sort of roof may also include additional layers such as a root barrier, drainage and irrigation systems [1, 21]. These vegetated roofs have existed for quite some time and in many places around the world. For example, a number of European countries including Germany, Switzerland, the Netherlands, Norway, Italy, Austria, Hungary, Sweden, the UK and Greece have very active associations promoting green roofs. Another example for the popularity of these roofs can be seen in the United States, where the popularity is increasing although not as much as is the case in Europe [42].

This popularity of green roofs around the world is happening because of their crucial benefits. Among these is that they can be used to address environmental issues in an urban setting. Research shows that green roofs can be used to mitigate problems associated with storm water runoff, pollution control, building insulation and recycling of carbon dioxide. In addition, these landscapes help in decreasing stress of the people around the roof [1, 21]

However, maintaining these green roofs is not an easy task. Due to their vulnerability, green roofs are subject to various stresses from the weather, in particular wind-loading and rainfall. An important task here is to understand where the water goes in order to design a roof that is able to achieve sustained healthy plants and loads that lie within the safe capacity of the supporting structure. In a typical green roof the degree of saturation should usually be less than 80% and it is important to be maintained at all times. High levels of saturation inside the structure of the roof will cut off the air supply to the plants. Low levels of supply, on the other hand, will result in plants dying from lack of water [21, 36].

These green roofs can be divided into either intensive or extensive roofs. This distinction is made based on the depth of the planting space within these roofs and the amount of maintenance they require. The first type, referred to as the intensive one, refers to a rooftop garden or park that contains large plants and trees and usually requires deep soils and high maintenance. The second type, referred to as an extensive green roof, usually requires shallower soils and contains one or two plants species and requires low maintenance compared to the first type. This type is usually constructed over flat roofs [27].

Understanding and investigating the fluid flow in these roofs has caught the attention of many researchers [5, 42]. Numerical models for simulating fluid flow and mass transport in the unsaturated zone of these roofs have been increasingly investigated over recent years. For example, Lacey and others presented a model for rainwater flow coming down through the soil layer of a green roof [1, 21]. They used Richards' equation which is the basic equation in the theory of groundwater flow through unsaturated porous media and which was first suggested in 1931 [36]. This non-linear convection-diffusion equation can be written as a conservation law for the water content, the quantity of water contained in a given soil volume. The convection term is due to gravity while the diffusive term comes from Darcy's law [5, 35]. Front solutions of the one-dimensional Richards' equation have been studied systematically for the three soil retention models known as Brooks-Corey, Mualem-Van Genuchten and Storm-Fujita [12].

The research undertaken here aims to solve the green roof model by [1] numerically using the exponential time differencing scheme and the finite difference method. It also aims to investigate travelling wave solutions, in particular the local behaviour of the solutions where the saturation approaches 0 and 1 and when it goes between 0 and 1, too. Most of the cases are studied for different values of saturation within the green roof material, which typically is formed of an expanded-clay soil. We also consider self-similar solutions to the green roof model for the two limiting cases; namely high saturation and low saturation.

Several different studies have been done on Richards' equation. For instance, Caputo and Stepanyants [12] have studied the front travelling wave solution for Richards' equation where the saturation goes between 0 and 1. They consider both problems when the convective and diffusive terms are present (infiltration problem) and when the convective term is absent (absorption problem). Also, travelling wave solutions for convection-diffusion and convection-diffusion-reaction equations have been obtained

by others [18, 28]. Self-similar front solutions for Richards' equation have been considered in [2, 4, 12, 20]. In [12], they were found only for the absorption problem.

1.2   Literature Review on Exponential Integrators

Many researchers have recently been interested in a particular class of numerical methods for the solution of ordinary differential equations (ODEs). These methods are known as "Exponential Integrators" which were first used around two decades ago, but have received more attention in recent years; see [11, 19, 25, 31, 32, 33] and related references. Exponential integrators can be defined as numerical methods which involve an exponential function (and related functions) of the Jacobian or an approximation to it. They give an alternative approach to the implicit methods to get the numerical solution of stiff or oscillatory differential equations [11, 23].

Historically speaking, exponential integrators were first introduced in a paper that was published in 1960 by Certaine [14]. In that paper, two exponential integrators were created based on the Adams-Moulton methods of order two and three. These methods are members of the Exponential Time Differencing (ETD) methods, which were developed for the solution of stiff problems. A simple example of an exponential integrator is the exponential time differencing Euler method, given later in equation (2.7).

ETD schemes are basically aimed to be used on ODEs that can be divided into a stiff linear part and a non-stiff nonlinear part. The main idea behind these schemes is to integrate exactly the linear part of the differential equation and then use an appropriate approximation of the integral involving the nonlinear terms. In fact, solving exactly the linear part of the equation is a crucial feature of the ETD scheme. In solving this linear part, an exponential of a matrix arises [31].

An issue that can be of concern is the computational cost of the matrix exponential functions. However, there are many efficient ways to compute a matrix exponential times a vector. Among these techniques in the literature is the Krylov subspace technique. The Krylov subspace technique is a powerful class of methods that are applicable to large problems and it is an approximation based on the Arnoldi process [6, 24, 32, 33, 34, 38, 40]. Also, the real fast Léja points technique was used efficiently in the computation of the matrix exponential and it is based on matrix interpolation polynomials at spectral sequences [9, 10, 40]. A detailed description of both techniques will be given in the next chapter. Another popular method for computing the matrix exponential is the scaling and squaring method. The function *expm* built into

MATLAB is based on this method [19, 32].

Linear systems of ODEs have been solved using the Krylov subspace method and Padé approximation based on variation of constants by Sidje [39]. Cox and Matthews [15] developed a class of numerical methods for stiff systems, based on the method of ETD. They extended the method so that it may be applied to systems whose linear parts are non-diagonal matrix exponential functions, the so-called φ functions. The matrix exponential of φ functions was computed using Padé approximations by Berland et al. [7] and they provided the MATLAB package EXPINT which is a tool to facilitate the easy testing of exponential integrators for semi-linear problems. The Padé approximation of φ functions is defined for a given positive integer p as the (p, p)-degree rational function $P_{pp}(z) \equiv N_{pp}(z)/D_{pp}(z)$.

The matrix exponentials of φ functions in the linear reaction-convection-diffusion equations have been treated using the Krylov subspace method and the real fast Léja points technique [6, 9, 10]. The exponential Rosenbrock-type integrators for solving semi-linear reaction-convection-diffusion equations have been implemented efficiently using the real fast Léja points technique [3, 14]. This technique has also been applied to the exponential Euler-Midpoint method for solving non-linear reaction-convection-diffusion equations [11]. Other references related to the above two techniques that have been applied to the computation of the matrix exponential are [24, 30, 31, 32, 33, 34, 38].

The ETD scheme was the theme of many other related studies such as Higham (2008), Minchev and Wright (2005) and Tambue, Lord and Geiger [31, 40]. Recently, Carr et al. [13] applied the exponential time integration method to initial value problems resulting from the semidiscrete systems of the unsaturated Richard's equation. In that paper, they compared the performance of the exponential Euler method EEM and the backward differentiation formulae BDF. In this thesis, one of our aims is to apply the exponential time differencing scheme to the Richards' equation for unsaturated flow and then the result will be compared to the results of [1] for the green roof model.

1.3   Thesis Outline

The outline of this thesis is as follows. In Chapter 2, we begin by showing the derivation of the exponential time differencing scheme. We also give background material on the Krylov subspace technique for computing the exponential function. We provide a brief summary of the upwind methods to be used later in Chapter 3.
In Chapter 3, The numerical results of convergence in time and space using the ETD

schemes and the semi-implicit Euler method for the Allen-Cahn equation in subsection 3.1.1 and in only time for the reaction-convection-diffusion equation in subsection 3.1.2 are presented.

In Chapter 4, we investigate numerically the solution of the green roof model without a sink term : to be more precise, we solve the nonlinear convection-diffusion model (4.5) for three different initial conditions using the ETD scheme. Those numerical results are compared to the results in paper [1].

In Chapter 5, we look for travelling wave solutions for the green roof model (5.13), in particular, the local behaviour of the solutions near 0 and 1. We investigate the solutions for fixed value of a parameter, m, which appears in the model for the expanded-clay soil, and also when $m \to 0$ and $m \to 1$.

In Chapter 6, we consider the nonlinear convection-diffusion problem, (4.5), without the sink term. We investigate self-similar solutions for this model for the two limiting cases of saturation $S \to 0$ and $S \to 1$. Three different cases of m are considered for those cases of limiting saturation.

We finally conclude this thesis with discussions on the outcomes and give some suggestions for possible future work in Chapter 7.

Chapter 2

The Exponential Time Differencing Scheme

2.1 Introduction

The exponential time differencing (ETD) Euler schemes make up a class of numerical methods that are used for integrating stiff systems of ordinary differential equations (ODEs). Those systems commonly appear when solving partial differential equations (PDEs) by spectral methods and finite difference methods, for example. ETD schemes basically give an exact integration, using a matrix exponential function, of the linear part of the system while treating efficiently the non-linear part. In this chapter, we derive the ETD scheme to be applied to reaction-diffusion equations. We also give a description of the Krylov subspace technique for the computation of the matrix exponential function.

2.2 Derivation of the Exponential Time Differencing Scheme

To derive the ETD methods let us consider a PDE with given boundary and initial conditions.

$$u_t(x,t) = \mathcal{A}u(x,t) + \mathcal{F}(u(x,t),t), \quad u(x,t_0) = u_0(x), \quad x \in \Omega,$$

$$u(x,t) = g(x,t), \quad x \in \partial\Omega, \tag{2.1}$$

for $t > t_0$, and $\mathcal{A}$ and $\mathcal{F}$ represent the linear and nonlinear terms respectively. When a PDE (2.1) is discretized in the spatial variables using finite difference approximations or other spatial approximations, a system of ordinary differential equations ODEs is

produced. The system can be written as

$$u'(t) = \mathbf{A}u(t) + \mathbf{F}(u, t), \quad u(t_0) = u_0, \tag{2.2}$$

where $u : \mathbb{R} \longrightarrow \mathbb{R}^J$, $\mathbf{A} \in \mathbb{R}^{J \times J}$, $\mathbf{F} : \mathbb{R}^J \longrightarrow \mathbb{R}^J$ and J is the dimensionality of the discretized problem.

2.2.1 Exponential Time Differencing Scheme

The ETD method [15, 30] is derived as follows.

We begin by multiplying (2.2) through by the integrating factor $e^{-t\mathbf{A}}$ to get

$$e^{-t\mathbf{A}}u' - e^{-t\mathbf{A}}\mathbf{A}u - e^{-t\mathbf{A}}\mathbf{F} = 0, \qquad \text{so}$$

$$(e^{-t\mathbf{A}}u)' - e^{-t\mathbf{A}}\mathbf{F} = 0. \tag{2.3}$$

Now, we integrate this equation over a single time step from $t = t_n$ to $t = t_{n+1} = t_n + \Delta t$ and multiply by $e^{t_{n+1}A}$ to give

$$u(t_{n+1}) = e^{\Delta t \mathbf{A}}u(t_n) + \int_{t_n}^{t_n + \Delta t} e^{(t_n + \Delta t - s)\mathbf{A}}\mathbf{F}(u(s), s)ds, \tag{2.4}$$

where s is integration time. Then if we do a change of variable and let $s = t_n + \tau$, (2.4) can be written as

$$u(t_{n+1}) = e^{\Delta t \mathbf{A}}u(t_n) + \int_0^{\Delta t} e^{(\Delta t - \tau)\mathbf{A}}\mathbf{F}(u(t_n + \tau), t_n + \tau)d\tau, \tag{2.5}$$

or

$$u(t_{n+1}) = e^{\Delta t \mathbf{A}}u(t_n) + e^{\Delta t \mathbf{A}}\int_0^{\Delta t} e^{-\tau \mathbf{A}}\mathbf{F}(u(t_n + \tau), t_n + \tau)d\tau. \tag{2.6}$$

This formula (2.6) is still an exact solution. The main point of the exponential time differencing is to approximate the nonlinear term $\mathbf{F}(u(t_n + \tau), t_n + \tau)$ by a suitable polynomial [15]. The easiest way of approximating $\mathbf{F}(u(t_n + \tau), t_n + \tau)$ is by the constant $\mathbf{F}(u(t_n), t_n)$. The corresponding ETD1 scheme is then given by

$$u_{n+1} = e^{\Delta t \mathbf{A}}u_n + \Delta t \varphi_1(\Delta t \mathbf{A})\mathbf{F}(u_n, t_n), \tag{2.7}$$

where $\varphi_1(\mathbf{\Gamma}) = \mathbf{\Gamma}^{-1}(e^{\mathbf{\Gamma}} - \mathbf{I})$ for any invertible matrix $\mathbf{\Gamma}$. We arrive now at the numerical scheme ETD1 given by

$$u_{n+1} = u_n + \Delta t \varphi_1(\Delta t \mathbf{A})(\mathbf{A}u_n + \mathbf{F}(u_n, t_n)), \tag{2.8}$$

where the function φ_1, which plays an important role in these methods, is one of a family of functions $\varphi_k(z) = \sum_{j=0}^{\infty} z^j/(j+k)!$, closely related to the exponential, and is defined by

$$\varphi_1(z) = \frac{e^z - 1}{z}.$$

Note that in the last equation (2.8) that represents the ETD1 scheme only one matrix exponential function has to be evaluated at each step.

2.3 Krylov subspace technique

The problem of evaluating the action of the matrix exponential operator on a given vector is of substantial importance in many applications in mathematics, physics and engineering. For example, this operator is the backbone of many methods for solving time-dependent partial differential equations or systems of ordinary differential equations [31]. When we are evaluating matrix functions using Krylov subspace techniques, reduced matrices can be obtained instead of large ones. Thus the basic idea behind this Krylov subspace approach is to approximately project the vector $\varphi_1(\Delta t \mathbf{A})v$ onto a small space of dimension m. Here $\mathbf{A}$ is an $n \times n$ matrix (with n large) and $v \in \mathbb{R}^n$. This smaller space is the Krylov subspace [6, 24, 31, 38, 40], which is given by

$$\mathcal{K}_m(\mathbf{A}, v) = \text{span}\{v, \mathbf{A}v, \mathbf{A}^2 v, \ldots, \mathbf{A}^{m-1}v\}.$$

By applying the stabilized Gram-Schmidt process [15], we get an orthonormal basis $\mathbf{V}_m = [v_1, v_2, \ldots, v_m]$ of the Krylov subspace $\mathcal{K}_m$. If $\mathbf{V}_m$ is the $n \times m$ matrix, then the $m \times m$ matrix $\mathbf{H}_m = \mathbf{V}_m^T \mathbf{A} \mathbf{V}_m$ is the projection of the action of $\mathbf{A}$ onto the Krylov subspace expressed in the basis $\mathbf{V}_m$. The matrices $\mathbf{H}_m$ and $\mathbf{V}_m$ can be computed by Arnoldi iteration [15, 40]. The projection of the action of $\mathbf{A}$ on the Krylov subspace $\mathcal{K}_m$ in the standard basis of $\mathbb{R}^n$ is $\mathbf{V}_m \mathbf{H}_m \mathbf{V}_m^T$. Then $\varphi_1(\Delta t \mathbf{A})v$ is approximated by $\varphi_1(\mathbf{V}_m \Delta t \mathbf{H}_m \mathbf{V}_m^T)v$. In detail we have $\varphi_1(\mathbf{V}_m \Delta t \mathbf{H}_m \mathbf{V}_m^T)v = \mathbf{V}_m \varphi_1(\Delta t \mathbf{H}_m)\mathbf{V}_m^T v$ as $\mathbf{V}_m^T \mathbf{V}_m = \mathbf{I}_m$ and $\mathbf{V}_m \mathbf{V}_m^T v = v$.

Therefore, $\mathbf{V}_m^T v = \beta e_1$, where $\beta = \|v\|$ and e_1 is the first unit basis vector. Then we obtain the following approximation

$$\varphi_1(\Delta t \mathbf{A})v \approx \|v\| \mathbf{V}_m \varphi_1(\Delta t \mathbf{H}_m)e_1. \tag{2.9}$$

We arrive finally at a smaller $m \times m$ matrix $\mathbf{H}_m$, which is much easier to evaluate compared to a big $n \times n$ matrix $\mathbf{A}$. The matrix $\mathbf{H}_m = [h_{i,j}]$ is an upper Hessenberg matrix, meaning that the (i,j) entry vanishes whenever $i > j + 1$ [39].

To sum up, the Krylov subspace technique reduces the problem of computing $\varphi_1(\Delta t \mathbf{A})v$ to that of computing $\varphi_1(\Delta t \mathbf{H}_m)e_1$.

From the theory, there is no specific way that allows us easily to choose the optimal value for the dimension of the Krylov subspace m. The default value used in [39] is $m = 30$, but in our case this seems not to be optimal. In our examples in Chapter 3, it appears that $m = 20$ is the best value. When m is small, the total number of iterations increases. However, the time spent in the orthogonalisation process is lower and this leads to a decrease in the memory requirements. When m is large, there is a decrease in the number of iterations but an additional time necessary to spend in the orthogonalisation process. The required memory increases in this case.

2.4   Upwind Methods

Upwind schemes are defined as a class of numerical methods for solving hyperbolic partial differential equations (HPDEs). They attempt to discretize hyperbolic PDE's depending on the sign of the characteristic speeds. In order to illustrate this method we consider the one space dimensional homogeneous linear convection equation, which is the simplest of all hyperbolic partial differential equations, with an initial condition [26].

$$\begin{cases} u_t(x,t) + au_x(x,t) = 0, \\ u(x,0) = u_0(x). \end{cases} \tag{2.10}$$

It describes a wave propagating in the x-direction with a velocity a which is considered to be a constant here. $u_0(x)$ is a given function.

The sign of a gives the wave direction and since this is important for the analytic solution of the convection equation it should be considered numerically as well. If $a > 0$, the wave moves to the right and when $a < 0$ the wave moves to the left.

To get the approximate solution of this equation we need to approximate the derivatives u_t and u_x. If we use the forward difference for approximating u_t and the backward difference approximation for u_x (when we say backward difference approximation for u_x we mean backward difference with respect to the space discretization), we then get a forward difference approximation in time and a backward difference approximation in space which is denoted by FTBS scheme. We can also consider a forward difference approximation for u_x to obtain briefly FTFS scheme. It can be noticed that the FTBS scheme is in line with the wave travelling to the right and, similarly, the other FTFS scheme can be used when the wave moves to the left.

Therefore, both those schemes depend on the sign of a. If a is positive we can use a backward difference in space and if a is negative we can use a forward difference in space. The FTBS and FTFS schemes are called the upwind schemes. Hence, the approximate solution of the convection equation (2.10) is as follows.

$$u_j^{n+1} = \begin{cases} (1 - \alpha)u_j^n + \alpha u_{j+1}^n & \text{if } a < 0, \\ (1 + \alpha)u_j^n - \alpha u_{j-1}^n & \text{if } a > 0, \end{cases} \qquad (2.11)$$

where $\alpha = a\Delta t/\Delta x$. The upwind schemes are first order in space and time and they are stable if $|\alpha| \leq 1$.

Chapter 3

Implementation

In this chapter we give the numerical results of our implementation for the well known equation from the area of reaction-diffusion systems (the Allen-Cahn equation which is a non-linear parabolic partial differential equation that describes evolution of interfaces by mean curvature). We also implement our method on a reaction-convection-diffusion (RCD) equation. For both equations we apply a finite difference method for the space discretization and then use the exponential time differencing (ETD) scheme on the resulting semi-linear system. We use the semi-implicit Euler method and the ETD with Krylov subspace for computing the matrix exponential to get the approximate solution for both equations. In addition, for the RCD equation we apply the ETD with real fast Léja points technique [3, 6, 10]. The aim here is to find out which one of these methods : the ETD, the semi-implicit Euler, the ETD with Krylov subspace technique and the ETD with real fast Léja points technique, is most accurate and efficient. We obtain the convergence in time and in space for the Allen-Cahn equation using only the ETD and semi-implicit Euler methods and compare the efficiency of those methods. Then, for the Allen-Cahn and RCD equations, we compare ETD, semi-implicit Euler, the ETD with Krylov subspace scheme and the ETD with real fast Léja points technique to see how well they converge in time (the last method is only tested for the RCD equation).

3.1   Numerical Experiments

3.1.1   Allen-Cahn equation

We consider the Allen-Cahn PDE equation, which is a one-dimensional reaction-diffusion equation given as

$$u_t = u_{xx} + u - u^3, \quad x \in (0,1), \quad t > 0,$$

$$u(x,0) = \sin(\pi x), \quad u(0,t) = u(1,t) = 0. \tag{3.1}$$

For the equation (3.1) above we use a finite difference method in order to discretize in space [8, 19, 26, 41]. Therefore our PDE is approximated by a system of ODEs which is much easier to treat and it is given by

$$u_t = \mathbf{A}u(t) + \mathbf{F}(u,t). \tag{3.2}$$

The following schemes: ETD, the semi-implicit Euler and the ETD with Krylov subspace for computing the matrix exponential have been used for solving the equation (3.2). In the ETD scheme we implement our code in the MATLAB function *expm*. Our aim here is to get the order of convergence in both time and space of the ETD and semi-implicit Euler methods, and the order of convergence in time of the ETD with Krylov for getting the solution of this problem. Then we have to determine, based on that (the orders of convergence), which of these is computationally the more accurate and efficient method. In order to do this we first establish a MATLAB code to implement the ETD and the semi-implicit schemes to get the order of convergence in time and we present the graphical results in Figures 3.1 and 3.2 respectively.

As we do not have an exact solution we estimate the global error by

$$\| u_h(t) - u_h^{\Delta t}(t) \|_{L^2} \approx 2 \| u_h^{\Delta t}(t) - u_h^{\frac{\Delta t}{2}}(t) \|_{L^2},$$

where $u_h^{\Delta t}(t)$ indicates the approximation of solution at time t with time step Δt.
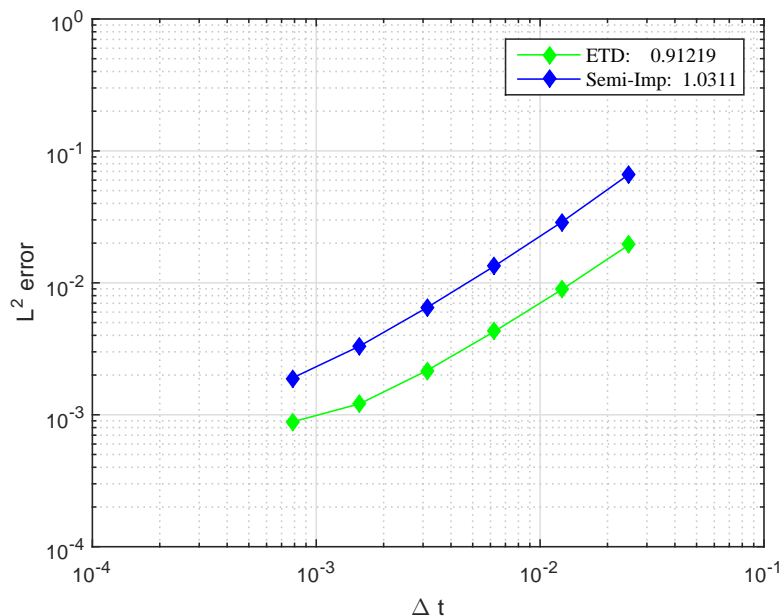
Figure 3.1: Error of the solutions using the ETD and Semi-Imp methods in solving (3.1), at the final time $T = 0.5$ as a function of Δt with fixed space step $\Delta x = 0.005$.

Figure 3.1 represents the convergence at the final time $T = 0.5$ in the L^2 norm as a function of the chosen time step Δt, measuring the error with fixed space step $\Delta x = 0.005$. It can be seen from this graph the rates of convergence for the ETD and semi-implicit Euler methods are 0.91219 and 1.0311 respectively. That is both schemes are of the first order $O(\Delta t)$ and they have similar error constants.

Figure 3.2 shows the L^2 error as a function of CPU time. In this case we find that the ETD scheme is more accurate and more efficient than the semi-implicit Euler scheme.
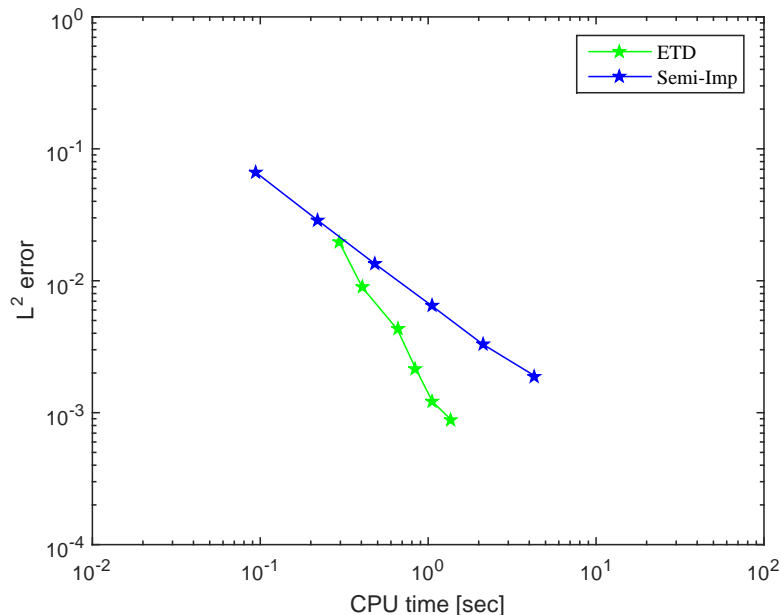
Figure 3.2: The L^2 error at $T = 0.5$ as a function of CPU time. Both plots above 3.1 and 3.2 are for the Allen-Cahn equation (3.1).

In the second MATLAB code we try to get the order of convergence in space for both ETD methods and semi-implicit Euler. It is worth mentioning that when we estimate the errors, we scale the norms so they converge as $N \to \infty$. Therefore, we will give an idea about the discrete L^2 norm [23] and how to scale it and why to do that.

Definition 3.1.1. *(Discrete L^2 Norm) The discrete L^2 norm is particularly for measuring errors in numerical schemes. The discrete L^2 norm for a vector v^h with a d-dimensional domain and a uniform grid spacing h is given by*

$$\|v^h\|_h = \left(h^d \sum_i (v_i^h)^2 \right)^{1/2}.$$

This Euclidean vector norm scaled by a factor h^d which depends on the geometry of the problem. In fact, because of this scaling factor the discrete L^2 norm approximates the continuous L^2 norm of a function $u(x)$ which is given by

$$\|u\|_2 = \left(\int_\Omega | u(x) |^2 \, dx \right)^{1/2}.$$

In Figure 3.3 we can see that the order of convergence for varying spatial dis-

cretization with fixed time step $\Delta t = 0.05$ for both the ETD and semi-implicit methods where the rate of convergence for ETD is 2.0722 and for semi-implicit is 2.0313. Since we found in this case the semi-implicit and ETD methods have very similar error constants, then both schemes have the same rate of convergence, namely $O(\Delta x^2)$. This means that the the order of convergence here is two.
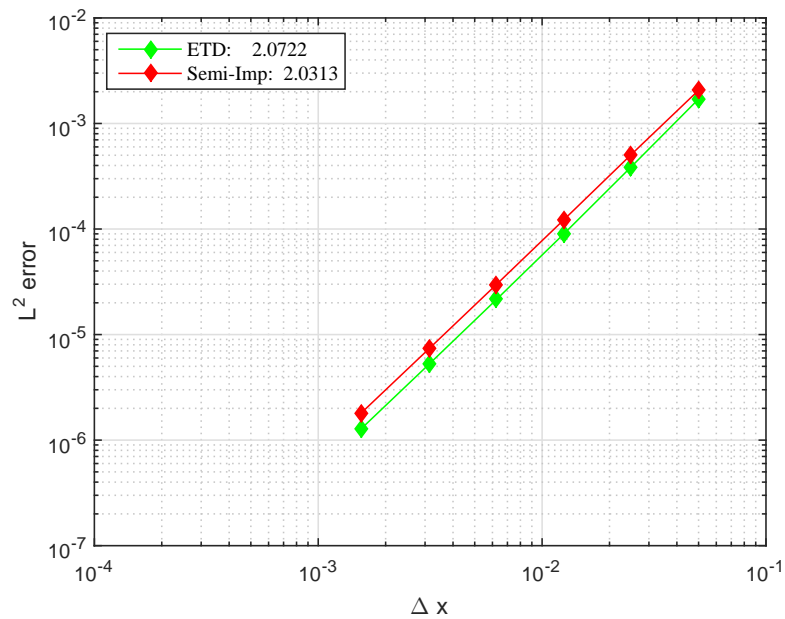
Figure 3.3: Convergence of the ETD and Semi-Imp methods at $T = 0.5$ as a function of Δx and fixed time step $\Delta t = 0.05$.
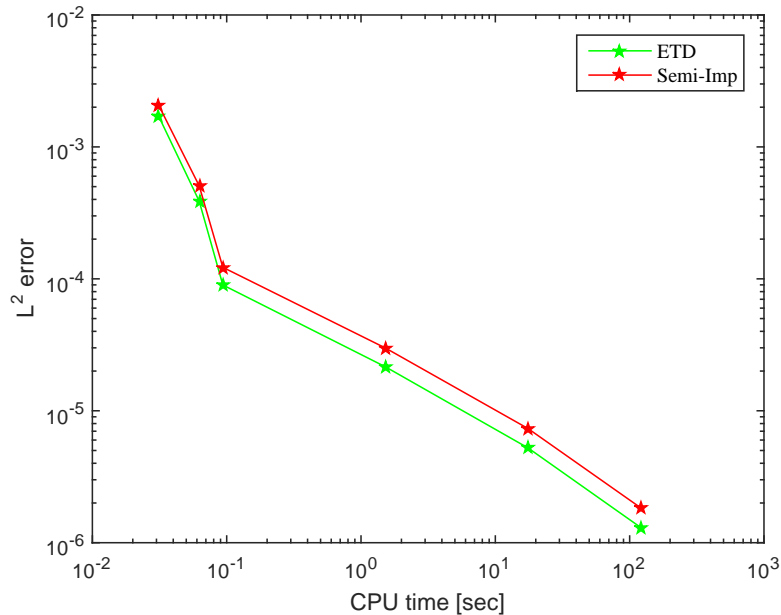
Figure 3.4: The L^2 error, which is represented in Figure 3.3, at $T = 0.5$ as a function of CPU time. Figures 3.3 and 3.4 belongs to the Allen-Cahn equation (3.1).

Figure 3.4 shows the L^2 error as a function of CPU time. We can simply see the reduction in the numerical error for both methods. The efficiency for solving this problem is approximately similar for both methods, however, ETD for the space convergence is considered rather better than the semi-implicit as it has a smaller CPU time than the semi-implicit method.

On the other hand, we also evaluate the matrix exponential using the Krylov subspace technique and we get the plot of the error versus different time steps which is shown in Figure 3.5. In this implementation we use the function *phiv* of the Expokit package [39] with fixed space step $\Delta x = 0.005$, the tolerance used is 10^{-7} and the Krylov subspace dimension used is $m = 20$. From this graph we can see the convergence for this method is achieved and the order of this method is 0.91219. The error in the L^2 norm is computed at time $T = 0.5$. Figure 3.6 shows the L^2 error as a function of CPU time, which is represented in Figure 3.5.
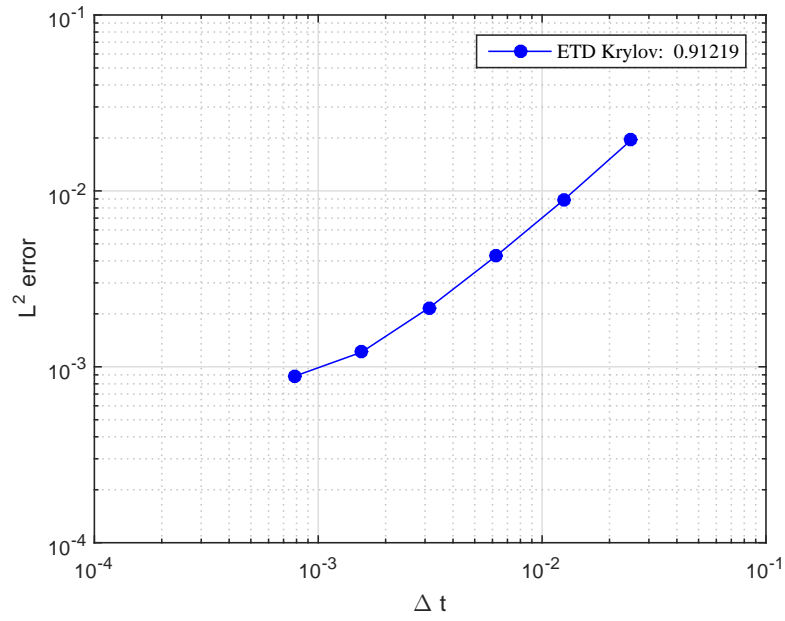
Figure 3.5: Convergence of the ETD Krylov method. This log-log plot shows the numerical error versus time step size Δt.
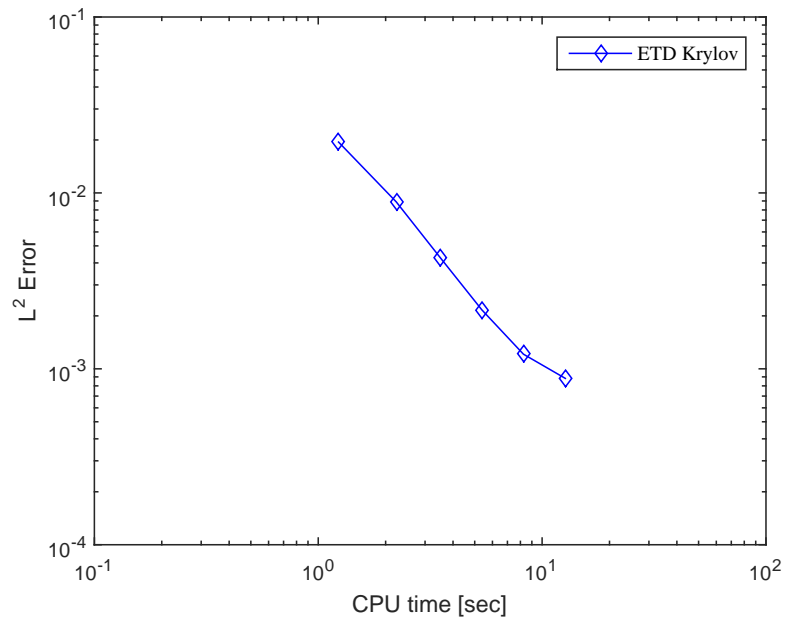
Figure 3.6: A log-log plot of the numerical error versus average computer time.

In Figures 3.7 and 3.8 we compare the convergence and the CPU time we got by the Krylov method with those we got by the ETD and the semi-implicit Euler schemes. We take here also a fixed space step of $\Delta x = 0.005$ and different time steps, while the dimension of Krylov subspace used is the same, $m = 20$, with tolerance 10^{-7}.
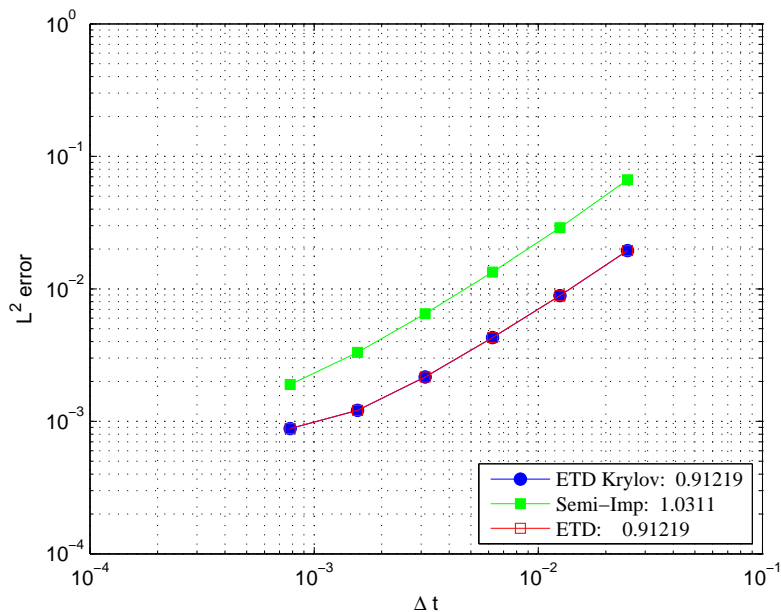
Figure 3.7: Convergence of the ETD, ETD Krylov and Semi-Imp methods at final time as a function of Δt with fixed $\Delta x = 0.005$. The Krylov subspace dimension is fixed to be 20.

As can be seen from Figure 3.7 all methods converge at essentially the same rate. The ETD method and ETD with Krylov method have exactly the same error constants, so they have the same rate of convergence which is 0.91219, whereas the semi-implicit Euler method have a similar error constants and its convergence of order 1.0311. Overall, all schemes show convergence rates of $O(\Delta t)$.
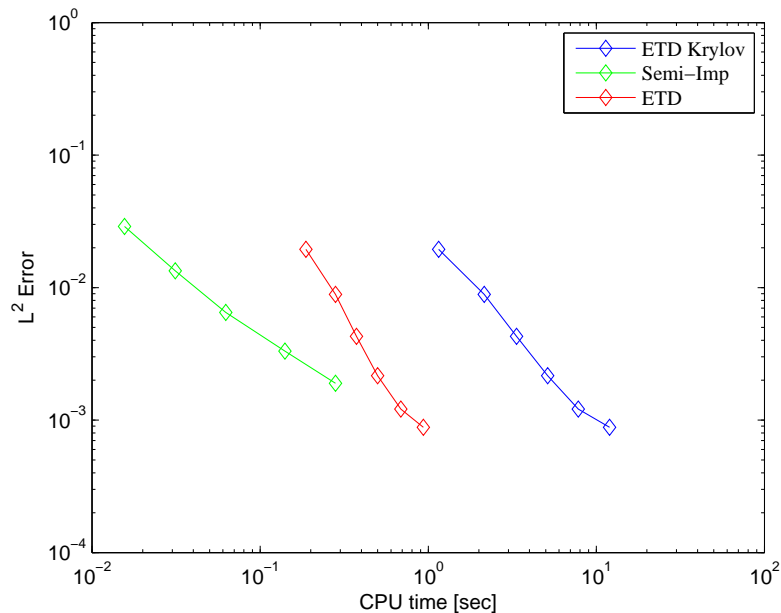
Figure 3.8: The L^2 error at the final time as a function of CPU time. Both Figures 3.7 and 3.8 represented the error of ETD, ETD Krylov and Semi-Imp methods in solving the Allen-Cahn equation (3.1).

Figure 3.8 shows us the error as a function of CPU time. The graphs indicate that, for relatively small CPU time, the semi-implicit Euler method gives more accurate results and appears to be the fastest and most efficient method. What happens for larger CPU time (above 10^0 sec) is less clear.

3.1.2 The 1D reaction-convection-diffusion equation with constant coefficients

We consider the one-dimensional linear constant coefficient reaction-convection-diffusion equation

$$u_t = \epsilon\, u_{xx} + a\, u_x + F(u), \quad x \in (0, 1), \quad t > 0, \tag{3.3}$$

with the Dirichlet boundary conditions $u(0, t) = u(1, t) = 0$. The initial condition is the function $u_0 = u(x, 0) = \sin(\pi x)$. Here ϵ is the diffusivity constant which is positive. We consider the function $F(u) = u - u^3$, and assume the constant velocity a to be positive.

For equation (3.3) we use the first-order upwind scheme to approximate the spatial derivative u_x. Based on our assumption that the sign of the constant a is positive,

we apply the forward space difference approximation for u_x and we use the central difference approximation to approximate the second derivative u_{xx}.

Hence, we arrive at a semi-discrete system of ODE which is much easier to treat and it is given by

$$u_t = (A + B)u + F(u). \tag{3.4}$$

This equation can be rewritten as

$$u_t = \mathcal{L}u + F(u), \tag{3.5}$$

where $\mathcal{L} = A + B$, $A = (1/\Delta x^2)\tilde{A}$ and $B = (1/\Delta x)\tilde{B}$.

$\tilde{A}$ and $\tilde{B}$ are given by

$$\tilde{A} = \begin{bmatrix} -2 & 1 & 0 & \cdots & 0 \\ 1 & -2 & 1 & & \vdots \\ 0 & \ddots & \ddots & \ddots & 0 \\ \vdots & & 1 & -2 & 1 \\ 0 & \cdots & 0 & 1 & -2 \end{bmatrix}, \quad \tilde{B} = \begin{bmatrix} -1 & 1 & 0 & \cdots & 0 \\ 0 & -1 & 1 & & \vdots \\ \vdots & \ddots & \ddots & \ddots & 0 \\ \vdots & & & \ddots & -1 & 1 \\ 0 & \cdots & \cdots & 0 & -1 \end{bmatrix}. \tag{3.6}$$

The following schemes : ETD, the semi-implicit Euler method, ETD with Krylov subspace and ETD with real fast Léja points tecnniques [3, 6, 9, 10] for computing the matrix exponential were used for solving the equation (3.5). In the ETD scheme we implemente our code in the MATLAB function *expm*.

We also use the function *phipm* [31] and the Krylov subspace dimension used here was $m = 20$ with tolerance 10^{-5} in our implementation for evaluating the matrix exponential using Krylov subspace and real fast Léja points techniques. We choose a fixed space step of $\Delta x = 0.0005$ and different time steps $\Delta t = 0.0001, 0.0002, 0.001, 0.002, 0.01$. Our target here is to obtain the order of convergence in time of the above mentioned schemes and then based on that, we have to determine which one is the more accurate and efficient scheme. The numerical results can be seen in the Figures 3.9 and 3.10.
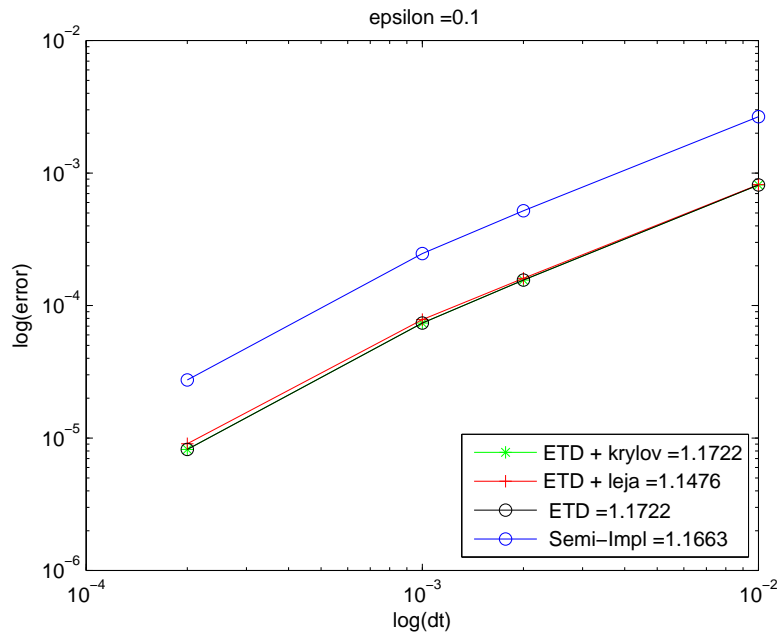
Figure 3.9: A log-log plot represent convergence of the ETD, ETD + Krylov, ETD + Léja and Semi-Impl methods at final time $T = 1$ as a function of Δt with fixed space step $\Delta x = 0.0005$.

Figure 3.9 displays the convergence at the final time $T = 1$ in the L^2 norm for different time steps Δt for all methods. As can be seen from this figure the rate of convergence is the first order $O(\Delta t)$ for all schemes. The ETD, ETD with Krylov subspace technique and ETD with real fast Léja points technique shows an obvious improvement in the error constans. There is a clear difference between the ETD schemes and the semi-implicit Euler method. Hence the ETD, ETD with Krylov subspace and ETD with real fast Léja points methods are more accurate than the semi-implicit Euler method.

We can see the efficiency of the methods from the second Figure 3.10. As the semi-implicit Euler method has a small CPU time compared to the other methods, it is considered significantly more efficient than the ETD schemes.
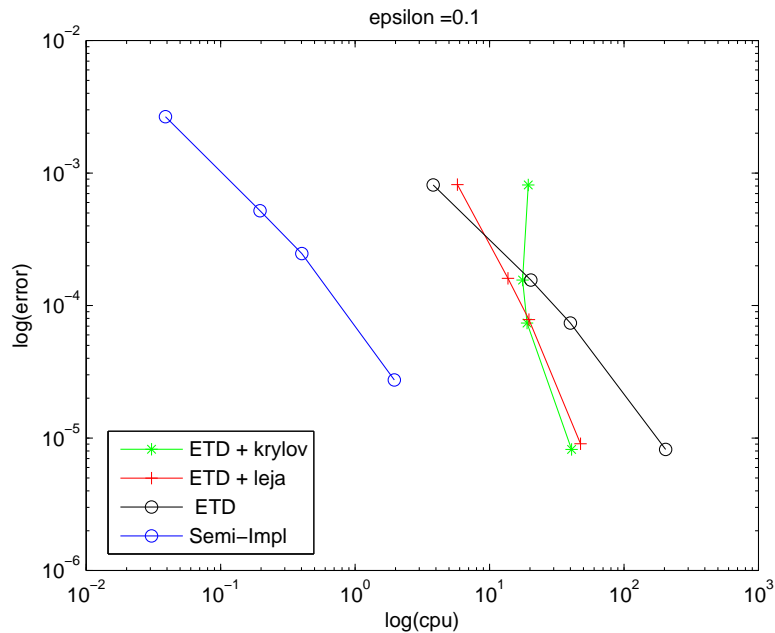
Figure 3.10: The error of the ETD, ETD + Krylov, ETD + Léja and Semi-Impl methods at the final time $T = 1$ as a function of CPU time. Both Figures 3.9 and 3.10 show the error of methods in solving the RCD equation (3.3).

3.2   Summary

From the numerical results for the two problems (3.1) and (3.3), we found out that the rate of convergence in time for all schemes : ETD, ETD with Krylov subspace technique, ETD with real fast Léja points technique and the semi-implicit Euler, are the first order $O(\Delta t)$. The three ETD schemes converge faster than the semi-implicit Euler method so that they are considered more accurate. However, we noticed that the semi-implicit Euler method is more efficient than the ETD schemes.

On the other hand, we can see from Figures 3.3 and 3.4 that the ETD scheme is more accurate and efficient than the semi-implicit method and this was for different space steps and fixed time step. The order of convergence in space for both schemes is the second order, $O(\Delta x^2)$.

Chapter 4

Green Roof Model Numerics

4.1 Introduction

In this chapter we solve the green roof model of [1] without the sink term (the one-dimensional Richards' equation) numerically. The model, based on the paper [1], describes the movement of water through a soil layer. This model is one-dimensional and represents a horizontal roof, here taken to have a single soil layer with thickness $L = 10^{-1}$ m. In reality, a green roof can contain two layers of soil, a rooting soil which is a thinner layer (< 2 cm) at the top and a thicker layer containing pellets of expanded clay which is about 5-10 cm thick [1, 21]. At the bottom of the soil, there is a soil-drainage-layer separated from the soil by a plastic sheet, taken to lie at $z = 0$. The soil upper surface is $z = L$; here water can be supplied to the system by rain fall. In practice, there can be saturated and unsaturated regions within the green roof soil. Figure 4.1 shows a case where a saturated layer occupies the lower part of the soil, $0 < z < h(t)$, so that the saturation $S = 1$ for $0 < z \leq h$, while the upper part is unsaturated : saturation S satisfies $0 \leq S < 1$ for $h < z < 1$. However, in this chapter we confine our attention to situation where the whole roof is unsaturated, $0 \leq S < 1$ for $0 \leq z \leq 1$ (and $h(t)$ has no meaning).

The central finite difference approximation is used for the spatial derivatives. The boundary conditions are discretized using the fictitious point method. Then we apply time integration with the exponential Euler method to the resulting system. We code this problem using MATLAB.
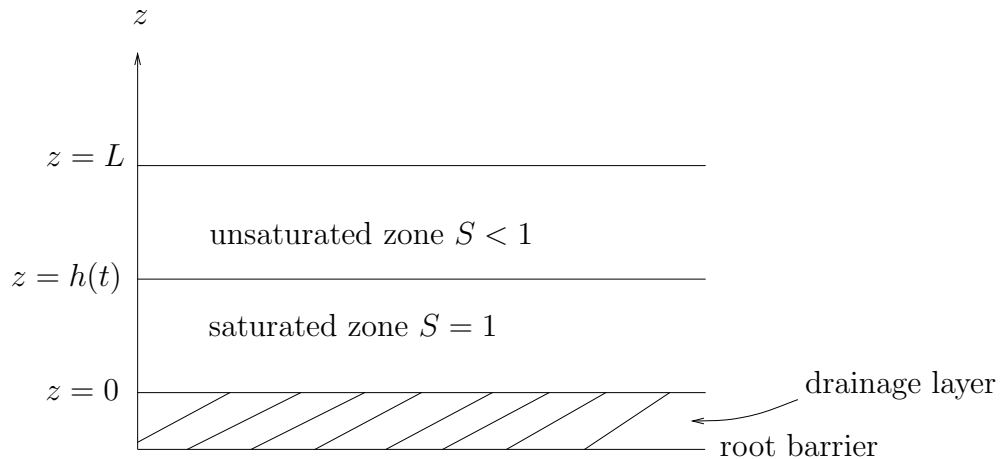
Figure 4.1: Green roof structure.

4.2   Green Roof Model : The Unsaturated Region

We assume the entire region $0 \leq z \leq L$ is unsaturated so that the soil saturation S, $S(z,t)$ denoting its value at a time t and a height z, is everywhere less than 1 ($S < 1$). The one-dimensional Richards' equation for water flow in the unsaturated soil [1] is

$$\phi \frac{\partial S}{\partial t} = \frac{\partial}{\partial z} \left(D_0 D(S) \frac{\partial S}{\partial z} + K_0 K(S) \right) - R, \tag{4.1}$$

where ϕ is the constant porosity of the soil, taken here to be 0.25, $D_0 D(S)$ is a diffusive term and $K_0 K(S)$ models the flow due to gravity. More generally, a similar term (with a different multiplicative constant) multiplies pressure gradient in giving mass flux in a concentration-dependent version of Darcy flow. R is the sink due to water uptake by the plant roots.

We have an initial condition $S = S_{init}$ at $t = 0$, the water saturation at time zero. Here, for simplicity, we take S_{init} to be independent of z with $0 < S_{init} < 1$. The boundary conditions that have been taken at the top and bottom of the soil layer are given in [1] by :

$$D_0 D(S) \frac{\partial S}{\partial z} + K_0 K(S) = Q_{in}(t) \quad \text{at} \quad z = L, \tag{4.2}$$

$$D_0 D(S) \frac{\partial S}{\partial z} + K_0 K(S) = 0 \quad \text{at} \quad z = 0. \tag{4.3}$$

Here Q_{in} is the rate of the rainfall at the ground level and (4.2) models the water input to the green roof from the atmosphere giving a specific flux at the upper surface $z = 1$. The other boundary condition, (4.3) represents an effectively impervious bottom boundary so the flux is zero at the bottom of the green roof $z = 0$.

Nondimensional variables are given in [1] by writing :

$$z = L\hat{z}, \quad p_r = |P|\hat{p}_r, \quad t = \frac{L}{K_0}\hat{t}, \quad p = p_a + p_c\hat{p}, \quad R = 2\pi a k_r l_d |P|\hat{R}, \quad Q_{in} = Q_{typ}\hat{Q},$$

$$(4.4)$$

where L is the thickness of the soil layer, p_r is an effective pressure in the roots, P is the pressure of root at the soil surface, p_a is atmospheric pressure, p_c is a characteristic suction pressure, a is the root radius, k_r is the root's radial conductivity of water and l_d is the average of roots per unit area.

The parameter values were taken from Roose and Fowler [37] as follows :
$|P| = 10^6$ N m^{-2}, $p_a = 0$, $p_c = 10^4$ N m^{-2}, $2\pi a k_r = 7.85 \times 10^{-16}$m^2 s^{-1} Pa^{-1}, $l_d = 5 \times 10^3$ m^{-2}, $K_0 = 10^{-1}$ m s^{-1} and $D_0 = 10^{-6}$ m^2 s^{-1}. This value of K_0, with the above L makes a nondimensional time $\hat{t} = 1$ correspond to $t = 1$ second.

After nondimensionalisation has been done to (4.1), and to the boundary conditions (4.2) and (4.3), the dimensionless Richards' equation (4.1) has the form

$$\phi\frac{\partial S}{\partial t} = \frac{\partial}{\partial z}\left(\delta D(S)\frac{\partial S}{\partial z} + K(S)\right) - \eta\left(\theta - \epsilon f(S) - p_r\right),$$

$$(4.5)$$

where $\delta = \frac{D_0}{LK_0} \approx 10^{-4}$, $\eta = \frac{2\pi a k_r l_d |P| L}{K_0} \approx 4 \times 10^{-6}$, $\theta = \frac{p_a}{|P|} \approx 10^{-1}$ and $\epsilon = \frac{p_c}{|P|} \approx 10^{-2}$ and $\hat{p}_r = \theta^{-1}$, on dropping the hats. The first term on the right hand side of (4.5) is the water diffusivity in the soil and the second term represents the water conductivity due to gravity. The last term containing η gives the water uptake by plant roots and based on the report [1], gives $\eta \ll 1$, suggesting that it is negligible over the chosen time scale (of order 1 s). The water flux measured upwards in the positive z direction is

$$q = -\left(\delta D(S)\frac{\partial S}{\partial z} + K(S)\right).$$

The dimensionless forms of the boundary conditions are given by

$$\delta D(S)\frac{\partial S}{\partial z} + K(S) = \nu Q \quad \text{at} \quad z = 1,$$

$$(4.6)$$

$$\delta D(S)\frac{\partial S}{\partial z} + K(S) = 0 \quad \text{at} \quad z = 0,$$

$$(4.7)$$

where

$$\nu = \frac{Q_{typ}}{K_0} \approx 3 \times 10^{-6},$$

$$(4.8)$$

with $Q_{typ} = 3 \times 10^{-7}$ m s^{-1} taken to be some typical rainfall for a wet day in Ireland. The functions $K(S)$, $D(S)$ and $f(S)$ are given by

$$K(S) = S^{1/2} \left[1 - \left(1 - S^{1/m} \right)^m \right]^2, \tag{4.9}$$

$$D(S) = \frac{\left[1 - \left(1 - S^{1/m} \right)^m \right]^2}{S^{1/m-1/2} \left(1 - S^{1/m} \right)^m}, \tag{4.10}$$

$$f(S) = \left(S^{-\frac{1}{m}} - 1 \right)^{1-m}, \tag{4.11}$$

where the constant m, $0 < m < 1$, is a property of the expanded-clay soil used in the green roofs [1]. The model problem with equations (4.5), (4.6) and (4.7) is a highly nonlinear problem and called the green roof model.

The water diffusivity $D(S)$ and hydraulic conductivity $K(S)$ are shown in Figures 4.2 and 4.3.
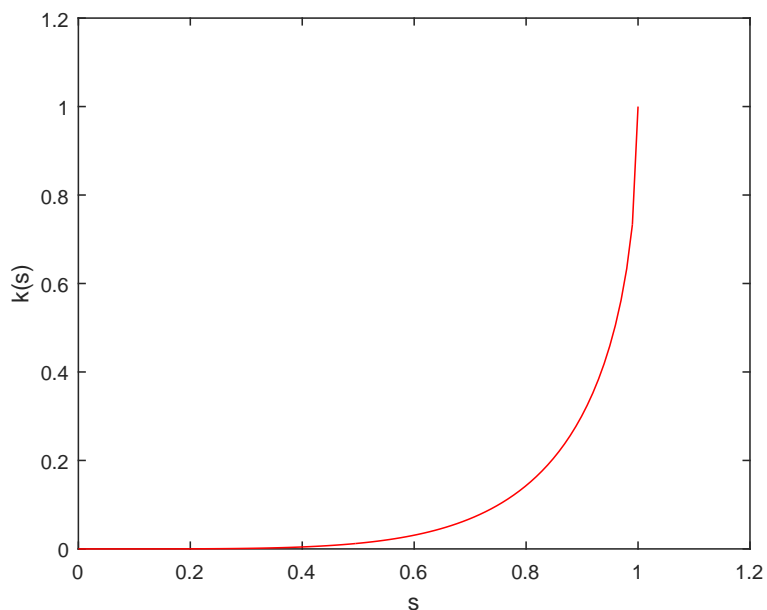
Figure 4.2: Graph of the saturation S dependence of hydraulic conductivity $K(S)$ given by (4.9), when $m = 0.5$.
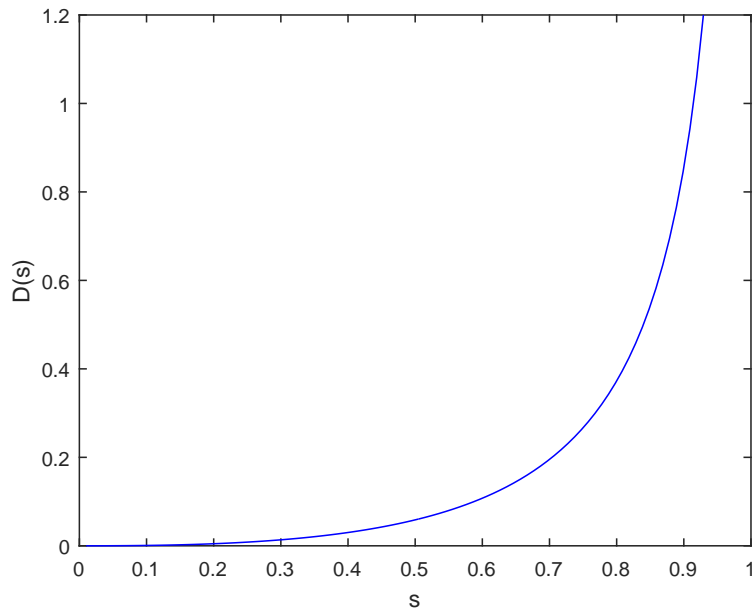
Figure 4.3: Graph of the saturation S dependence of soil water diffusivity $D(S)$ given by (4.10), when $m = 0.5$.

The function $K(S)$ represents dimensionless hydraulic conductivity and it is the factor of proportionality multiplying negative pressure gradient in Darcy's law. $D(S)$ comes about from having a local capillary pressure dependent upon saturation S. Combining the derivatives of this capillary pressure with $K(S)$ in Darcy's law gives a flux term $\left(-D_0 D(S) \frac{\partial S}{\partial z}\right)$ in 1D.

$K(S)$ and $D(S)$ both are increasing functions of the moisture content and vanish for $S = 0$, there is no flow when the soil is dry. There is then a free boundary between regions of $S = 0$ and $S > 0$. Also $D(S) \to \infty$ as $S \to 1$, $K(1) = 1$ but $K' \to \infty$ as $S \to 1$. These give anomolous behaviour for $S = 1$, which corresponds to saturation. Neglecting $D(S)$, the simpler hyperbolic model, $\phi \frac{\partial S}{\partial t} = \frac{\partial}{\partial z} \left(K(S)\right) - R$, has characteristic velocity $c(S) \to \infty$ as $S \to 1$.

In the next chapter we will approximate $D(S)$ and $K(S)$ when m is fixed, $m \to 0^+$ for the high and low saturation cases.

Taking $m \to 0$ gives a soil in which flow has extremely sensitive dependence upon saturation, due to the appearance of terms in $S^{\frac{1}{m}}$ in the expressions (4.9) and (4.10) for $K(S)$ and $D(S)$, respectively (this can be seen more clearly in the limiting forms, (5.1) and (5.2), in the next chapter). The limit of $m \to 1$ is rather subtle. For $m < 1$, $K' \to \infty$ as $S \to 1$, so that characteristics for a model with $D(S)$ neglected have infinite speed at $S = 1$ (although flow velocity is still finite). Therefore, in situations

with m and S near 1, disturbances propagate fast. However, for $m = 1$, $K'(1)$ is finite and the simpler convection only model has bounded characteristic speeds, indicating slower changes, at least when the diffusion term is neglected.

4.3   The Discretized Problem

We consider the finite grid $\Omega_{\Delta z} = \{z_i\}$ with nodes $z_i = z_0 + i\Delta z$, $i = 0, \ldots, J$ for the space interval $[0, 1]$, $z_0 = 0$, $z_J = 1$ and the space step $\Delta z = \frac{1}{J}$, where J here is the number of the spatial nodes. We discretize $\frac{\partial}{\partial z}\left(D\left(S\right)\frac{\partial S}{\partial z}\right)$ in two steps.

First, the "outer derivative" is discretized according to

$$\left.\frac{\partial G}{\partial z}\right|_{z=z_i} \simeq \frac{1}{\Delta z}\left(G|_{z=z_{i+\frac{1}{2}}} - G|_{z=z_{i-\frac{1}{2}}}\right) = \frac{1}{\Delta z}\left(G_{i+\frac{1}{2}} - G_{i-\frac{1}{2}}\right), \qquad i = 0, \ldots, J,$$

(4.12)

where $G = D\left(S\right)\frac{\partial S}{\partial z}$.

Then G is discretized by a central finite difference method as follows :

$$
\begin{aligned}
G_{i+\frac{1}{2}} = \left.\left(D\left(S\right)\frac{\partial S}{\partial z}\right)\right|_{z=z_{i+\frac{1}{2}}} &= D\left(S_{i+\frac{1}{2}}\right)\frac{\partial S_{i+\frac{1}{2}}}{\partial z} \\
&\simeq D_{i+\frac{1}{2}}\left(\frac{S_{i+1} - S_i}{\Delta z}\right),
\end{aligned}
$$

(4.13)

$$
\begin{aligned}
G_{i-\frac{1}{2}} = \left.\left(D\left(S\right)\frac{\partial S}{\partial z}\right)\right|_{z=z_{i-\frac{1}{2}}} &= D\left(S_{i-\frac{1}{2}}\right)\frac{\partial S_{i-\frac{1}{2}}}{\partial z} \\
&\simeq D_{i-\frac{1}{2}}\left(\frac{S_i - S_{i-1}}{\Delta z}\right).
\end{aligned}
$$

(4.14)

The most obvious choice to express $D_{i+\frac{1}{2}}$ in terms of D_i and D_{i+1}, and $D_{i-\frac{1}{2}}$ in terms of D_i and D_{i-1} is the arithmetic mean as follows :

$$D_{i+\frac{1}{2}} = D\left(S_{i+\frac{1}{2}}\right) = D\left(\frac{S_i + S_{i+1}}{2}\right),$$

$$D_{i-\frac{1}{2}} = D\left(S_{i-\frac{1}{2}}\right) = D\left(\frac{S_i + S_{i-1}}{2}\right).$$

Then

$$G_{i+\frac{1}{2}} \simeq D\left(\frac{S_{i+1} + S_i}{2}\right)\left(\frac{S_{i+1} - S_i}{\Delta z}\right),$$

$$G_{i-\frac{1}{2}} \simeq D\left(\frac{S_{i-1} + S_i}{2}\right)\left(\frac{S_i - S_{i-1}}{\Delta z}\right).$$

Then (4.12) becomes

$$\frac{\partial}{\partial z}\left(D(S)\frac{\partial S}{\partial z}\right) \quad \simeq \quad \frac{1}{\Delta z}\left\{D\left(\frac{S_i + S_{i+1}}{2}\right)\left(\frac{S_{i+1} - S_i}{\Delta z}\right) - D\left(\frac{S_i + S_{i-1}}{2}\right)\left(\frac{S_i - S_{i-1}}{\Delta z}\right)\right\}$$

$$\simeq \quad \frac{1}{\Delta z^2}\left\{D\left(\frac{S_i(t) + S_{i-1}(t)}{2}\right)(S_{i-1}(t) - S_i(t))\right.$$

$$\left. - D\left(\frac{S_i(t) + S_{i+1}(t)}{2}\right)(S_i(t) - S_{i+1}(t))\right\}. \tag{4.15}$$

We use the central finite difference method to approximate the first derivative $\frac{\partial}{\partial z}(K(S))$ in (4.5) as follows :

$$\frac{\partial}{\partial z}(K(S)) = \frac{K(S_{i+1}) - K(S_{i-1})}{2\Delta z}. \tag{4.16}$$

Therefore, equation (4.5) gives the following semi-discrete approximation :

$$\frac{\partial S_i}{\partial t} = \frac{\delta}{\phi\Delta z^2}\left[D\left(\frac{S_{i-1}(t) + S_i(t)}{2}\right)(S_{i-1}(t) - S_i(t))\right.$$

$$\left. - D\left(\frac{S_{i+1}(t) + S_i(t)}{2}\right)(S_i(t) - S_{i+1}(t))\right]$$

$$+ \frac{1}{2\phi\Delta z}\left[K(S_{i+1}(t)) - K(S_{i-1})\right]$$

$$- \eta\left(\theta - \epsilon f(S_i(t)) - p_r\right), \qquad i = 0, \ldots, J. \tag{4.17}$$

If we ignore η then (4.17) can be written as follows :

$$S_i'(t) = P\left[D\left(\frac{S_{i-1}(t) + S_i(t)}{2}\right)(S_{i-1}(t) - S_i(t))\right.$$

$$\left. - D\left(\frac{S_{i+1}(t) + S_i(t)}{2}\right)(S_i(t) - S_{i+1}(t))\right]$$

$$+ r\left[K(S_{i+1}(t)) - K(S_{i-1})\right], \qquad i = 0, \ldots, J, \tag{4.18}$$

where $P = \frac{\delta}{\phi\Delta z^2}$ and $r = \frac{1}{2\phi\Delta z}$.

4.4 Discretization of the Boundary Conditions

We also need to discretize the boundary conditions (4.6) and (4.7) as follows.

If we consider the boundary condition at the bottom (lower B.C.) as the left boundary condition and the boundary condition at the top (upper B.C.) as the right one, we will use the central finite differences for the Robin B.C.'s.

First, the B.C. at the bottom $(z = 0)$,

$$\delta D\left(S\right)\frac{\partial S}{\partial z} + K\left(S\right) = 0$$

can be written as

$$\frac{\partial S}{\partial z} = -\frac{K\left(S\right)}{\delta D\left(S\right)} = \gamma_0(S),$$

Using the fictitious point method, we have that the B.C. at $i = 0$ can be approximated by

$$\frac{\partial S_i}{\partial z} \simeq \frac{D_z}{2\Delta z}S_0^n = \frac{S_1^n - S_{-1}^n}{2\Delta z} = \gamma_0(S_0)$$

$$\text{so} \qquad S_1^n - S_{-1}^n = 2\Delta z\gamma_0(S_0)$$

$$\text{or} \qquad S_{-1}^n = S_1^n - 2\Delta z\gamma_0(S_0). \qquad (4.19)$$

Second, the B.C. at the top $(z = 1)$ is

$$\delta D\left(S\right)\frac{\partial S}{\partial z} + K\left(S\right) = \nu Q$$

and can be written as

$$\frac{\partial S}{\partial z} = \frac{\nu Q - K\left(S\right)}{\delta D\left(S\right)} = \gamma(S_J).$$

We then have the B.C. at $i = J$ approximated as

$$\frac{\partial S_i}{\partial z} \simeq \frac{D_z}{2\Delta z}S_J^n = \frac{S_{J+1}^n - S_{J-1}^n}{2\Delta z} = \gamma(S_J)$$

$$\text{so} \qquad S_{J+1}^n - S_{J-1}^n = 2\Delta z\gamma(S_J)$$

$$\text{or} \qquad S_{J+1}^n = S_{J-1}^n + 2\Delta z\gamma(S_J). \qquad (4.20)$$

Now our semi-discrete system with the values of solution on the boundaries will be in the following form :

$$\frac{dS_i}{dt} = P\left[D\left(\frac{S_{i-1}(t) + S_i(t)}{2}\right)(S_{i-1}(t) - S_i(t)) \right.$$

$$- D\left(\frac{S_{i+1}(t) + S_i(t)}{2}\right)(S_i(t) - S_{i+1}(t)) \Big]$$

$$+ r\left[K\left(S_{i+1}(t)\right) - K\left(S_{i-1}(t)\right) \right] = g_i, \qquad i = 0, 1, \dots, J, \tag{4.21}$$

where S_{-1} and S_{J+1} are eliminated using (4.19) and (4.20). Equation (4.21) can be written in the form :

$$\frac{dS}{dt} = g(S), \qquad S(0) = S_0. \tag{4.22}$$

4.5   Time Integration with Exponential Euler Method

We linearize $g(S)$ in (4.22) about the state at $t = t_n$ using the first order linear approximation, in other words, the first order Taylor polynomial. At each step this results in the linear initial value problem :

$$\frac{dS}{dt} = g_n + J_n\left(S - S_n\right), \qquad S(t_n) = S_n \tag{4.23}$$

to advance the solution from $t = t_n$ to $t = t_{n+1}$. We consider the simplest exponential integrator for (4.22). Employing a time stepping strategy with $S_n = S(t_n)$ and setting $\tau_n = t_{n+1} - t_n$, we obtain the formula

$$S_{n+1} = S_n + J_n^{-1}\left(e^{\tau_n J_n} - I\right)g_n. \tag{4.24}$$

Here $J_n \in \mathbb{R}^{N \times N}$ denotes the Jacobian matrix $\frac{\partial g}{\partial S}$ evaluated at $S = S_n$, $g_n = g(S_n)$. I refers to the identity matrix.

The previous equation (4.24) can be simply rewritten in the following form :

$$S_{n+1} = S_n + \tau_n \varphi(\tau_n J_n)g_n, \tag{4.25}$$

and this provides an approximate solution to (4.22) in time.

4.6 Numerical Solutions

In the previous sections, 4.3, 4.4 and 4.5, we set up our numerical method for solving the green roof model (4.5) subject to the boundary conditions (4.6) and (4.7). We approximated the spatial derivatives given in (4.5) using the central finite difference method and we now apply the ETD method (2.8) to solve the resulting system of ODEs (4.22). The last term in our model (4.5) was neglected.

We investigate the numerical solution for three different initial conditions of the saturation $S_{init} = 0.05, 0.1, 0.15$. This work was based on the work of, and will be compared with results in, the paper [1]. For all the cases, this work was implemented in MATLAB and the parameter values are taken as : $m = \frac{1}{2}$, $\nu = 3 \times 10^{-6}$ and $\delta = 10^{-4}$. In the top boundary condition, (4.6), we take $Q = 1$. The program was stopped when S reaches 1 except that for the initial condition $S_{init} = 0.05$ we halted our computations at the dimensionless time of $t = 100$, consistent with the results in the paper [1], where $S_{bottom} = S(0, t)$ is still far from 1.

The profiles obtained for the saturation S for the three initial values are shown at some final times in Figure 4.4. A boundary layer of thickness δ in S near the bottom boundary $z = 0$ can be seen in the semi-log plot in the second set of plots, Figure 4.5. For $S_{init} = 0.1$ and 0.15, we notice that two of the plots of saturation S cross. This crossing is due to the two plots corresponding to two different times : the computation for initial conditions $S_{init} = 0.1$ and 0.15 were halted when the value of S at $z = 0$, S_{bottom}, reaches 1, as shown in Figure 4.6. The time taken for $S_{bottom} = 1$ to be reached is greater for $S_{init} = 0.1$ and this larger time allows S to increase more for $z > 0$.

Figure 4.6 shows plots of S_{bottom} against the dimensionless time for the three values of initial conditions. The saturation S at $z = 1$ (S_{top}) against dimensionless time is presented in Figure 4.7.
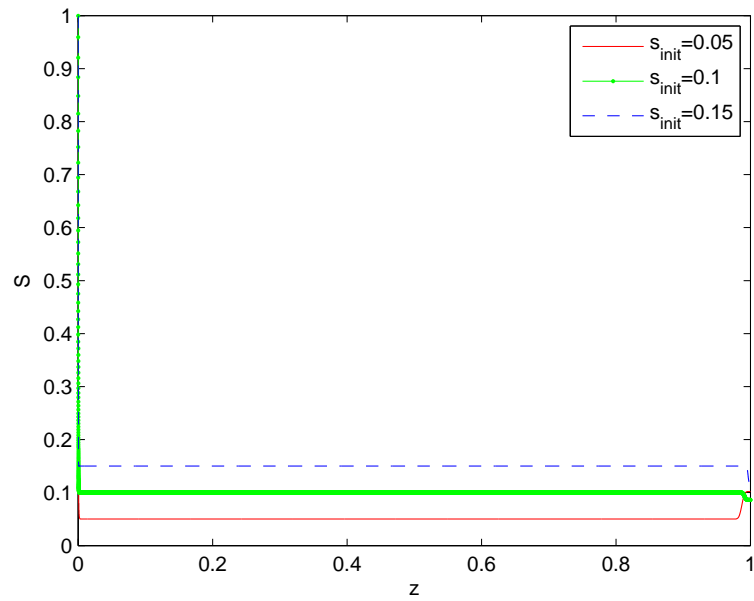
Figure 4.4: Saturation S against z for three different initial conditions ($S_{init} = 0.05, 0.1, 0.15$) when S approximately reaches 1 at $z = 0$ ($S_{init} = 0.1, 0.15$) and at the dimensionless time 100, meaning about two minutes in terms of the original time variable ($S_{init} = 0.05$).
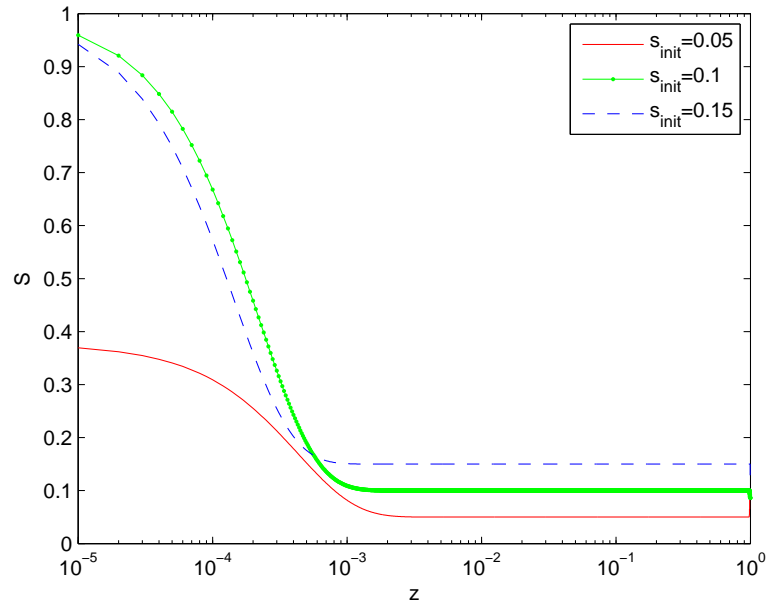
Figure 4.5: A semi-log plot of saturation S against z for three different initial conditions ($S_{init} = 0.05, 0.1, 0.15$) when S approximately reaches 1 at $z = 0$ ($S_{init} = 0.1, 0.15$) and at the dimensionless time 100 ($S_{init} = 0.05$).
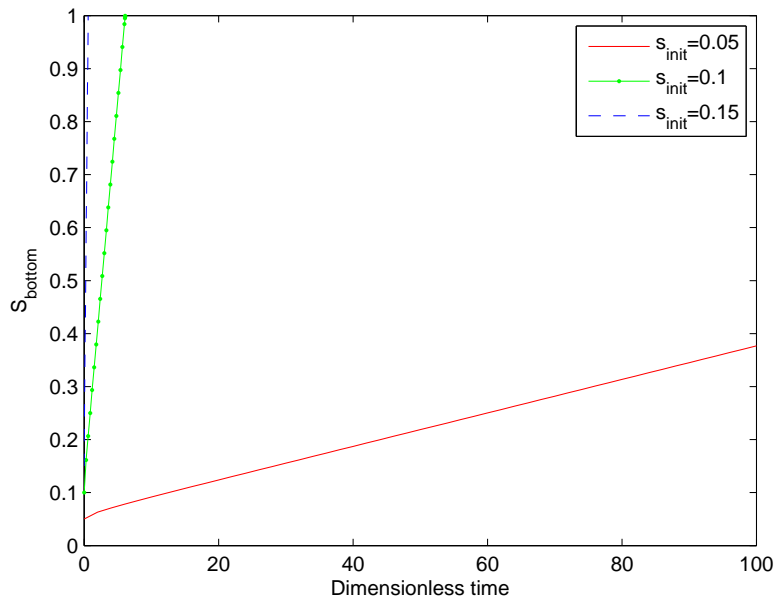
Figure 4.6: S_{bottom} against the dimensionless time for three different initial conditions $(S_{init} = 0.05, 0.1, 0.15)$.
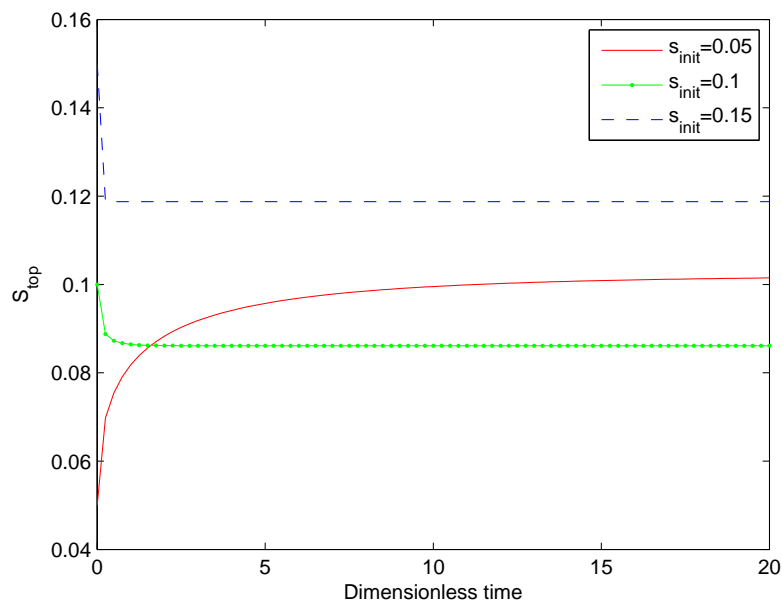
Figure 4.7: S_{top} against the nimensionless time for three different initial conditions $(S_{init} = 0.05, 0.1, 0.15)$ with $Q = 1$ in the top condition.

As can be seen from the results, the saturation is completed at the bottom of the soil at different times when the values of the initial saturation S_{init} are 0.1 and 0.15. From Figure 4.4, we can see something appears to be a travelling wave (see next chapter) developing downwards from the top boundary at $z = 1$ in $S_{init} = 0.05$ case and it looks sharp as the value of the parameter δ is very small. We also can recognize that the value below the travelling wave is the initial condition.

4.7   Summary

The work in this chapter is based on the work in the paper [1]. A description of the evolution of the saturation in the soil layer of a mathematical model of a flat green roof has been done using the ETD and finite difference methods. The results are compared to those in the paper [1] and we noticed that they are very similar to each other where the saturation S reached 1, at $z = 0$, for the two initial conditions $S_{init} = 0.1$ and 0.15 while for $S_{init} = 0.05$, the S_{bottom} did not reach 1 even for $t = 100$. One problem seen with the implementation of the method at present is as exhibited by the plots in Figure 4.7. The limiting values of saturation S_{top} at the top boundary $z = 1$ shown they are all different; they depend upon the initial concentration S_{init} as well as on the prescribed flux at the boundary, νQ. In contrast, the results in the paper [1] show that S_{top} approaches the same value irrespective of the initial data, S_{init}, in agreement with theory (for cases of small δ) which says we should get a limiting value S_{top} satisfying $K(S_{top}) = \nu Q$. Although the interior part of the numerical approximation is mass conserving (like the PDE), the boundary approximations do not exactly conserve mass, and this is the likely cause of these differences.

According to the results, we found that the finite difference and the ETD methods were slower than the finite element method used in the paper [1], however, they otherwise worked well with this green roof model.

In the next chapter, we investigate the local behaviour of the solutions of the same model (5.13) for the saturation near 0 and 1. These solutions are looked at for varying values of the parameter m which appears in the model for water saturation in the expanded-clay soil.

Chapter 5

Travelling Wave Solutions

5.1 Introduction

We saw in section 4.6 that a travelling wave could be formed linking a smaller value S_- for $z \to -\infty$ (or at least z far enough to the left) with a larger value S_+ for $z \to \infty$ (or at least z far enough to the right). In section 4.6, both these values of S satisfies $0 < S < 1$. In this chapter, we investigate travelling wave solutions for our nonlinear convection-diffusion model. We look for frontal travelling waves connecting such limiting values of saturation S_- and S_+. We are particularly interested in whether such waves exist for different cases for different ranges of S_- and S_+ in $[0, 1]$. For example, the travelling wave which was seen numerically, developing from $z = 1$ in Chapter 4, had $0 < S_- < S_+ < 1$ (this we shall call Case 4). We find travelling waves for all our cases with $0 \leq S_- < S_+ \leq 1$ but the cases with $0 < S_+ < S_- < 1$ and $0 = S_+ < S_- < 1$ do not give travelling waves. We also particularly look at the local behaviour of the solutions for S close to 0 (dry region) and when S is close to 1 (saturated region). Most of the cases have a fixed value of m for the expanded-clay soil and we also consider $m \to 0$ and $m \to 1$.

We must start by discussing the approximations of the functions $D(S)$ and $K(S)$ for the low and high saturations.

5.2 Approximation of the Functions $D(S)$ and $K(S)$ when $S \to 0^+$

We shall want to approximate the functions $D(S)$ and $K(S)$ for various cases of the constant m.

- When m is fixed $(0 < m < 1)$

$$
\begin{aligned}
D(S) &= \frac{\left[1 - \left(1 - S^{1/m}\right)^m\right]^2}{S^{(1/m-1/2)}\left(1 - S^{1/m}\right)^m} \\[2mm]
&\sim S^{(1/2-1/m)}\left[1 - \left(1 - mS^{1/m}\cdots\right)\right]^2 \\[2mm]
&\sim S^{(1/2-1/m)}\left(m^2 S^{2/m}\right) \\[2mm]
&\sim m^2 S^{(1/m+1/2)}. \tag{5.1}
\end{aligned}
$$

and

$$
\begin{aligned}
K(S) &= S^{1/2}\left[1 - \left(1 - S^{1/m}\right)^m\right]^2 \\[2mm]
&\sim S^{1/2}\left[1 - \left(1 - mS^{1/m}\cdots\right)\right]^2 \\[2mm]
&\sim S^{1/2}\left(m^2 S^{2/m}\right) \\[2mm]
&\sim m^2 S^{(2/m+1/2)}. \tag{5.2}
\end{aligned}
$$

- When $m \to 0^+$

In this case, the functions $D(S)$ and $K(S)$ are approximated simply as in equations (5.1) and (5.2).

5.3   Approximation of the Functions $D(S)$ and $K(S)$ when $S \to 1^-$

- When m is fixed $(0 < m < 1)$

We set $S \sim 1 - m\sigma$, $\sigma \to 0+$ and $0 < m < 1$.

$$
\begin{aligned}
D(1 - m\sigma) &= \frac{\left[1 - \left(1 - (1 - m\sigma)^{1/m}\right)^m\right]^2}{(1 - m\sigma)^{(1/m - 1/2)} \left(1 - (1 - m\sigma)^{1/m}\right)^m} \\[2mm]
&\sim \frac{\left[1 - (1 - (1 - \sigma \cdots))^m\right]^2}{\left(1 - m\left(1/m - 1/2\right)\sigma \cdots\right)\left(1 - (1 - \sigma \cdots)\right)^m} \\[2mm]
&\sim \frac{\left[1 - \sigma^m \cdots\right]^2}{\left(1 - m\left(1/m - 1/2\right)\sigma \cdots\right)\sigma^m} \\[2mm]
&\sim \sigma^{-m}\left(1 - 2\sigma^m \cdots\right) \\[2mm]
&\sim \sigma^{-m} \quad \text{for} \quad \sigma \to 0 \quad \text{(i.e.} \quad S \to 1). \tag{5.3}
\end{aligned}
$$

This leads to the following equation :

$$
D(S) \sim \left(\frac{1 - S}{m}\right)^{-m} \quad \text{for} \quad S \to 1^-. \tag{5.4}
$$

Also

$$
\begin{aligned}
K(1 - m\sigma) &\sim (1 - m\sigma)^{1/2}\left[1 - \left(1 - (1 - m\sigma)^{1/m}\right)^m\right]^2 \\[2mm]
&\sim \left(1 - \frac{m}{2}\sigma\right)(1 - \sigma^m)^2 \\[2mm]
&\sim (1 - \sigma^m)^2 \\[2mm]
&\sim 1 - 2\sigma^m \cdots \\[2mm]
&\sim 1 \quad \text{for} \quad \sigma = \left(\frac{1 - S}{m}\right) \to 0^+, \quad m < 1. \tag{5.5}
\end{aligned}
$$

- When $m \to 0^+$

  We set $S = 1 - m\sigma$, σ is not too small and $m \to 0^+$. We can simply write S like this $S = e^{\ln S} \sim e^{-m\sigma}$.

$$D(S) \quad \sim \quad \frac{\left[1 - \left(1 - (e^{-m\sigma})^{1/m}\right)^m\right]^2}{(e^{-m\sigma})^{(1/m-1/2)} \left(1 - (e^{-m\sigma})^{1/m}\right)^m}$$

$$\sim \quad \frac{\left[1 - (1 - e^{-\sigma})^m\right]^2 e^{-(1/2-1/m)m\sigma}}{(1 - e^{-\sigma})^m}$$

$$\sim \quad \frac{e^{\sigma - \frac{1}{2}m\sigma} \left[1 - e^{\ln\left(1 - e^{-\sigma}\right)^m}\right]^2}{(1 - e^{-\sigma})^m}$$

$$\sim \quad \frac{e^{\sigma} \left[1 - e^{m\ln\left(1 - e^{-\sigma}\right)}\right]^2}{(1 - e^{-\sigma})^m}$$

$$\sim \quad \frac{e^{\sigma} \left[1 - (1 + m\ln(1 - e^{-\sigma})\cdots)\right]^2}{(1 - e^{-\sigma})^m}$$

$$\sim \quad \frac{e^{\sigma} m^2 \left(\ln(1 - e^{-\sigma})\right)^2}{(1 - e^{-\sigma})^m}.$$

$$\sim \quad e^{\sigma} m^2 \left(\ln(1 - e^{-\sigma})\right)^2. \tag{5.6}$$

Now to approximate $K(S)$ we set $S = e^{-m\sigma}$, $S^{\frac{1}{m}} = e^{-m\sigma/m} = e^{-\sigma}$.

$$K(S) \quad \sim \quad (e^{-m\sigma})^{1/2} \left[1 - (1 - e^{-\sigma})^m\right]^2$$

$$\sim \quad (e^{-m\sigma})^{1/2} \left[1 - e^{\ln\left(1 - e^{-\sigma}\right)^m}\right]^2$$

$$\sim \quad (e^{-m\sigma})^{1/2} \left[1 - e^{m\ln\left(1 - e^{-\sigma}\right)}\right]^2$$

$$\sim \quad (e^{-m\sigma})^{1/2} \left[1 - (1 + m\ln(1 - e^{-\sigma})\ldots)\right]^2$$

$$\sim \quad m^2 \left(\ln(1 - e^{-\sigma})\right)^2. \tag{5.7}$$

Here we see that σ is not too small means $m\left|\ln(1 - e^{-\sigma})\right|$ is size 1. This choice goes wrong if σ is exponentially small in $1/m$, in other words, S is exponentially close in

$1/m$ to 1. With S so close to 1, let us then choose another variable, α such that

$$1 - e^{-\sigma} = e^{-\alpha/m} \Leftrightarrow e^{-\sigma} = 1 - e^{-\alpha/m} \Leftrightarrow \sigma = -\ln\left(1 - e^{-\alpha/m}\right) \sim e^{-\alpha/m}$$

i.e. $S \sim 1 - me^{-\alpha/m}$, $(\alpha \gg m)$. S decreases with σ and increases with α, thus $S \to 1$ when $\alpha \to \infty$. Then $K(S)$ and $D(S)$ can be obtained as follows :

$$K(S) \sim \left[1 - \left(1 - \left(1 - me^{-\alpha/m}\right)^{1/m}\right)^m\right]^2$$

$$\sim \left[1 - \left(1 - \left(1 - e^{-\alpha/m}\right)\right)^m\right]^2$$

$$\sim \left[1 - \left(e^{-\alpha/m}\right)^m\right]^2$$

$$\sim \left[1 - e^{-\alpha}\right]^2$$

$$\sim 1 - 2e^{-\alpha}. \tag{5.8}$$

$$D(S) \sim \frac{\left[1 - e^{-\alpha}\right]^2}{\left(1 - me^{-\alpha/m}\right)^{(1/m - 1/2)}\left(e^{-\alpha}\right)}$$

$$\sim \frac{\left[1 - e^{-\alpha}\right]^2}{\left(e^{-\alpha}\right)}$$

$$= e^\alpha \left[1 - e^{-\alpha}\right]^2. \tag{5.9}$$

If $\alpha \to \infty$ then $K(S) \to 1$ and $D(S) \to \infty$.

5.4   The Properties of the Function $K(S)$

Here we have the forms and graphs of the hydraulic conductivity $K(S)$ and its first and second derivatives. The function $K(S)$ is an increasing function and approaches zero for $S \to 0$ and $K(S) = 1$ for $S = 1$. For the range $0 < m < 1$, we have these forms as follows

$$K(S) = S^{1/2} \left[1 - \left(1 - S^{1/m} \right)^m \right]^2, \tag{5.10}$$
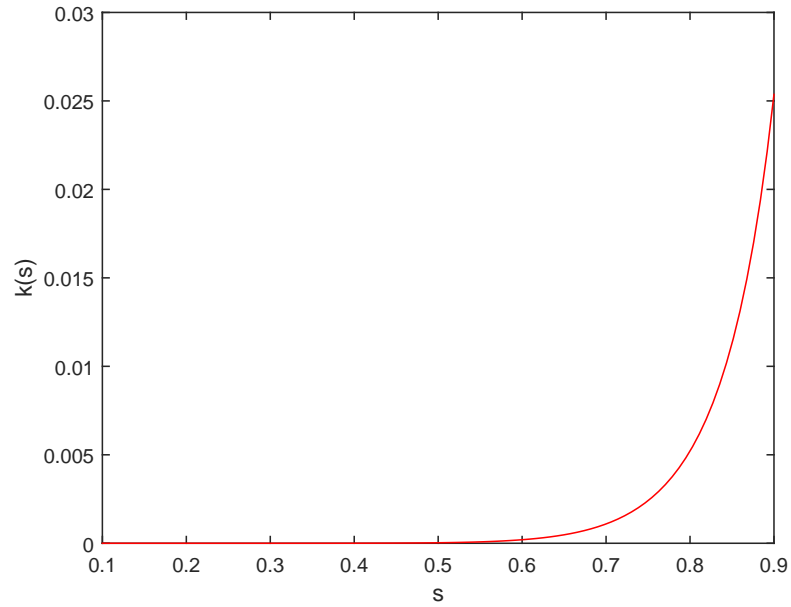
Figure 5.1: The function $K(S)$ with $m = 0.2$ and $0.1 \le S \le 0.9$.

$$
\begin{aligned}
K'(S) &= 2S^{\left(\frac{1}{m} - \frac{1}{2}\right)} \left(1 - S^{\frac{1}{m}} \right)^{m-1} \left(1 - \left(1 - S^{\frac{1}{m}} \right)^m \right) \\
&+ \frac{1}{2} S^{-\frac{1}{2}} \left(1 - \left(1 - S^{\frac{1}{m}} \right)^m \right)^2.
\end{aligned}
\tag{5.11}
$$

From (5.11) it is not immediately obvious as to whether the first derivative K' is an increasing function of S or not. Let us then set $K' = K_a + K_b$ with

$$K_a = 2S^{\left(\frac{1}{m} - \frac{1}{2}\right)} \left(1 - S^{\frac{1}{m}} \right)^{m-1} \left(1 - \left(1 - S^{\frac{1}{m}} \right)^m \right),$$

and

$$K_b = \frac{1}{2} S^{-\frac{1}{2}} \left(1 - \left(1 - S^{\frac{1}{m}} \right)^m \right)^2 .$$

K_a is clearly increasing since $0 < m < 1 < 2$.

For K_b, we write

$$K_b = K_b(s) \quad \text{for} \quad s = 1 - S^{\frac{1}{m}}, \quad \text{then} \quad S = (1 - s)^m$$

$$\text{so that} \quad 0 < s < 1 \quad \text{for} \quad 0 < S < 1 \quad \text{and} \quad \frac{ds}{dS} < 0.$$

Then

$$K_b = \frac{1}{2} (1 - s)^{-\frac{m}{2}} (1 - s^m)^2 .$$

$$
\begin{aligned}
\frac{dK_b}{ds} &= -m (1 - s)^{-\frac{m}{2}} (1 - s^m) s^{m-1} + \frac{m}{4} (1 - s)^{-\frac{m}{2}-1} (1 - s^m)^2 \\[2mm]
&= -\frac{m}{4} (1 - s)^{-\frac{m}{2}-1} (1 - s^m) \left(4 (1 - s) s^{m-1} - (1 - s^m) \right) \\[2mm]
&= -\frac{m}{4} (1 - s)^{-\frac{m}{2}-1} (1 - s^m) \left(4 s^{m-1} - 3 s^m - 1 \right) \\[2mm]
&= -\frac{m}{4} (1 - s)^{-\frac{m}{2}-1} (1 - s^m) \left(3 s^{m-1} (1 - s) + \left(s^{m-1} - 1 \right) \right) . \quad (5.12)
\end{aligned}
$$

From (5.12) we get $\frac{dK_b}{ds} < 0 \Rightarrow \frac{dK_b}{dS} > 0 \Rightarrow K'$ increasing. Therefore, $K'' > 0$ for $0 < S < 1$.
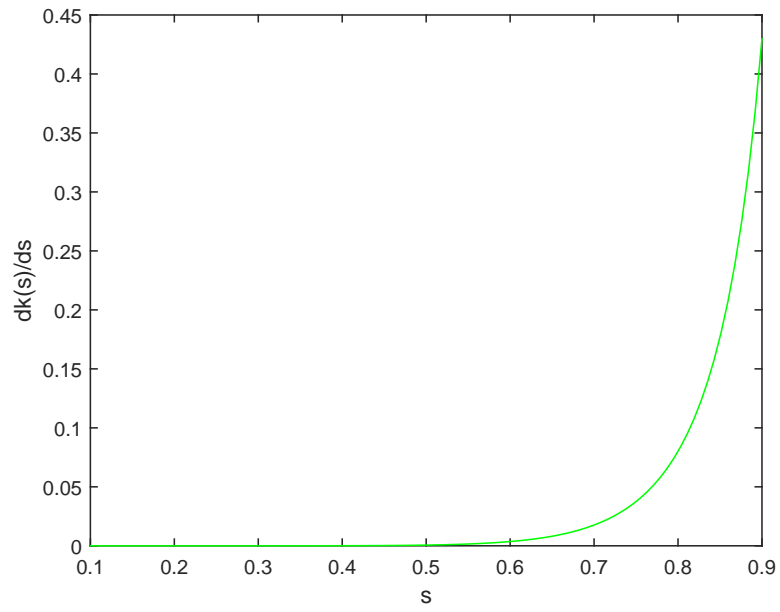
Figure 5.2: The first derivative of the function $K(S)$ with $m = 0.2$ and $0.1 \leq S \leq 0.9$.
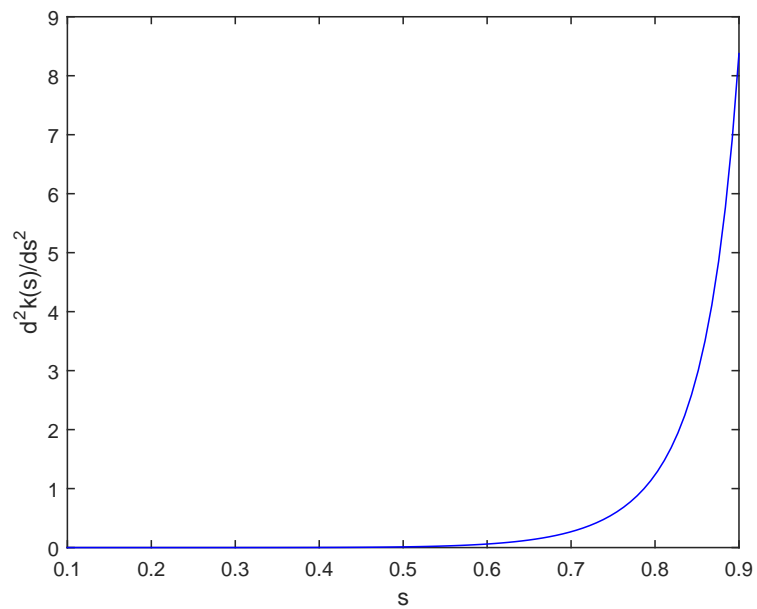
Figure 5.3: The second derivative of the function $K(S)$ with $m = 0.2$ and $0.1 \leq S \leq 0.9$.

As shown in Figures 5.1, 5.2 and 5.3, we can see that $K(S)$ and its first and second derivatives are all positive functions, with both first and second derivatives vanishing at $S = 0$ but becoming infinite as S tends to 1.

5.5 Solving the Unsaturated Region Model Using Travelling Wave Solutions

We now investigate the existence of a travelling wave solution of our model (4.5) when we neglect the last term ($\eta \ll 1$) :

$$\phi \frac{\partial S}{\partial t} = \frac{\partial}{\partial z} \left(\delta D(S) \frac{\partial S}{\partial z} + K(S) \right). \tag{5.13}$$

A travelling wave solution of our model (5.13) is a solution of the form :

$$S(z, t) = S(\psi), \quad \text{where} \quad \psi = z - ct, \tag{5.14}$$

where c is the wave velocity. From (5.14), (5.13) becomes :

$$\frac{d}{d\psi} \left(\delta D(S) \frac{dS}{d\psi} + K(S) \right) + c\phi \frac{dS}{d\psi} = 0. \tag{5.15}$$

By integrating both sides of (5.15) we get

$$\delta D(S) \frac{dS}{d\psi} + K(S) + c\phi S = A, \tag{5.16}$$

where A is a constant of integration. From (5.16) we have

$$\frac{dS}{d\psi} = \frac{A - K(S) - c\phi S}{\delta D(S)} \tag{5.17}$$

so

$$\frac{d\psi}{dS} = \frac{\delta D(S)}{A - (K(S) + c\phi S)}. \tag{5.18}$$

Since $0 < S < 1$, integrating (5.18) again gives

$$\psi = \psi_0 + \int_{S_0}^{S} \frac{\delta D(S)}{A - (K(S) + c\phi S)} \, dS, \quad 0 < S_0 < 1. \tag{5.19}$$

Here S_0 is the value of S at $\psi = \psi_0$. Now we seek travelling wave solutions of different forms for our model (5.13) for different values of the expanded-clay soil constant m.

5.6 Different Travelling Waves : m is fixed $(0 < m < 1)$

We will go through all possible cases and see which work and which do not. If they work then we want to know how they reach the limiting S_+ and S_- where $\lim_{\psi \to \infty} S = S_+$ and $\lim_{\psi \to -\infty} S = S_-$. We look for different travelling waves for different S_+ and S_-. Here we have cases as follows :

Case 1 : $\quad 0 < S_- < S_+ = 1$

We wish to check if a travelling wave in this case has $S = S_+$ at a finite value of ψ. In equation (5.17), we need $\frac{dS}{d\psi} > 0$ for $0 < S_- < S < S_+ = 1$. We also need $A = K(S_-) + c\phi S_-$ and then

$$A > K(S) + c\phi S \qquad \text{for} \qquad S_- < S < 1. \qquad (5.20)$$

This means we need $K(S) + c\phi S$ to be decreasing at S_-. But $K(S)$ is increasing, so c must be negative $(c < 0)$.

Indeed, we need $K'(S_-) + c\phi \leq 0$, i.e. $c \leq -\frac{K'(S_-)}{\phi}$. It follows from (5.20), for this case, that we have two possible cases for A. In both cases, $A < 0$ as we have :

$$K'(S_-) + c\phi \leq 0 \quad \text{with} \quad K > 0, K' > 0 \quad \text{and} \quad K'' > 0,$$

(see Figures 5.1, 5.2 and 5.3).

$$
\begin{aligned}
A &= K(S_-) + c\phi S_-, \\
&= S_- \left(\frac{K(S_-)}{S_-} + c\phi \right), \\
&< S_- (K'(S_-) + c\phi) \leq 0.
\end{aligned}
$$

This follows as from Taylor's theorem we find :

$$K(0) = 0 = K(S_-) - S_- K'(S_-) + \frac{1}{2} K''(\bar{S}) S_-^2 > K(S_-) - S_- K'(S_-),$$

$$\Rightarrow \frac{K(S_-)}{S_-} < K'(S_-),$$

where $\bar{S}$ is some value in the range $0 \leq \bar{S} \leq S$.

Case 1(i) : $\quad 1 + c\phi < A < 0$
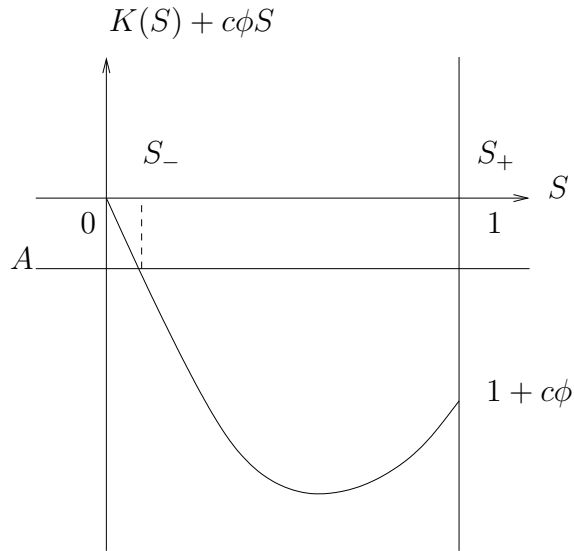
Figure 5.4: $K(S) + c\phi S$ for Case 1(i) : $1 + c\phi < A < 0$, where $c < -\frac{1}{\phi} \left(\frac{1 - K(S_-)}{1 - S_-} \right) < 0$, $A = K(S_-) + c\phi S_-$ and $K(S) + c\phi S < A$ for $S_- < S \leq S_+ = 1$.
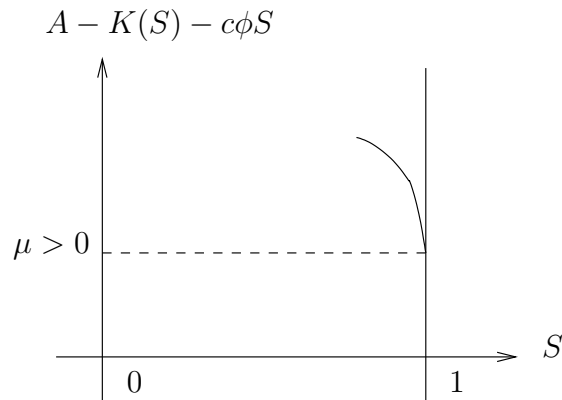
Figure 5.5: $A - K(S) - c\phi S > 0$ in $[S_-, 1]$ when $A > 1 + c\phi$.

When $S \to 1^-$ we can approximate $A - K(S) - c\phi S$ by $A - 1 - c\phi = \mu > 0$ (see Figures 5.4 and 5.5). In particular, $A - K(S) - c\phi S \geq \mu > 0$ as $S \to 1^-$.

By assumption for this case,

$$1 + c\phi < A = K(S_-) + c\phi S_-$$

so

$$\phi c(1 - S_-) < K(S_-) - 1 \qquad (< 0 \quad \text{because} \quad K(S_-) < 1),$$

and hence

$$c < \frac{K(S_-) - 1}{\phi(1 - S_-)} = \frac{-1}{\phi} \left(\frac{1 - K(S_-)}{1 - S_-} \right). \tag{5.21}$$

Here :

$$\frac{1 - K(S_-)}{1 - S_-} = \begin{cases} = 1 & \text{for} \quad S_- = 0 \\ > 1 & \text{for} \quad 0 < S_- < 1 \\ \to \infty & \text{for} \quad S_- \to 1^- \end{cases} \tag{5.22}$$

(see Figure 5.26).

The travelling wave solution is given by

$$\psi = \psi_0 + \delta \int_{S_0}^{S} \frac{D(S)}{A - K(S) - c\phi S} \, \mathrm{d}S, \qquad S_0 \le S < 1, \tag{5.23}$$

where $\psi_0 = \psi(S_0)$, $S_- < S_0 < S_+$. We know that the quantity $\frac{D(S)}{A - K(S) - c\phi S}$ is positive for $S_0 \le S \le 1$.
When $S \to 1^-$, $\sigma = \frac{(1-S)}{m} \to 0^+$ with $0 < m < 1$, so that $D(S)$ and $K(S)$ are approximated by :

$$D(S) \sim D(1 - m\sigma) \sim \sigma^{-m} \sim \left(\frac{1 - S}{m} \right)^{-m} \quad \text{for} \quad S = 1 - m\sigma \to 1^-, \tag{5.24}$$

$$K(S) \sim 1. \tag{5.25}$$

Using $A - K(S) - c\phi S = \mu = A - 1 - c\phi$ when $S \to 1^-$, we have the following :

$$\frac{D(S)}{A - K(S) - c\phi S} \sim \frac{m^m}{\mu} (1 - S)^{-m} \quad \text{for} \quad S \to 1. \tag{5.26}$$

Then the integral $\int_{S_0}^{1} \frac{D(S)}{A - K(S) - c\phi S} \, dS < \infty$, i.e. the integrand is integrable. Then we have a ψ_1 as the value of ψ at which S reaches 1 and we have a travelling wave as sketched in Figure 5.6.
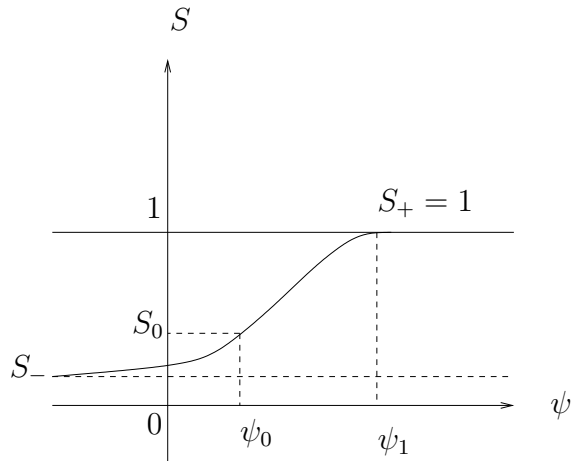
Figure 5.6: The travelling wave solution for $0 < S_- < S_+ = 1$ with $1 + c\phi < K(S_-) + c\phi S_-$ (Case 1(i)).

Then

$$\psi_1 = \psi_0 + \delta \int_{S_0}^{1} \frac{D(S)}{A - K(S) - c\phi S} \, dS. \tag{5.27}$$

Now we subtract ψ from ψ_1 ((5.23) from (5.27)) to get :

$$\psi_1 - \psi = \delta \int_{S_0}^{1} \frac{D(S)}{A - K(S) - c\phi S} \, dS - \delta \int_{S_0}^{S} \frac{D(S)}{A - K(S) - c\phi S} \, dS$$

$$= \delta \int_{S}^{1} \frac{D(S)}{A - K(S) - c\phi S} \, dS. \tag{5.28}$$

From (5.26) and (5.28), we have :

$$\psi_1 - \psi \sim \frac{\delta m^m}{\mu} \int_{S}^{1} (1 - S)^{-m} \, dS$$

$$\sim \frac{\delta m^m}{\mu(1 - m)} (1 - S)^{(1-m)}, \quad \text{for} \quad S \to S_+ = 1. \tag{5.29}$$

In this case, we have a local solution (5.29) with A given by $A = K(S) + c\phi S$ for $S = S_-$ and for given c satisfying (5.21).

Case 1(ii) : $\quad 0 > A = K(S_-) + c\phi S_- = 1 + c\phi$
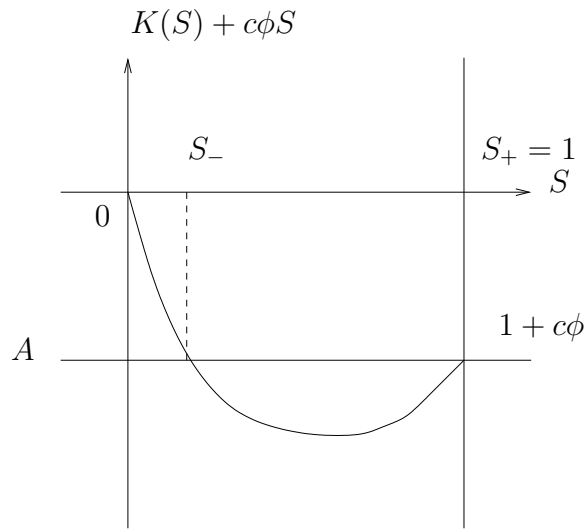
Figure 5.7: $K(S) + c\phi S$ for Case 1(ii) : $0 > A = 1 + c\phi$, $c = -\frac{1}{\phi}\left(\frac{1-K(S_-)}{1-S_-}\right) < 0$, $A = K(S) + c\phi S$ for $S = S_-$ and $A > K(S) + c\phi S$ for $S_- < S < S_+ = 1$.

Here we have from the value of A.

$$A - K(S) - c\phi S = 1 + c\phi - K(S) - c\phi S = 1 - K(S) + c\phi(1 - S).$$

$$A - K(S) - c\phi S$$

$$\mu = 0$$
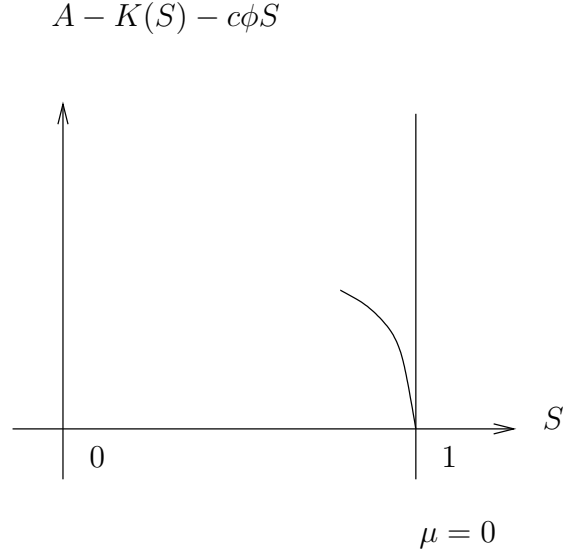
Figure 5.8: $A - K(S) - c\phi S$, showing that $\mu = A - 1 - c\phi = 0$ when $A = 1 + c\phi$.

We had earlier :

$$K(S) \sim 1 - 2\sigma^m \sim 1 - 2\left(\frac{1-S}{m}\right)^m \quad \text{for} \quad \sigma = \left(\frac{1-S}{m}\right) \to 0.$$

Then we have :

$$A - K(S) - c\phi S \quad \sim \quad 2\left(\frac{1-S}{m}\right)^m + c\phi(1-S)$$

$$\sim \quad 2\left(\frac{1-S}{m}\right)^m \quad \text{for} \quad S \to 1^-, \quad \text{since} \quad m < 1. \quad (5.30)$$

The wave velocity c will be given as follows :

$$K(S_-) + c\phi S_- = 1 + c\phi,$$

$$c = \frac{K(S_-) - 1}{\phi(1 - S_-)} = \frac{-1}{\phi}\left(\frac{1 - K(S_-)}{1 - S_-}\right), \quad (5.31)$$

where $\frac{1-K(S_-)}{1-S_-}$ satisfies the properties in (5.22). Then,

$$\frac{\delta D(S)}{A - K(S) - c\phi S} \sim \frac{\delta m^{(2m)}}{2}(1-S)^{-2m} \qquad \text{for} \qquad S \to 1. \quad (5.32)$$

For this integrand $\frac{\delta D(S)}{A - K(S) - c\phi S}$, there are two cases :

Case 1(ii)* : This case does the same as Case 1(i) and the integrand here is integrable at $S = 1$ and we have ψ_1 as in equation (5.27). We get this behaviour if $0 < 2m < 1$, i.e. $0 < m < \frac{1}{2}$ (see Figure 5.9).
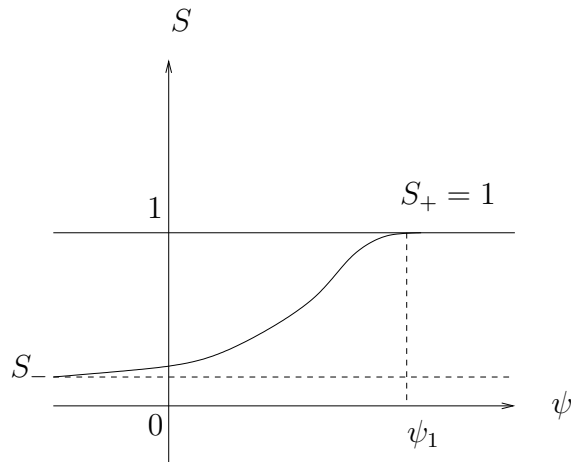
Figure 5.9: Case 1(ii)* : The travelling wave solution for $S_- < S_+ = 1$ and $1 + c\phi = K(S_-) + c\phi S$ if $0 < m < \frac{1}{2}$.

From (5.28), we have

$$\psi_1 - \psi \; = \; \delta \int_S^1 \frac{D(S)}{A - K(S) - c\phi S} \, \mathrm{d}S$$

$$\sim \; \frac{\delta}{2} \int_S^1 \left(\frac{1 - S}{m} \right)^{-2m} \mathrm{d}S$$

$$\sim \; \frac{\delta m^{(2m)}}{2(-2m + 1)} (1 - S)^{-2m+1} \quad \text{for} \quad S \to 1^-. \tag{5.33}$$

Case 1(ii)** : In this case, the integrand is not integrable at $S = 1$ and applies for $1 \le 2m < 2$, i.e. $\frac{1}{2} \le m < 1$ and then ψ_1 does not exist. Therefore, S does not reach 1 for finite ψ in this case (see Figure 5.10).
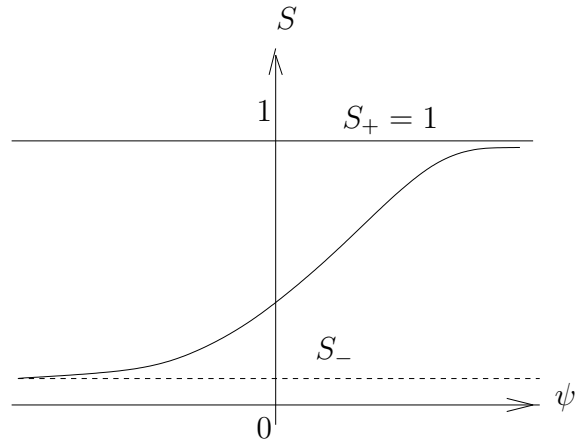
Figure 5.10: Case 1(ii)** : The behaviour of travelling wave solution for $\frac{1}{2} \leq m < 1$ where ψ_1 does not exist.

To explain this, from (5.18) and (5.32) we can see that for S close to 1 :

$$\frac{d\psi}{dS} \sim \frac{\delta m^{(2m)}}{2} (1 - S)^{-2m} .$$

By integrating both sides, we get, taking, for simplicity, $m > \frac{1}{2}$,

$$\psi \sim \frac{\delta m^{(2m)}}{2(2m - 1)} (1 - S)^{-(2m-1)} \qquad \text{for} \qquad S \to 1^{-},$$

$$\left(\frac{2(2m - 1)}{\delta m^{(2m)}} \right) \psi^{\frac{-1}{2m-1}} \sim 1 - S,$$

$$\text{so} \quad S \sim 1 - \left(\frac{2(2m - 1)}{\delta m^{(2m)}} \right) \psi^{\frac{-1}{2m-1}} \qquad \text{as} \qquad \psi \to \infty. \tag{5.34}$$

Case 2 : $0 = S_{-} < S_{+} = 1$

In this case, we look for a travelling wave between fully saturated and fully dry regions. Here $A = 0$ because :

$$\frac{dS}{d\psi} = \frac{A - K(S) - c\phi S}{\delta D(S)} \to 0 \quad \text{as} \quad S \to S_{-} = 0,$$

so that $A = K(0) = 0$ whether S_{-} is reached 0 as $\psi \to -\infty$ or at some finite value of ψ (see Figure 5.11). Note again that $\frac{dS}{d\psi} > 0$ so $A - K(S) - c\phi S > 0$ for $0 < S < 1$.
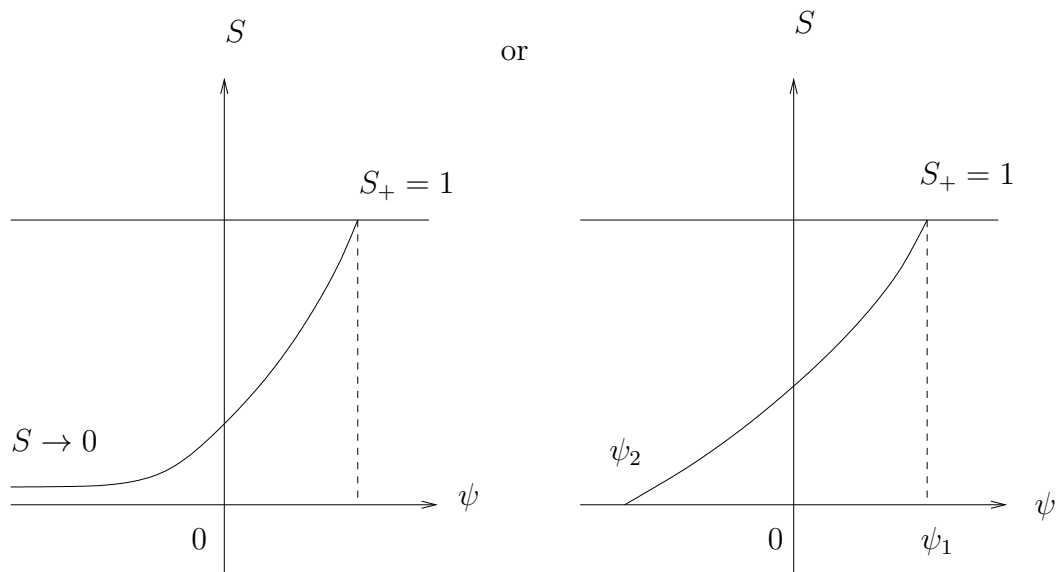
Figure 5.11: The travelling wave solution between fully saturated and fully dry regions where $0 = S_- < S < S_+ = 1$. If $S = S_- = 0$, the limiting value is either reached at finite ψ ($\psi \to \psi_2$) on right or as $\psi \to -\infty$ on left. $c < 0$ in both cases.

We again want to get the local behaviour of solution near $S_+ = 1$. In this case, we have two cases of $K(S) + c\phi S$ as shown in Figure 5.12.
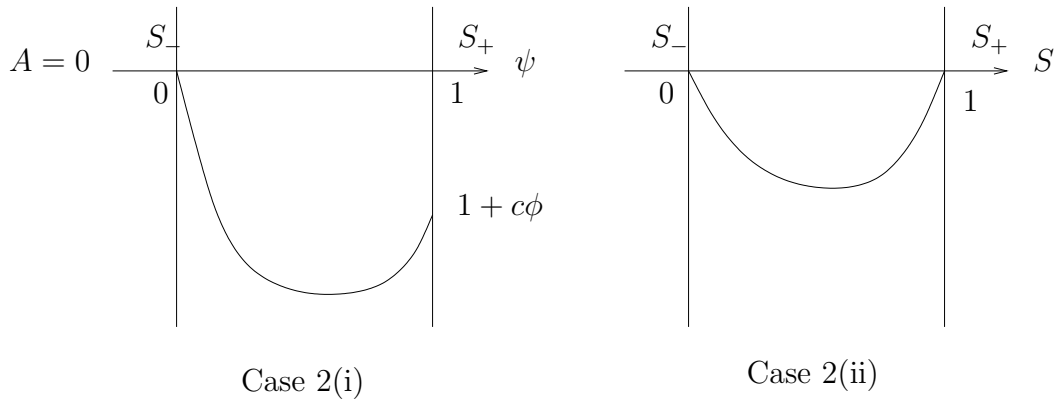
Figure 5.12: $K(S) + c\phi S$ for Case 2, $0 = S_- < S_+ = 1$. Case 2(i), $1 + c\phi < A = 0$, and Case 2(ii), $1 + c\phi = A = 0$.

Case 2(i) :

We need to check if the integrand $\frac{\delta D(S)}{-K(S) - c\phi S}$ is integrable. We also want to check the value of c.

$$0 = A > 1 + c\phi \quad \Rightarrow \quad c\phi < -1 \quad \Rightarrow \quad c < -\frac{1}{\phi}. \tag{5.35}$$

Then, from (5.35), $-K(S) - c\phi S$ is as sketched in Figure 5.13.
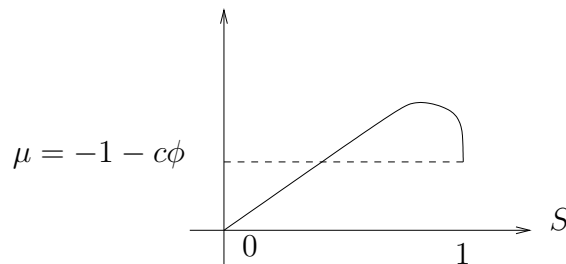
Figure 5.13: The graph of $-K(S) - c\phi S$. Here $\mu = -1 - c\phi$.

As can be seen from Figure 5.13,

$$\text{at} \quad S = 1, \quad -K(S) - c\phi S = -1 - c\phi \quad \Rightarrow \quad \mu = -1 - c\phi > 0.$$

Following Case 1(i), $\frac{D(S)}{A - K(S) - c\phi S} = \frac{D(S)}{-K(S) - c\phi S} \sim \frac{-m^m}{1 + c\phi} (1 - S)^{-m}$ is integrable at $S = 1$,

so that S reaches 1 at finite value ψ_1 and we can write :

$$\psi_1 - \psi = \delta \int_S^1 \frac{D(S)}{-K(S) - c\phi S} \, dS, \tag{5.36}$$

and

$$\psi_1 - \psi \ \sim \ \delta \int_S^1 \frac{\left(\frac{1-S}{m}\right)^{-m}}{-1 - c\phi} \, dS$$

$$\sim \ \frac{-\delta m^m}{(1 + c\phi)} \int_S^1 (1 - S)^{-m} \, dS$$

$$\sim \ \frac{-\delta m^m}{(1 + c\phi)(1 - m)} (1 - S)^{-m+1} \Big|_S^1$$

$$\sim \ \frac{\delta m^m}{(1 - m)(1 + c\phi)} (1 - S)^{1-m} . \tag{5.37}$$

Equation (5.37) gives the local behaviour of the travelling wave solution with ψ near ψ_1 (S near 1).

Now when $S \to 0^+$ and $0 < m < 1$, we have the approximations of $D(S)$ and $K(S)$ given in (5.1) and (5.2). The integrand $\frac{D(S)}{-K(S) - c\phi S}$ depends on c with $c \neq 0$. Then

$$\frac{D(S)}{-K(S) - c\phi S} \sim \frac{m^2 S^{\left(\frac{1}{m} + \frac{1}{2}\right)}}{-m^2 S^{\left(\frac{2}{m} + \frac{1}{2}\right)} - c\phi S} \sim \frac{m^2}{-c\phi} S^{\left(\frac{1}{m} + \frac{1}{2}\right) - 1} \sim \frac{m^2}{-c\phi} S^{\left(\frac{1}{m} - \frac{1}{2}\right)}$$

is integrable. We have ψ is given by :

$$\psi = \psi_1 - \delta \int_S^1 \frac{D(S)}{K(S) + c\phi S} \, dS, \tag{5.38}$$

and ψ_2 is given by :

$$\psi_2 = \psi_1 - \delta \int_0^1 \frac{D(S)}{K(S) + c\phi S} \, dS. \tag{5.39}$$

By subtracting (5.38) from (5.39), we get the local behaviour for ψ when S near 0 as follows :

$$\psi_2 - \psi \ = \ \delta \int_0^S \frac{-D(S)}{K(S) + c\phi S} \, dS$$

$$\sim \ \frac{-\delta m^2}{c\phi} \int_0^S S^{\left(\frac{1}{m} - \frac{1}{2}\right)} \, dS$$

$$\sim \ \frac{-2\delta m^3}{c\phi \, (2 + m)} S^{\left(\frac{1}{m} + \frac{1}{2}\right)} . \tag{5.40}$$

Case 2(ii) :

First note that $c = -\frac{1}{\phi} \neq 0$ and then, following Case 2(i), ψ falls to $S_- = 0$ at a finite value ψ_2 and has local behaviour as (5.40) :

$$\psi \sim \psi_2 - \frac{2\delta m^3}{c\phi(2+m)} S^{\left(\frac{1}{m}+\frac{1}{2}\right)}.$$

For this second case, we have the following two sub-cases according to whether $m < \frac{1}{2}$ or $m \geq \frac{1}{2}$.

Case 2(ii)* : For $m < \frac{1}{2}$, as with Case 1(ii)*, the integral is bounded at 1 so that $S_+ = 1$ is reached at a finite value ψ_1, see Figure 5.14.
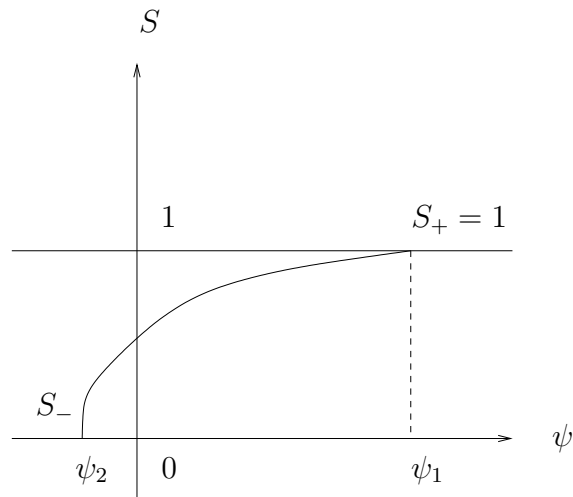
Figure 5.14: The travelling wave solution for Case 2(ii)*, $S_- = 0$, $S_+ = 1$, $A = 1 + c\phi = 0$, $c = -\frac{1}{\phi}$ and $m < \frac{1}{2}$.

Case 2(ii)** : In this case, the integrand is not integrable at $S = 1$ if $m \geq \frac{1}{2}$, therefore, ψ_1 does not exist (see Figure 5.15). This case is exactly as Case 1(ii)** in the previous part.
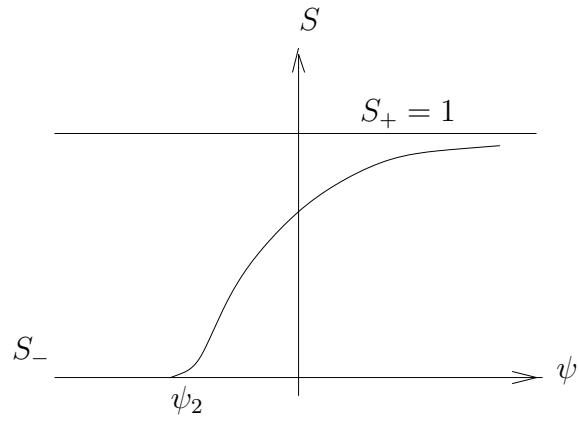
Figure 5.15: The travelling wave solution for Case 2(ii)** when $S_- = 0$, $S_+ = 1$ and $m \geq \frac{1}{2}$ and in this case ψ_1 does not exist.

Case 3 : $0 = S_- < S_+ < 1$
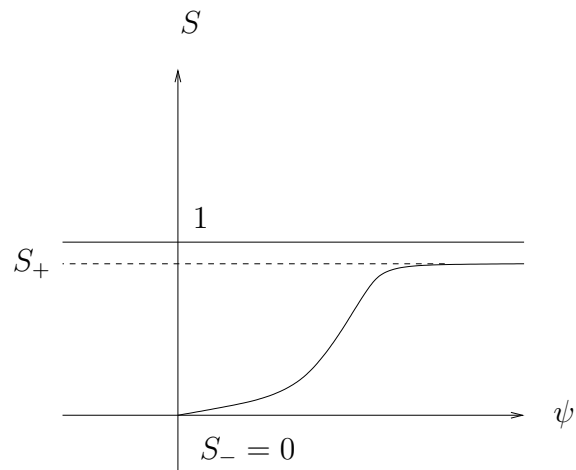
Figure 5.16: The travelling wave for Case 3, when $0 = S_- < S_+ < 1$.

For this case, based on Figure 5.16, one thing of particular interest is the local behaviour of the travelling wave solution near $S_- = 0$. The approximations of the functions $D(S)$ and $K(S)$ are given by equations (5.1) and (5.2).

In this case, $A = \lim_{S \to 0} K(S) + c\phi S = 0$ (as Case 2). Also, we have $\frac{dS}{d\psi} \to 0$ as $S \to S_+ < 1$ and note again that $\frac{dS}{d\psi} > 0$ so $A - K(S) - c\phi S > 0$ for $0 < S < S_+$ (see Figure 5.17).

The wave velocity c can be obtained from the following formula :

$$K(S_+) + c\phi S_+ = K(S_-) + c\phi S_-,$$

$$c = -\frac{1}{\phi}\left(\frac{K(S_+) - K(S_-)}{S_+ - S_-}\right), \qquad (5.41)$$

so

$$
\begin{aligned}
c &= -\frac{1}{\phi}\left(\frac{K(S_+) - 0}{S_+ - 0}\right) \\
&= \frac{-K(S_+)}{\phi S_+}. \qquad (5.42)
\end{aligned}
$$
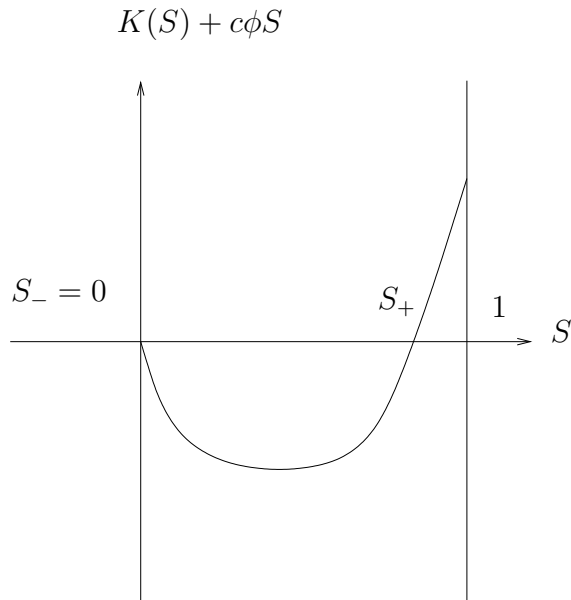
$$K(S) + c\phi S$$

Figure 5.17: Graph of $K(S) + c\phi S$, $A = 0$ and $0 = S_- < S_+ < 1$.

Following Case 2, we have integrability near $S = 0$ because $c \neq 0$ so that the travelling wave solution is given by :

$$\psi = \psi_2 + \delta \int_0^S \frac{D(S)}{A - K(S) - c\phi S} \, dS = \psi_2 - \delta \int_0^S \frac{D(S)}{K(S) + c\phi S} \, dS, \qquad (5.43)$$

where ψ_2 is the value of ψ when $S = 0$.

From equations (5.1), (5.2) and (5.43), we have

$$\psi \;\sim\; \psi_2 + \delta \int_0^S \frac{m^2 S^{\left(\frac{1}{m}+\frac{1}{2}\right)}}{-m^2 S^{\left(\frac{2}{m}+\frac{1}{2}\right)} - c\phi S}\, dS$$

$$\sim\; \psi_2 - \frac{\delta m^2}{c\phi} \int_0^S S^{\left(\frac{1}{m}-\frac{1}{2}\right)}\, dS$$

$$\sim\; \psi_2 - \frac{\delta m^2}{c\phi \left(\frac{1}{m}+\frac{1}{2}\right)}\, S^{\left(\frac{1}{m}+\frac{1}{2}\right)} \Big|_0^S$$

$$\sim\; \psi_2 - \frac{\delta m^2}{c\phi \left(\frac{1}{m}+\frac{1}{2}\right)} S^{\left(\frac{1}{m}+\frac{1}{2}\right)}, \quad \text{for} \quad S \to 0, \quad 0 < m < 1, \quad c \neq 0. \quad (5.44)$$

Equation (5.44) gives the form of the travelling wave solution for S small.

Case 4 : $\quad 0 < S_- < S_+ < 1$
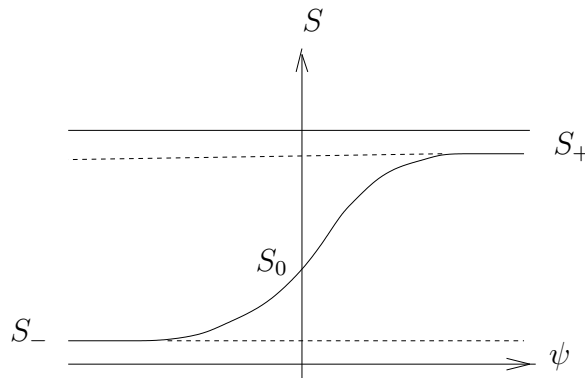
Figure 5.18: The travelling wave when $0 < S_- < S_+ < 1$, where $S_- < S_0 < S_+$.

Here from Figure 5.18, we must have $\lim_{\psi \to -\infty} S(\psi) = S_-$ and $\lim_{\psi \to +\infty} S(\psi) = S_+$. Hence, from equation (5.17), $A - K(S) - c\phi S$ must be 0 when $S = S_-$ and $S = S_+$.

Then

$$A = K(S_-) + c\phi S_- = K(S_+) + c\phi S_+. \quad (5.45)$$

The wave velocity c is then easily obtained from (5.45) to be

$$c = -\frac{1}{\phi}\left(\frac{K(S_+) - K(S_-)}{S_+ - S_-}\right) < 0. \quad (5.46)$$

Based on that, the travelling wave will be moving left (see Figure 5.18).

Now $\frac{d^2}{dS^2}\left(K(S) + c\phi S\right) = \frac{d^2 K}{dS^2} > 0$ so to have $K(S) + c\phi S = A$ at $S = S_-$ and $S = S_+$ we automatically get $\frac{d}{dS}\left(K(S) + c\phi S\right) < 0$ at $S = S_-$ and likewise $\frac{d}{dS}\left(K(S) + c\phi S\right) > 0$ at $S = S_+$. Indeed,

$$K(S) + c\phi S - A \quad < \quad K(S_-) + c\phi S_- - A$$

$$= \quad K(S_+) + c\phi S_+ - A = 0,$$

for $S_- < A < S_+$ (see Figure 5.19), which is what we need to get $\frac{dS}{d\psi} = \frac{A - K(S) - c\phi S}{D(S)} > 0$. We then have the travelling wave is given by :

$$\psi = \psi_0 + \delta \int_{S_0}^{S} \frac{D(S)}{A - K(S) - c\phi S}\, dS, \quad 0 < S_- < S < S_+ < 1. \tag{5.47}$$
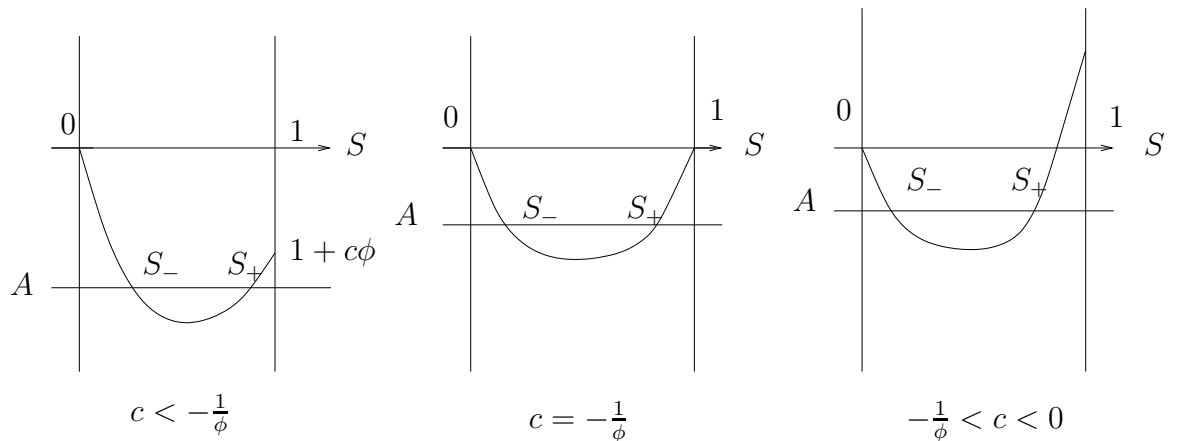
Figure 5.19: Three plots of $K(S) + c\phi S$ with $A = K(S_-) + c\phi S_- = K(S_+) + c\phi S_+ < 1 + c\phi$, where $c < -\frac{1}{\phi}$ in the first graph (left), in the second (middle) $c = -\frac{1}{\phi}$ and $-\frac{1}{\phi} < c < 0$ in the last one (right).

Case 5 : $0 = S_+ < S_- = 1$
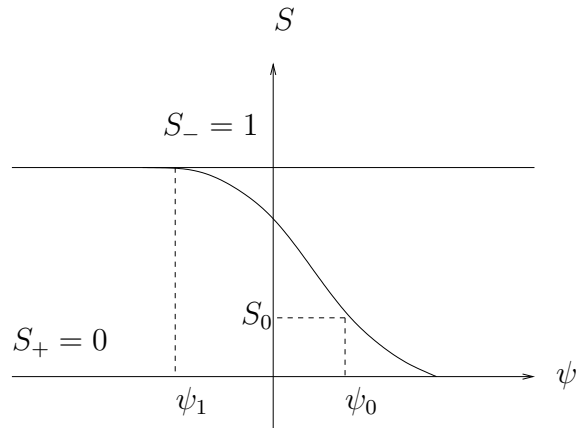
Figure 5.20: A graph of a travelling wave when $0 = S_+ < S_- = 1$.

From equation (5.16) and Figure 5.20, we have :

$$\delta D(S)\frac{dS}{d\psi} = A - K(S) - c\phi S = 0 \quad \text{for} \quad S = S_+ = 0.$$

Therefore,

$$A = 0 = K(S_+) + c\phi S_+.$$

Also,

$$\frac{dS}{d\psi} = -\left(\frac{K(S) + c\phi S}{\delta D(S)}\right) < 0 \quad \text{for} \quad 0 < S < 1$$

so

$$K(S) + c\phi S > 0 \quad \text{for} \quad 0 < S < 1.$$

Then the velocity of the wave c should be non-negative since $\frac{dK}{dS}(0) = 0$, and we have the two cases of $K(S) + c\phi S$ shown in Figure 5.21.
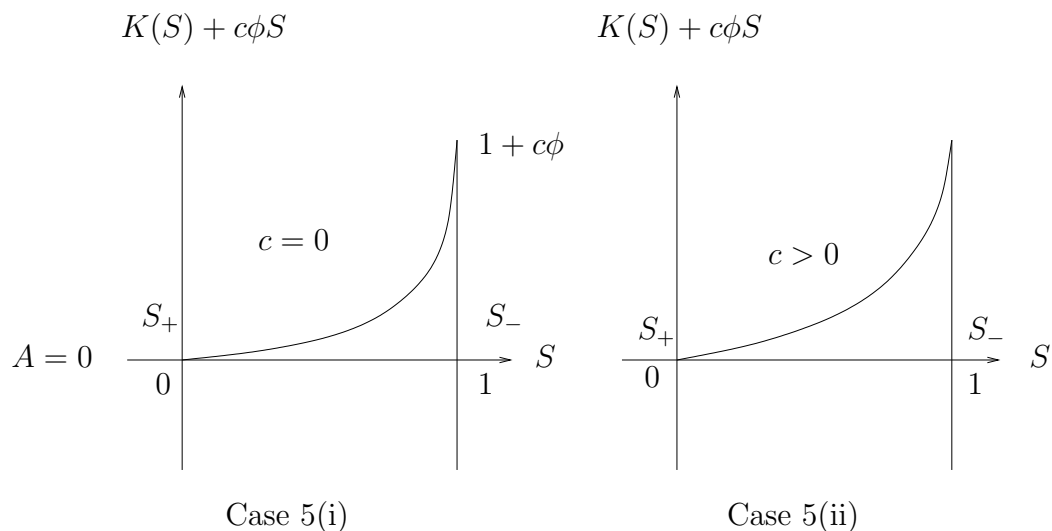
Figure 5.21: The graph of $K(S) + c\phi S$ when the velocity of the wave c is non-negative, $c = 0$ in Case 5(i) and $c > 0$ in Case 5(ii).

Case 5(i)
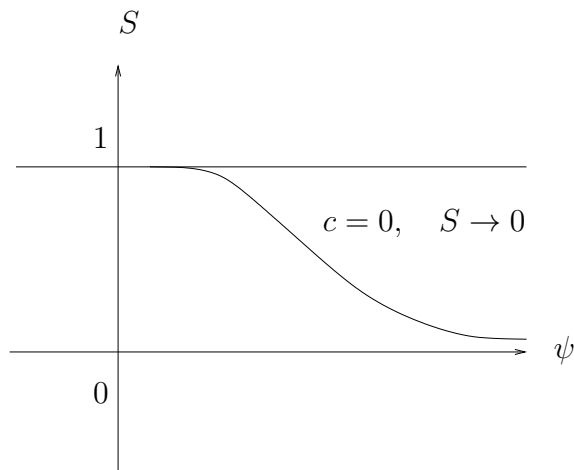
Figure 5.22: Case 5(i) shows the travelling wave behaviour when $c = 0$ and $S \to 0$.

We need to check if the integrand $\frac{-\delta D(S)}{K(S) + c\phi S}$ is integrable at $S = 1$ first and afterward at $S = 0$. For $c = 0$, we have :

$$K(S) + c\phi S = 1 \quad \text{at} \quad S = 1,$$

and

$$D(S) \sim D(1 - m\sigma) \sim \sigma^{-m}, \quad \sigma = \frac{1 - S}{m} \to 0 \quad \text{where} \quad 0 < m < 1.$$

Then

$$\frac{-\delta D(S)}{K(S) + c\phi S} \sim \frac{-\delta \left(\frac{1-S}{m}\right)^{-m}}{1} \sim -\delta m^m (1 - S)^{-m}$$

is integrable at $S = 1$. Therefore, S reaches 1 at finite ψ_1 given by equation (5.27). From (5.23) and (5.27), where $A = 0$, we subtract ψ from ψ_1 to get

$$\psi_1 - \psi = -\delta \int_S^1 \frac{D(S)}{K(S) + c\phi S} \, dS.$$

Then

$$\psi_1 - \psi \sim -\delta m^m \int_S^1 (1 - s)^{-m} \, dS$$

$$\sim \frac{-\delta m^m}{(1 - m)} (1 - S)^{1-m} \quad \text{for} \quad S \to 1. \tag{5.48}$$

Equation (5.48) gives the local behaviour of the travelling wave solution with ψ near ψ_1.

Now for $c = 0$ and $S \to 0$, the functions $D(S)$ and $K(S)$ are approximated by equations (5.1) and (5.2), then

$$\frac{\delta D(S)}{-K(S) - c\phi S} \sim \frac{\delta m^2 S^{\left(\frac{1}{m} + \frac{1}{2}\right)}}{-m^2 S^{\left(\frac{2}{m} + \frac{1}{2}\right)}} \sim -\delta S^{-\frac{1}{m}}$$

is not integrable at 0 when $m < 1$. Therefore, S does not reach 0 at a finite value of ψ.
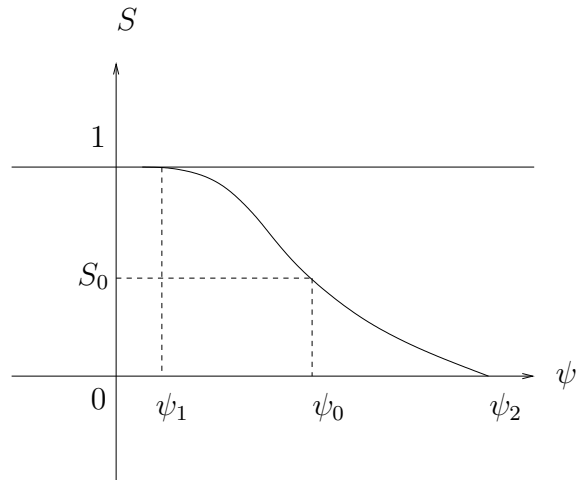
Case 5(ii)

Figure 5.23: Case 5(ii) represents the travelling wave when $c > 0$ and $-K(S) - c\phi S < 0$.

In this case (Figure 5.23) we have, $c > 0$ and $-K(S) - c\phi S < 0$. Then

$$\frac{\delta D(S)}{-K(S) - c\phi S} \sim \frac{\delta m^2 S^{\left(\frac{1}{m} + \frac{1}{2}\right)}}{-m^2 S^{\left(\frac{2}{m} + \frac{1}{2}\right)} - c\phi S} \sim \frac{\delta m^2}{-c\phi} S^{\left(\frac{1}{m} - \frac{1}{2}\right)} \quad \text{for} \quad S \to 0.$$

Hence, $\frac{dS}{d\psi} \sim \frac{\delta m^2}{-c\phi} S^{\left(\frac{1}{m} - \frac{1}{2}\right)}$ is integrable at 0, $S = 0$ at $\psi = \psi_2$. When S close to 0, ψ and ψ_2 are given respectively earlier by (5.38) and (5.39).
Then

$$\psi_2 - \psi \quad \sim \quad \frac{\delta m^2}{-c\phi} \int_0^S S^{\left(\frac{1}{m} - \frac{1}{2}\right)} \, dS$$

$$\sim \quad \frac{2\delta m^3}{-c\phi(2 + m)} S^{\left(\frac{1}{m} + \frac{1}{2}\right)}.$$

Now, when $S \to 1$,

$$\frac{\delta D(S)}{-K(S) - c\phi S} \sim \frac{\delta \left(\frac{1-S}{m}\right)^{-m}}{-1 - c\phi} \sim \frac{-\delta(1 - S)^{-m}}{(1 + c\phi)m^{-m}} \sim \frac{-\delta m^m}{1 + c\phi}(1 - S)^{-m}.$$

is integrable at $S = 1$. Hence,

$$\psi_1 - \psi \; \sim \; \frac{-\delta m^m}{1 + c\phi} \int_S^1 (1 - S)^{-m} \, dS$$

$$\sim \; \frac{-\delta m^m}{(1 + c\phi)(1 - m)} \left. (1 - S)^{1-m} \right|_S^1$$

$$\sim \; \frac{\delta m^m}{(1 + c\phi)(1 - m)} (1 - S)^{1-m},$$

gives the local behaviour of the travelling wave solution with ψ near ψ_1.

Case 6 : $0 < S_+ < S_- = 1$
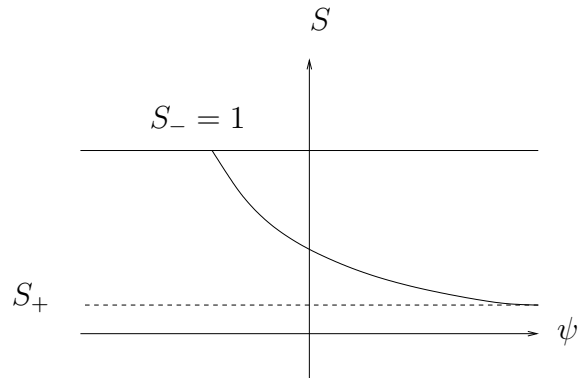
Figure 5.24: The travelling wave in Case 6 when $0 < S_+ < S_- = 1$.

We need to check that such a travelling wave solution exists with $S = S_- = 1$ at a finite value of ψ (see Figure 5.24). We again need

$$A = K(S_+) + c\phi S_+, \tag{5.49}$$

and

$$\frac{dS}{d\psi} = -\left(\frac{K(S) + c\phi S - A}{\delta D(S)}\right) < 0 \quad \text{for} \quad S_+ < S < 1 \tag{5.50}$$

so that

$$K(S) + c\phi S > A \quad \text{for} \quad S_+ < S < 1.$$

This means we need $K(S)+c\phi S$ increasing at S_+. Because K is an increasing function, as can be seen in Figure 5.25, c can now be positive or negative, as long as $\frac{dK}{dS}(S_+) + c\phi \geq 0$. $K(S) + c\phi S > 0$ is then guaranteed for $S > S_+$ since $\frac{d^2K}{dS^2} > 0$.
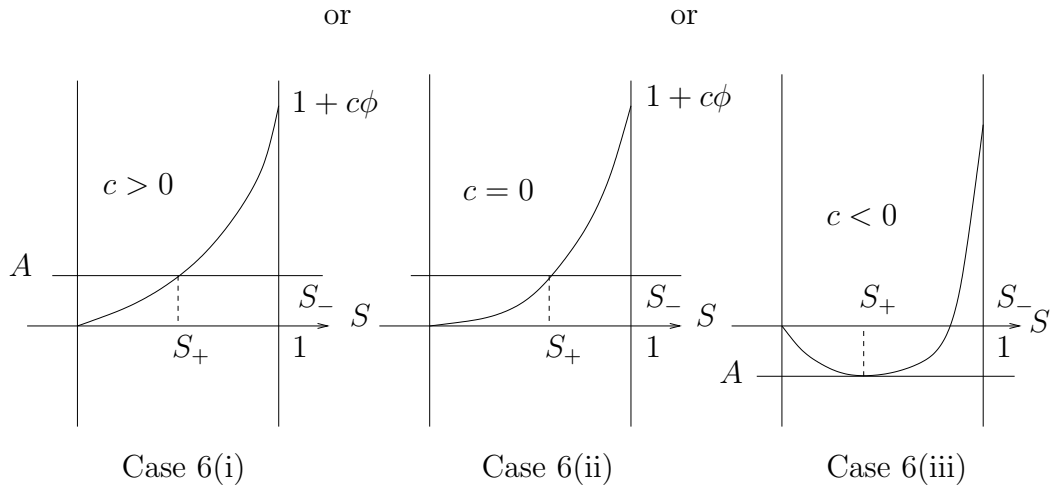
Figure 5.25: Three graphs of the function $K(S) + c\phi S$ with three possibilities of the velocity of the wave c respectively, Case 6(i) : when $c > 0$, Case 6(ii) : $c = 0$ and a very special Case 6(iii) : $c < 0$ (that shown is a most extreme case).

Figure 5.25 shows sketches of $K(S) + c\phi S$ compared with A for cases $c > 0$, $c = 0$ and $c < 0$. For the third case we need $K'(S_+) + c\phi \geq 0$ and the particular example shown is for the largest negative c so that the condition on c in this case is $c = \frac{-K'(S_+)}{\phi}$.

In all cases, the restriction on A is $A < 1 + c\phi$. Because of this, the calculations for getting the behaviour of the travelling wave solution are the same.

When $S \to 1^+$ we can approximate $K(S) + c\phi S - A$ by $1 + c\phi - A = \mu > 0$.

Therefore

$$K(S) + c\phi S - A > 0 \quad \text{for} \quad S_+ < S \leq 1,$$

$$K(S) + c\phi S > A,$$

$$1 + c\phi > K(S_+) + c\phi S_+,$$

$$\text{so} \quad c\phi(1 - S_+) > -(1 - K(S_+)) < 0 \quad \text{because} \quad K(S_+) < 1.$$

Then $c\phi > \frac{-(1-K(S_+))}{(1-S_+)}$ and we also have $c\phi \geq -K'(S_+)$.
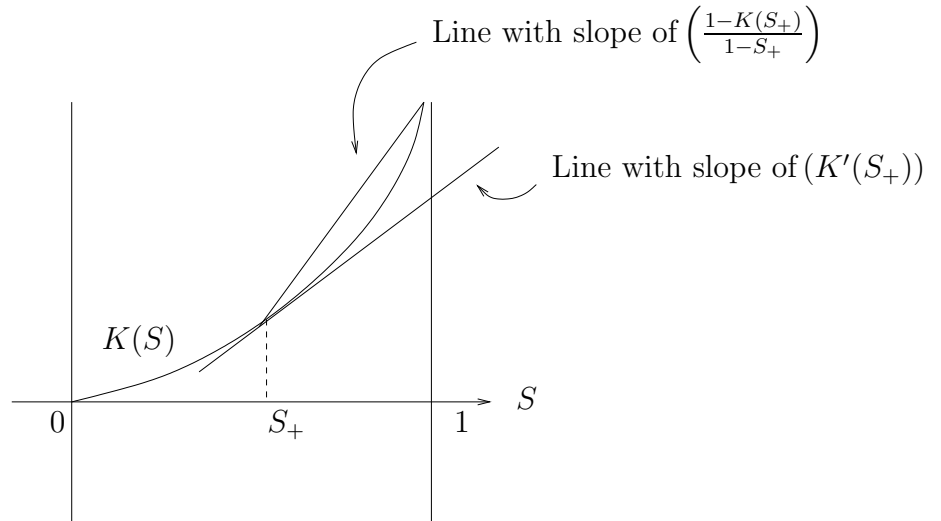
Figure 5.26: This graph shows us $K(S)$, and lines with slopes of interest : the tangent at S_+, and the line joining $(S_+, K(S_+))$ to $(1, K(1)) = (1, 1)$.

From the convexity of K (recall that $\frac{d^2 K}{dS^2} > 0$, see Figure 5.26), we see that $K'(S_+)$ is smaller than $\frac{1-K(S_+)}{1-S_+}$. That means the bound on c from $\frac{1-K(S_+)}{1-S_+}$ is guaranteed by the bound given by $K'(S_+)$.

The general behaviour of travelling wave solution when $S \to 1^+$ is given by

$$\psi = \psi_0 + \delta \int_{S_0}^{S} \frac{D(S)}{A - K(S) - c\phi S} \, \mathrm{d}S, \qquad S_0 \leq S < 1.$$

Here $\frac{D(S)}{A-K(S)-c\phi S}$ is positive for $S_0 \leq S < 1$ and $D(S) \sim D(1 - m\sigma) \sim \sigma^{-m}$ when $S \to 1^+$, $\sigma = \frac{1-S}{m} \to 0+$ and $0 < m < 1$.

$$\frac{D(S)}{A - K(S) - c\phi S} \sim \frac{\left(\frac{1-S}{m}\right)^{-m}}{A - 1 - c\phi} \sim \frac{m^m}{-\mu}(1 - S)^{-m} \quad \text{for} \quad S \to 1 \quad \text{with} \quad \mu > 0.$$

$$(5.51)$$

Then the integral $\int_{S_0}^{1} \frac{D(S)}{A-K(S)-c\phi S} \, \mathrm{d}S < \infty$. Then we have a ψ_1 as the value of ψ at which S reaches 1 (see Figure 5.27).
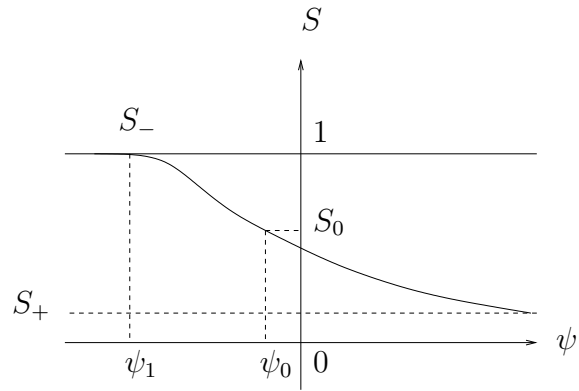
Figure 5.27: The travelling wave when $0 < S_+ < S_- = 1$, $\psi_0 = \psi(S_0)$ and $\psi_1 = \psi(S_-)$.

Then

$$\psi_1 = \psi_0 + \delta \int_{S_0}^{1} \frac{D(S)}{A - K(S) - c\phi S} \, dS,$$

$$\psi_1 - \psi = \delta \int_{S}^{1} \frac{D(S)}{A - K(S) - c\phi S} \, dS.$$

From (5.51) :

$$\psi_1 - \psi \quad \sim \quad \frac{\delta m^m}{-\mu} \int_{S}^{1} (1 - S)^{-m} \, dS$$

$$\sim \quad \frac{-\delta m^m}{\mu(1 - m)}(1 - S)^{(1-m)} \quad \text{for} \quad S \to S_- = 1.$$

Case 7 : $0 = S_+ < S_- < 1$
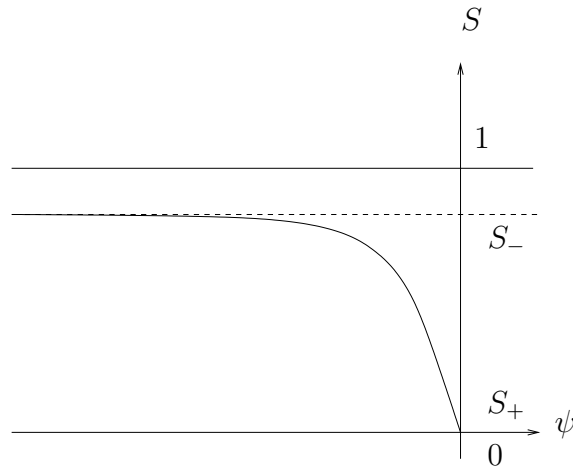
Figure 5.28: The possible travelling wave in Case 7 when $0 = S_+ < S_- < 1$.

In this case, $A = 0$ because $\frac{dS}{d\psi} \to 0$ as $\psi \to \infty$ (see Figure 5.28), and we need

$$\delta D(S)\frac{dS}{d\psi} = -\left(K(S) + c\phi S\right) < 0 \quad \text{for} \quad 0 < S < S_-. \tag{5.52}$$

For (5.52) to hold, $c \geq 0$, since $\frac{dK}{dS}(0) = 0$.
But then

$$K(S) + c\phi S > 0 \quad \text{for} \quad S > 0 \quad \text{since} \quad K(S) > 0 \quad \text{for} \quad S > 0.$$

However, for our travelling wave, we should have that S is constant at $S = S_-$ so that

$$\frac{dS}{d\psi} = 0 \quad \text{and} \quad K(S) + c\phi S = 0 \quad \text{at} \quad S = S_- > 0,$$

giving a contradiction. Consequently, there is no travelling wave solution in this case.

Case 8 : $0 < S_+ < S_- < 1$

Just like Case 7, this case fails to give a travelling wave for such S_- and S_+.

5.6.1   Conclusion

When m is fixed, travelling wave solutions exist for the following cases :

- Case 1 : $0 < S_- < S_+ = 1$, $S \to S_-$ as $\psi \to -\infty$, we have the following cases :
  Case 1(i), with $c < -\frac{1}{\phi}\left(\frac{1-K(S_-)}{1-S_-}\right)$, $S = 1$ at $\psi = \psi_1 < \infty$.
  Case 1(ii), with $c = -\frac{1}{\phi}\left(\frac{1-K(S_-)}{1-S_-}\right)$, we have then these subcases :
  Case 1(ii)*, $S = 1$ at $\psi = \psi_1 < \infty$ for $0 < m < \frac{1}{2}$.
  Case 1(ii)**, $S \to 1^-$ as $\psi \to \infty$ for $\frac{1}{2} \le m < 1$.

- Case 2 : $0 = S_- < S_+ = 1$, $S = 0$ at $\psi_2 > -\infty$, we have the two cases :
  Case 2(i), with $c < -\frac{1}{\phi}$, $S = 1$ at $\psi = \psi_1 < \infty$ (as Case 1(i)).
  Case 2(ii), with $c = -\frac{1}{\phi} \neq 0$, we have here the two subcases :
  Case 2(ii)*, $S = 1$ at $\psi = \psi_1 < \infty$ for $0 < m < \frac{1}{2}$.
  Case 2(ii)**, $S = 1^-$ as $\psi \to \infty$ for $\frac{1}{2} \le m < 1$.

- Case 3 : $0 = S_- < S_+ < 1$, $c < 0$, $S = 0$ at $\psi = \psi_2 < \infty$, and $S \to S_+$ as $\psi \to \infty$.

- Case 4 : $0 < S_- < S_+ < 1$, $c < 0$, $S \to S_-$ as $\psi \to -\infty$ and $S \to S_+$ as $\psi \to \infty$.

- Case 5 : $0 = S_+ < S_- = 1$ for which $c \ge 0$. For the two subcases :
  Case 5(i), $c = 0$, $S \to 0$ as $\psi \to \infty$.
  Case 5(ii), $c > 0$, $S = 0$ at $\psi = \psi_2 < \infty$.
  For both Cases 5(i) and 5(ii), we have $S = 1$ at $\psi = \psi_1 > -\infty$.

- Case 6 : $0 < S_+ < S_- = 1$, with $c \ge 0$ and $c < 0$, $S_- = 1$ at $\psi = \psi_1 > -\infty$. Also $S \to S_+$ as $\psi \to \infty$.

On the other hand, there were no travelling wave solutions for Case 7 : $0 = S_+ < S_- < 1$, with $c \ge 0$, $S = S_-$ and Case 8 : $0 < S_+ < S_- < 1$.
In the next section, we will look at the limiting cases, especially when $m \to 0^+$.

5.7   Different Travelling Waves : $m \to 0^+$

Case 1 : $0 < S_- < S_+ = 1$

We consider Case 1(i) and Case 1(ii)* together as they are so similar. Note that Case 1(ii)** does not apply because $m \ll 1$ so we always have $m < \frac{1}{2}$.
We have here three regimes for the travelling wave as shown by the graphs of Figure 5.29.
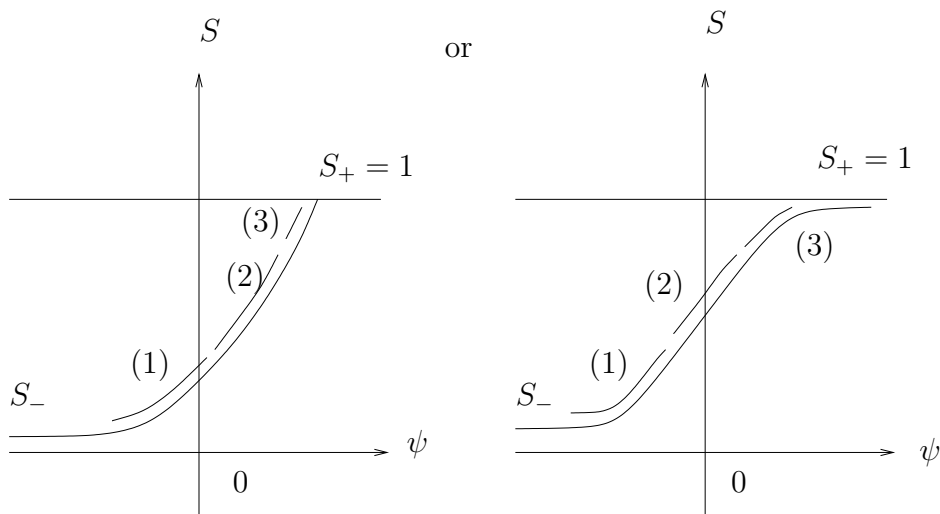
Figure 5.29: These graphs show the three regimes for the travelling wave when $m \to 0^+$: regime 1, where $1 - S$ is not small; regime 2, where $1 - S$ is of order m; and regime 3, where $1 - S$ is exponentially small in $\frac{1}{m}$.

In this case, we consider fixed S_-, in regime 1, and we have $1 + c\phi \leq A = K(S_-) + c\phi S_- < 0$ (see Figures 5.4 and 5.7). We also assume that A and c are of order 1. As before

$$c \leq -\frac{1}{\phi}\left(\frac{1 - K(S_-)}{1 - S_-}\right),$$

and

$$A = K(S_-) + c\phi S_-.$$

In regime 1, we have that $D(S)$ and $K(S)$ are given by (5.1) and (5.2).

Therefore

$$\frac{d\psi}{dS} \sim \frac{\delta m^2 S^{\left(\frac{1}{m}+\frac{1}{2}\right)}}{A - m^2 S^{\left(\frac{2}{m}+\frac{1}{2}\right)} - c\phi S}$$

$$\sim \frac{\delta m^2 S^{\left(\frac{1}{m}+\frac{1}{2}\right)}}{A - c\phi S} \quad \text{for} \quad S \quad \text{not close to} \quad \frac{A}{c\phi}. \tag{5.53}$$

Looking closer to $S = 1$, we now consider S just $O(m)$ away.
In this regime 2 : $S = 1 - m\sigma$, $m \to 0$, we have that $D(S)$ and $K(S)$ are approximated by (5.6) and (5.7). Then

$$\frac{d\psi}{d\sigma} = \frac{d\psi}{dS}\frac{dS}{d\sigma} = -m\frac{d\psi}{dS}$$

so

$$\frac{d\psi}{d\sigma} = \frac{-m\delta D(S)}{A - K(S) - c\phi S}$$

$$\sim \frac{-m^3 \delta e^\sigma \left(\ln\left(1 - e^{-\sigma}\right)\right)^2}{A - m^2 \left(\ln\left(1 - e^{-\sigma}\right)\right)^2 - c\phi}. \tag{5.54}$$

For $\sigma \to \infty$

$$\frac{d\psi}{d\sigma} = \frac{-m^3 \delta e^\sigma \left(\ln\left(1 - e^{-\sigma}\right)\right)^2}{A - c\phi}$$

$$\sim \frac{-\delta m^3 e^\sigma e^{-2\sigma}}{A - c\phi}$$

$$\sim \left(\frac{-\delta m^3}{A - c\phi}\right) e^{-\sigma}. \tag{5.55}$$

Then

$$\psi \sim \left(\frac{\delta m^3}{A - c\phi}\right) e^{-\sigma} + \text{Const.} \tag{5.56}$$

To match the solutions in regime 1 and 2, we have, from (5.53),

$$\frac{d\psi}{dS} \sim \frac{\delta m^2}{A - c\phi S} S^{\left(\frac{1}{m}+\frac{1}{2}\right)}.$$

But $S = 1 - m\sigma$, in regime 2, then

$$\frac{d\psi}{d\sigma} = -m\frac{d\psi}{dS}$$

so

$$\frac{d\psi}{d\sigma} \quad \sim \quad \frac{-\delta m^3}{A - c\phi\,(1 - m\sigma)}\,(1 - m\sigma)^{\left(\frac{1}{m} + \frac{1}{2}\right)}$$

$$\sim \quad \frac{-\delta m^3}{A - c\phi + c\phi m\sigma}\,e^{\left(\frac{1}{m} + \frac{1}{2}\right)\ln(1 - m\sigma)}$$

$$\sim \quad \frac{-\delta m^3}{A - c\phi}\,e^{-\sigma}. \tag{5.57}$$

Integrating (5.57), we get :

$$\psi \sim \frac{\delta m^3}{A - c\phi}\,e^{-\sigma} + \text{Const.}, \tag{5.58}$$

agreeing with (5.56). We saw that the approximations used in regime 2 failed for S exponentially close to 1 and we must now consider an even smaller zone, regime 3. In regime 3, we have $S = 1 - me^{-\alpha/m}$ and the functions $D(S)$ and $K(S)$ are approximated in Section 1.3 by (5.9) and (5.8). Then (5.18) becomes :

$$\frac{d\psi}{dS} \sim \frac{\delta e^\alpha\,(1 - e^{-\alpha})^2}{A - (1 - e^{-\alpha})^2 - c\phi}.$$

But

$$\frac{d\psi}{d\alpha} = \frac{d\psi}{dS}\frac{dS}{d\alpha} = e^{-\alpha/m}\frac{d\psi}{dS} \sim \frac{\delta e^{\alpha\left(1 - \frac{1}{m}\right)}\,(1 - e^{-\alpha})^2}{A - (1 - e^{-\alpha})^2 - c\phi}. \tag{5.59}$$

Now, we want to match both regimes 2 and 3 together.
When $\sigma \to 0$ in (5.54) :

$$\frac{d\psi}{d\sigma} \sim \frac{-m^3\delta e^\sigma\,(\ln(1 - e^{-\sigma}))^2}{A - m^2\,(\ln(1 - e^{-\sigma}))^2 - c\phi}$$

but $1 - e^{-\sigma} \sim \sigma \sim e^{-\alpha/m}$ so

$$\frac{d\psi}{d\sigma} \quad \sim \quad \frac{-m^3\delta e^\sigma\frac{\alpha^2}{m^2}}{A - m^2\left(\frac{\alpha^2}{m^2}\right) - c\phi}$$

$$\sim \quad \frac{-m\delta e^\sigma\alpha^2}{A - \alpha^2 - c\phi}.$$

Then

$$\psi \quad \sim \quad \left(\frac{-m\delta\alpha^2}{A - \alpha^2 - c\phi}\right) e^\sigma + \text{Const.}$$

$$\sim \quad \frac{-m\delta\alpha^2}{\alpha^2 \left(-1 + \frac{1}{\alpha^2}(A - c\phi)\right)}(1 + \sigma + \ldots) + \text{Const.}$$

$$\sim \quad \frac{-m\delta}{\left(\frac{1}{\alpha^2}(A - c\phi) - 1\right)}\sigma + \text{Const.} \tag{5.60}$$

Now, from (5.59), on taking $\alpha \to 0$,

$$\frac{d\psi}{d\alpha} \sim \frac{\delta e^{\alpha(1 - 1/m)}(1 - e^{-\alpha})^2}{A - (1 - e^{-\alpha})^2 - c\phi},$$

where $(1 - e^{-\alpha})^2 \sim (1 - (1 - \alpha))^2 \sim \alpha^2$ so,

$$\frac{d\psi}{d\alpha} \quad \sim \quad \frac{\delta e^{\alpha(1 - 1/m)}\alpha^2}{A - \alpha^2 - c\phi}$$

$$\sim \quad \frac{\delta\alpha^2 e^{-\alpha/m}}{A - \alpha^2 - c\phi}$$

$$\sim \quad \frac{\delta\alpha^2 e^{-\alpha/m}}{\alpha^2 \left(-1 + \frac{1}{\alpha^2}(A - c\phi)\right)}$$

$$\sim \quad \frac{\delta e^{-\alpha/m}}{\left(\frac{1}{\alpha^2}(A - c\phi) - 1\right)}.$$

Integrating,

$$\psi \quad \sim \quad \frac{-m\delta e^{-\alpha/m}}{\left(\frac{1}{\alpha^2}(A - c\phi) - 1\right)} + \text{Const.}$$

$$\sim \quad \frac{-m\delta}{\left(\frac{1}{\alpha^2}(A - c\phi) - 1\right)}\sigma + \text{Const.} \quad \text{as} \quad e^{-\alpha/m} \sim \sigma. \tag{5.61}$$

Equations (5.60) and (5.61) match. In Figure 5.30 we can see the regimes of the travelling wave for this case. In regime 1 for m small, excluding regime 1a where the approximations are valid but its integral diverges, we have from (5.53) that ψ changes an exponentially small amount. According to (5.54), in regime 2, ψ changes an amount of size m^3. In regime 3, from (5.59) with $0 < \alpha < \infty$, we also see ψ changes an exponentially small amount.

All in all, apart from regime 1a $(S \to S_-)$, most of change of ψ occurs in regime 2. For completeness, we should worry about regime 1a, here $A - m^2 S^{\left(\frac{2}{m} + \frac{1}{2}\right)} - c\phi S$

becomes small.

Now S_- satisfies

$$A = c\phi S_- + K(S_-) \quad \sim \quad c\phi S_- + m^2 S_-^{\left(\frac{2}{m}+\frac{1}{2}\right)} \quad \text{(for} \quad S_- \quad \text{in regime 1)}.$$

$$\sim \quad c\phi S_- \quad \text{(for} \quad c \quad \text{order} \quad 1).$$

Then we have

$$1 + c\phi(1 - S_-) = 1 + c\phi - c\phi S_- \sim 1 + c\phi - A \leq 0.$$
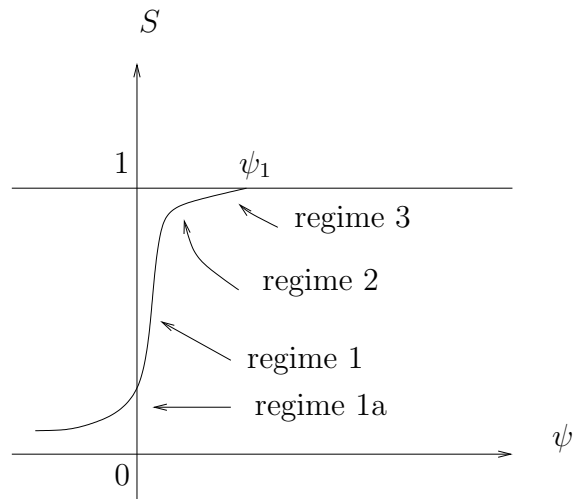
Figure 5.30: This figure shows us the changes in ψ in all regimes of the travelling wave. Regime 1a has S close to S_-.

For $\alpha \to \infty$, $(S \to 1)$, then

$$\frac{d\psi}{d\alpha} \sim \frac{\delta e^{\alpha\left(1-\frac{1}{m}\right)}}{A - c\phi}. \tag{5.62}$$

Integrating (5.62),

$$\psi \sim \left(\frac{\delta}{(A - c\phi)\left(1 - \frac{1}{m}\right)} \right) e^{\alpha\left(1 - \frac{1}{m}\right)} + \text{Const.}$$

$$\sim \left(\frac{\delta m}{(A - c\phi)(m - 1)} \right) e^{\alpha\left(1 - \frac{1}{m}\right)} + \text{Const.}$$

$$\sim \left(\frac{\delta m}{A - c\phi} \right) e^{\alpha\left(1 - \frac{1}{m}\right)} + \text{Const.}, \tag{5.63}$$

and we see that ψ reaches a finite value, ψ_1, as above, (5.27).

Case 2 : $0 = S_- < S_+ = 1$

As Case 1, we also consider both Case 2(i) and Case 2(ii)* together as they are so similar with Case 2(ii)** not applying because $m \ll 1$ so we always have $m < \frac{1}{2}$. In this case, we are looking for a travelling wave such that :

$$0 = A \geq 1 + c\phi \quad \Rightarrow \quad c\phi \leq -1 \quad \Rightarrow \quad c \leq -\frac{1}{\phi}.$$

For c fixed of order 1, $m \to 0^+$ and S not close to 1, the travelling wave in the first regime is given by :

$$\psi = -\delta \int_0^S \frac{D(S)}{K(S) + c\phi S} \, dS. \tag{5.64}$$

Using (5.1) and (5.2), then (5.64) becomes :

$$\psi \sim -\delta \int_0^S \frac{m^2 S^{\left(\frac{1}{m} + \frac{1}{2}\right)}}{m^2 S^{\left(\frac{2}{m} + \frac{1}{2}\right)} + c\phi S} \, dS$$

$$\sim -\delta \int_0^S \frac{m^2 S^{\left(\frac{1}{m} + \frac{1}{2}\right)}}{c\phi S} \, dS$$

$$\sim \frac{-m^2 \delta}{c\phi} \int_0^S S^{\left(\frac{1}{m} - \frac{1}{2}\right)} \, dS$$

$$\sim \frac{-m^2 \delta}{c\phi} \frac{1}{\left(\frac{1}{m} + \frac{1}{2}\right)} S^{\left(\frac{1}{m} + \frac{1}{2}\right)}$$

$$\sim \frac{-m^3 \delta}{c\phi} S^{\left(\frac{1}{m} + \frac{1}{2}\right)}. \tag{5.65}$$

Now, let us see the travelling wave in regime 2 when S is close to 1 ($S = 1 - m\sigma$). In this regime, the approximations of $D(S)$ and $K(S)$ are given by (5.6) and (5.7).

Then from (5.18), we have :

$$\frac{d\psi}{dS} \sim \frac{-\delta m^2 e^{\sigma} \left(\ln\left(1 - e^{-\sigma}\right)\right)^2}{m^2 \left(\ln\left(1 - e^{-\sigma}\right)\right)^2 + c\phi},$$

$$\frac{d\psi}{d\sigma} \sim \frac{\delta m^3 e^{\sigma} \left(\ln\left(1 - e^{-\sigma}\right)\right)^2}{m^2 \left(\ln\left(1 - e^{-\sigma}\right)\right)^2 + c\phi}. \tag{5.66}$$

σ in this regime is order 1. When $\sigma \to \infty$ (σ is large), this takes us back into S not close to 1, regime 1. On the other hand, σ is exponentially small in $\frac{1}{m}$ takes us into S very close to 1, regime 3.

For σ not small, (5.66) becomes

$$\frac{d\psi}{d\sigma} \sim \left(\frac{\delta m^3}{c\phi}\right) e^{\sigma} \left(\ln\left(1 - e^{-\sigma}\right)\right)^2.$$

For $\sigma \to \infty$, as before in (5.55), this gives :

$$\frac{d\psi}{d\sigma} \sim \left(\frac{\delta m^3}{c\phi}\right) e^{\sigma} e^{-2\sigma}$$

$$\sim \left(\frac{\delta m^3}{c\phi}\right) e^{-\sigma} \tag{5.67}$$

Integrating (5.67), we get :

$$\psi \sim \left(\frac{-\delta m^3}{c\phi}\right) e^{-\sigma} + \text{Const.} \tag{5.68}$$

Now, we need to make ψ match together for the two regimes 1 and 2. For this, we know that the previous regime gives, from (5.65) :

$$\psi \sim \left(\frac{-\delta m^3}{c\phi}\right) S^{\left(\frac{1}{m} + \frac{1}{2}\right)}.$$

But $S = 1 - m\sigma$, then

$$\psi \sim \left(\frac{-\delta m^3}{c\phi}\right) (1 - m\sigma)^{\left(\frac{1}{m} + \frac{1}{2}\right)} + \text{Const.}$$

$$\sim \left(\frac{-\delta m^3}{c\phi}\right) e^{\left(\frac{1}{m} + \frac{1}{2}\right)\ln(1 - m\sigma)} + \text{Const.}$$

$$\sim \left(\frac{-\delta m^3}{c\phi}\right) e^{-\sigma} + \text{Const..} \tag{5.69}$$

Equations (5.68) and (5.69) are the same, so that means the expressions for ψ match

for both regimes 1 and 2 of the travelling wave taking the constant in (5.68) to vanish. Figure 5.31 shows both regimes :
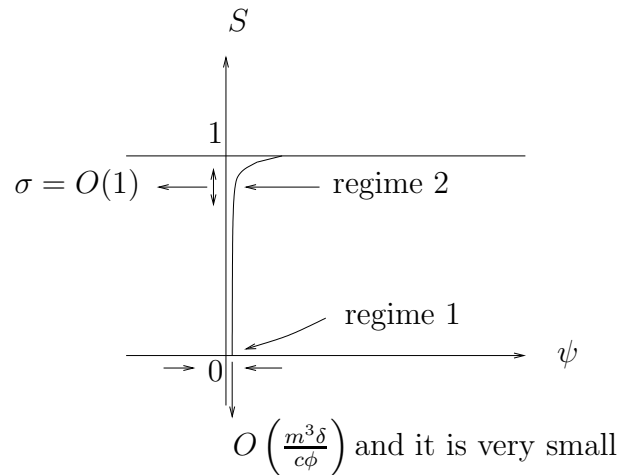
Figure 5.31: The changes in ψ over regimes 1 and 2 of the travelling wave.

Now, when S is very close to 1, so that we are in regime 3, we again write $S = 1 - me^{-\alpha/m}$. In this regime, the approximations of $D(S)$ and $K(S)$ are given earlier by (5.9) and (5.8). Then, from (5.66), we get :

$$\frac{d\psi}{d\alpha} \sim \frac{-\delta e^{\alpha\left(1-\frac{1}{m}\right)}\left(1-e^{-\alpha}\right)^2}{\left(1-e^{-\alpha}\right)^2 + c\phi}. \tag{5.70}$$

For $\alpha \to \infty$, so that $S \to 1$, we have :

$$\frac{d\psi}{d\alpha} \sim \left(\frac{-\delta}{c\phi}\right) e^{\alpha\left(1-\frac{1}{m}\right)}. \tag{5.71}$$

By integrating (5.71), we get :

$$\psi \sim \left(\frac{-\delta}{c\phi\left(1-\frac{1}{m}\right)}\right) e^{\alpha\left(1-\frac{1}{m}\right)} + \text{Const.}$$

$$\sim \left(\frac{-\delta m}{c\phi\left(m-1\right)}\right) e^{\alpha\left(1-\frac{1}{m}\right)} + \text{Const.}$$

$$\sim \left(\frac{-\delta m}{c\phi}\right) e^{\alpha\left(1-\frac{1}{m}\right)} + \text{Const.,} \tag{5.72}$$

82

again giving that ψ tends to a finite value, ψ_1.

Now, we want to match ψ in regime 3 with the expression in regime 2 as follows
From (5.66) :

$$\frac{d\psi}{d\sigma} \sim \frac{\delta m^3 e^\sigma \left(\ln\left(1 - e^{-\sigma}\right)\right)^2}{m^2 \left(\ln\left(1 - e^{-\sigma}\right)\right)^2 + c\phi}$$

But $1 - e^{-\sigma} \sim e^{-\alpha/m}$, then

$$\frac{d\psi}{d\sigma} \sim \frac{\delta m^3 e^\sigma \left(\ln\left(e^{-\alpha/m}\right)\right)^2}{m^2 \left(\ln\left(e^{-\alpha/m}\right)\right)^2 + c\phi}$$

$$\sim \frac{\delta m e^\sigma \alpha^2}{\alpha^2 + c\phi}$$

$$\sim \frac{\delta m e^\sigma}{\left(1 + \frac{c\phi}{\alpha^2}\right)}.$$

By integrating both sides, we have :

$$\psi \sim \left(\frac{\delta m}{1 + \frac{c\phi}{\alpha^2}}\right) e^\sigma + \text{Const.}$$

$$\sim \left(\frac{\delta m}{1 + \frac{c\phi}{\alpha^2}}\right) (1 + \sigma + \ldots) + \text{Const.}$$

$$\sim \left(\frac{\delta m}{1 + \frac{c\phi}{\alpha^2}}\right) \sigma + \text{Const.} \qquad (5.73)$$

From (5.70) :

$$\frac{d\psi}{d\alpha} \sim \frac{-\delta e^{\alpha\left(1 - \frac{1}{m}\right)} \left(1 - e^{-\alpha}\right)^2}{\left(1 - e^{-\alpha}\right)^2 + c\phi}.$$

But $\left(1 - e^{-\alpha}\right)^2 \sim \left(1 - (1 - \alpha)\right)^2 \sim \alpha^2$ for α small ($\alpha \to 0$), then

$$\frac{d\psi}{d\alpha} \sim \frac{-\delta e^{\alpha\left(1 - \frac{1}{m}\right)} \alpha^2}{\alpha^2 + c\phi}$$

$$\sim \left(\frac{-\delta}{1 + \frac{c\phi}{\alpha^2}}\right) e^{\alpha\left(1 - \frac{1}{m}\right)}$$

$$\sim \left(\frac{-\delta}{1 + \frac{c\phi}{\alpha^2}}\right) e^{-\alpha/m}.$$

Integrating both sides gives

$$\psi \sim \left(\frac{m\delta}{1 + \frac{c\phi}{\alpha^2}} \right) e^{-\alpha/m} + \text{Const.},$$

but $\sigma = -\ln\left(1 - e^{-\alpha/m}\right) \sim e^{-\alpha/m}$, then we get :

$$\psi \sim \left(\frac{\delta m}{1 + \frac{c\phi}{\alpha^2}} \right) \sigma + \text{Const.} \tag{5.74}$$

From (5.73) and (5.74), we can see that the expressions for ψ in regimes 2 and 3 match.

Case 3 : $0 = S_- < S_+ < 1$
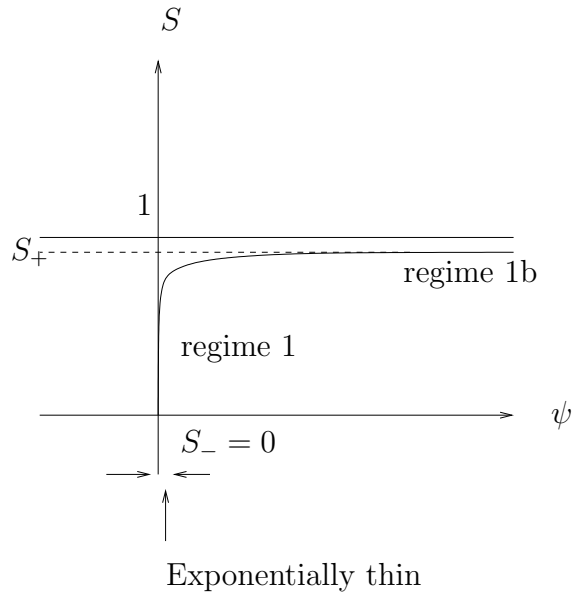
Figure 5.32: Shows Case 3 when $0 = S_- < S_+ < 1$.

In this case, we have that the wave speed c is given by

$$c \sim \frac{-m^2}{\phi} S_+^{\left(\frac{2}{m} - \frac{1}{2}\right)} \quad \text{for} \quad 0 < S_+ < 1$$

on taking S_+ not close to 1 (see (5.42)).
We now only have one regime, regime 1, and we have $A = 0$. Then from (5.18) we get :

$$\frac{d\psi}{dS} = \frac{-\delta D(S)}{K(S) + c\phi S},$$

and from (5.1) and (5.2), we have :

$$\frac{d\psi}{dS} \sim \frac{-\delta m^2 S^{\left(\frac{1}{m} + \frac{1}{2}\right)}}{m^2 S^{\left(\frac{2}{m} + \frac{1}{2}\right)} + c\phi S}$$

$$\sim \frac{-\delta m^2 S^{\left(\frac{1}{m} + \frac{1}{2}\right)}}{c\phi S}$$

$$\sim \left(\frac{-\delta m^2}{c\phi}\right) S^{\left(\frac{1}{m} - \frac{1}{2}\right)} \quad \text{for} \quad S \quad \text{not too close to} \quad S_+.$$

85

Then

$$\psi \quad \sim \quad \frac{-\delta m^2}{c\phi\left(\frac{1}{m}+\frac{1}{2}\right)} S^{\left(\frac{1}{m}+\frac{1}{2}\right)}$$

$$\sim \quad \left(\frac{-\delta m^3}{c\phi}\right) S^{\left(\frac{1}{m}+\frac{1}{2}\right)}.$$

Given the value of c, this asymptotic approximation clearly is not valid if S is too close to S_+. As before, there will be a regime 1b ($S \to S_+$), similar to regime 1a in Case 1, as shown in Figure 5.32.

Case 4 : $\quad 0 < S_- < S_+ < 1$

We take both S_- and S_+ to be fixed and away from $S = 1$, so that they are in regime 1. From (5.18), (5.1) and (5.2), we have

$$\frac{d\psi}{dS} \sim \frac{\delta m^2 S^{\left(\frac{1}{m}+\frac{1}{2}\right)}}{A - m^2 S^{\left(\frac{2}{m}+\frac{1}{2}\right)} - c\phi S}. \tag{5.75}$$

But

$$A \quad = \quad K(S_-) + c\phi S_- = K(S_+) + c\phi S_+$$

$$\sim \quad m^2 S_-^{\left(\frac{2}{m}+\frac{1}{2}\right)} + c\phi S_- \sim m^2 S_+^{\left(\frac{2}{m}+\frac{1}{2}\right)} + c\phi S_+. \tag{5.76}$$

For $0 < m \ll 1$ with $0 < S_- < S_+ < 1$ we assume S_+ not close to S_- or 1 and S_- not small, then $S_-^{\left(\frac{2}{m}+\frac{1}{2}\right)} \ll S_+^{\left(\frac{2}{m}+\frac{1}{2}\right)}$.
From (5.76) we have

$$c \quad = \quad -\left(\frac{K(S_+) - K(S_-)}{\phi\left(S_+ - S_-\right)}\right)$$

$$\sim \quad -\left(\frac{m^2 S_+^{\left(\frac{2}{m}+\frac{1}{2}\right)} - m^2 S_-^{\left(\frac{2}{m}+\frac{1}{2}\right)}}{\phi\left(S_+ - S_-\right)}\right).$$

Using the assumption above, we have

$$c \sim \frac{-m^2 S_+^{\left(\frac{2}{m}+\frac{1}{2}\right)}}{\phi\left(S_+ - S_-\right)}. \tag{5.77}$$

Therefore, (5.76) becomes

$$A \sim m^2 S_+^{\left(\frac{2}{m}+\frac{1}{2}\right)} - \frac{m^2 S_+ S_+^{\left(\frac{2}{m}+\frac{1}{2}\right)}}{S_+ - S_-}$$

$$\sim \frac{m^2 S_+^{\left(\frac{2}{m}+\frac{1}{2}\right)} (S_+ - S_-) - m^2 S_+^{\left(\frac{2}{m}+\frac{3}{2}\right)}}{S_+ - S_-}$$

$$\sim \frac{-m^2 S_- S_+^{\left(\frac{2}{m}+\frac{1}{2}\right)}}{(S_+ - S_-)}. \tag{5.78}$$

Therefore, using (5.75), (5.77) and (5.78), we get :

$$\frac{d\psi}{dS} \sim \frac{\delta m^2 S^{\left(\frac{1}{m}+\frac{1}{2}\right)}}{A - m^2 S^{\left(\frac{2}{m}+\frac{1}{2}\right)} - c\phi S} \tag{5.79}$$

$$\sim \frac{\delta m^2 (S_+ - S_-) S^{\left(\frac{1}{m}+\frac{1}{2}\right)}}{-m^2 \left(S_- S_+^{\left(\frac{2}{m}+\frac{1}{2}\right)} + S^{\left(\frac{2}{m}+\frac{1}{2}\right)} (S_+ - S_-) - S_+^{\left(\frac{2}{m}+\frac{1}{2}\right)} S\right)} \tag{5.80}$$

$$\sim \frac{-\delta (S_+ - S_-) S^{\left(\frac{1}{m}+\frac{1}{2}\right)}}{S_+^{\left(\frac{2}{m}+\frac{1}{2}\right)} (S_- - S) + S^{\left(\frac{2}{m}+\frac{1}{2}\right)} (S_+ - S_-)} \tag{5.81}$$

$$\sim \frac{-\delta (S_+ - S_-) S^{\left(\frac{1}{m}+\frac{1}{2}\right)}}{S_+^{\left(\frac{2}{m}+\frac{1}{2}\right)} (S_- - S)}. \tag{5.82}$$

On integrating (5.79), we have :

$$\psi \sim -\left(\frac{\delta (S_+ - S_-)}{S_+^{\left(\frac{2}{m}+\frac{1}{2}\right)}}\right) \int_{S_-}^{S} \frac{\hat{S}^{\left(\frac{1}{m}+\frac{1}{2}\right)}}{S_- - \hat{S}} \, d\hat{S},$$

$$\sim -\left(\frac{\delta (S_+ - S_-)}{S_+^{\left(\frac{2}{m}+\frac{1}{2}\right)}}\right) \int_{S_-}^{S} \frac{e^{\left(\frac{1}{m}+\frac{1}{2}\right)\ln \hat{S}}}{S_- - \hat{S}} \, d\hat{S}. \tag{5.83}$$

Choosing $\quad \sigma = \left(\frac{1}{m} + \frac{1}{2}\right)\left(\ln S - \ln \hat{S}\right)$ then $\quad d\sigma = -\left(\frac{1}{m} + \frac{1}{2}\right)\frac{d\hat{S}}{\hat{S}}$,

$$\ln \hat{S} = \ln S - \frac{\sigma}{\left(\frac{1}{m} + \frac{1}{2}\right)} \quad \Rightarrow \quad \ln \hat{S} \sim \ln S \quad \Rightarrow \quad \hat{S} \sim S,$$

therefore,

$$d\sigma \sim -\left(\frac{1}{m} + \frac{1}{2}\right)\frac{d\hat{S}}{S} \sim -\frac{1}{m}\frac{d\hat{S}}{S} \quad \Rightarrow \quad d\hat{S} \sim -mS d\sigma.$$

When $S = \hat{S}$, $\sigma = 0$ and when $S = S_-$ then $\sigma = \left(\frac{1}{m} + \frac{1}{2}\right) \ln \frac{S}{S_-} \gg 1$.
Equation (5.83) becomes

$$
\psi \sim \left(\frac{\delta\,(S_+ - S_-)}{S_+^{\left(\frac{2}{m}+\frac{1}{2}\right)}}\right) \int_0^\infty \frac{mS^{\left(\frac{1}{m}+\frac{3}{2}\right)}e^{-\sigma}}{S - S_-}\mathrm{d}\sigma
$$

$$
\sim \frac{m\delta\,(S_+ - S_-)\,S^{\left(\frac{1}{m}+\frac{3}{2}\right)}}{S_+^{\left(\frac{2}{m}+\frac{1}{2}\right)}(S - S_-)}. \tag{5.84}
$$

Note that (5.84) is only valid for S not close to S_- and S_+.

Case 5 : $0 = S_+ < S_- = 1$
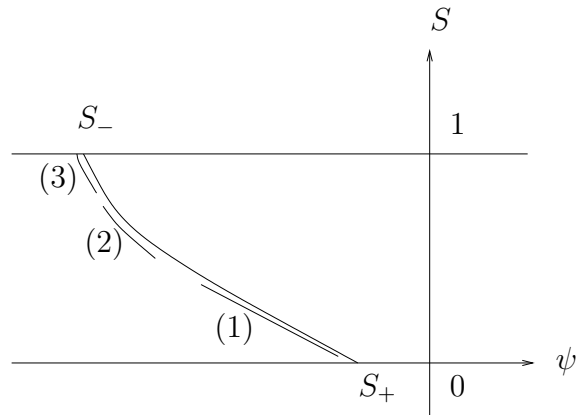
Figure 5.33: The three regimes of the travelling wave ψ when $0 = S_+ < S_- = 1$.

When $m \to 0$, we have the following two cases :

Case 5(i) :

In this case $c = 0$, the travelling wave is given by equation (5.64). In regime 1, $D(S)$ and $K(S)$ are approximated by equations (5.1) and (5.2) so that the travelling

wave can be given by :

$$\psi \quad \sim \quad -\delta \int_0^S \frac{m^2 S^{\left(\frac{1}{m}+\frac{1}{2}\right)}}{m^2 S^{\left(\frac{2}{m}+\frac{1}{2}\right)} + c\phi S} dS$$

$$\sim \quad -\delta \int_0^S \frac{S^{\left(\frac{1}{m}+\frac{1}{2}\right)}}{S^{\left(\frac{2}{m}+\frac{1}{2}\right)}} dS$$

$$\sim \quad -\delta \int_0^S S^{\left(-\frac{1}{m}\right)} dS$$

$$\sim \quad \delta m S^{\left(-\frac{1}{m}+1\right)} + \text{Const.}$$

Now, we will examine the travelling wave in regime 2 when S is close to 1. Using equations (5.6) and (5.7), we have :

$$\frac{d\psi}{dS} \quad = \quad \frac{-\delta D(S)}{K(S) + c\phi S}$$

$$\sim \quad \frac{-\delta m^2 e^{\sigma} \left(\ln\left(1 - e^{-\sigma}\right)\right)^2}{m^2 \left(\ln\left(1 - e^{-\sigma}\right)\right)^2}$$

$$\sim \quad -\delta e^{\sigma},$$

$$\frac{d\psi}{d\sigma} \quad = \quad -m\frac{d\psi}{dS}$$

$$\sim \quad \delta m e^{\sigma}.$$

For $\sigma \to \infty$, this gives
$$\frac{d\psi}{d\sigma} \sim \delta m e^{\sigma}.$$

Integrating this, we get
$$\psi \sim \delta m e^{\sigma} + \text{Const.} \tag{5.85}$$

Now to match the solution ψ for the two regimes 1 and 2, we have from the first regime :
$$\psi \sim \delta m S^{\left(-\frac{1}{m}+1\right)} \tag{5.86}$$

With $S = 1 - m\sigma$, (5.86) becomes :

$$\psi \quad \sim \quad m\delta \left(1 - m\sigma\right)^{\left(-\frac{1}{m}+1\right)}$$

$$\sim \quad m\delta e^{\left(-\frac{1}{m}+1\right)\ln(1-m\sigma)}$$

$$\sim \quad m\delta e^{\sigma} \tag{5.87}$$

so (5.85) and (5.87) match together.

Now, when S is very close to 1, regime 3, $S = 1 - me^{\frac{-\alpha}{m}}$. In this regime, the functions $D(S)$ and $K(S)$ are approximated by equations (5.9) and (5.8). Then

$$\frac{d\psi}{dS} \sim \frac{-\delta e^{\alpha}\left(1 - e^{-\alpha}\right)^2}{\left(1 - e^{-\alpha}\right)^2} \sim -\delta e^{\alpha}.$$

But

$$\frac{d\psi}{d\alpha} = e^{\frac{-\alpha}{m}}\frac{d\psi}{dS} \sim -\delta e^{\alpha\left(1-\frac{1}{m}\right)}.$$

For $\alpha \to \infty$, i.e. $S \to 1$,

$$\frac{d\psi}{d\alpha} \sim -\delta e^{\alpha\left(1-\frac{1}{m}\right)}.$$

Integrating this, we get

$$\psi \quad \sim \quad \frac{-\delta m}{(m-1)}e^{\alpha\left(1-\frac{1}{m}\right)} + \text{Const.}$$

$$\sim \quad -\delta m e^{\alpha\left(1-\frac{1}{m}\right)} + \text{Const.}$$

On the other hand, to match ψ in regime 3 with ψ in regime 2, we have from regime 2

$$\frac{d\psi}{d\sigma} \sim \delta m e^{\sigma}.$$

Integrating this, we have

$$\psi \sim \delta m e^{\sigma} \sim \delta m\left(1 + \sigma + \ldots\right) \sim \delta m\sigma + \text{Const.} \quad \text{for} \quad \sigma \to 0. \tag{5.88}$$

We also have from regime 3

$$\frac{d\psi}{d\alpha} \sim -\delta e^{\alpha\left(1-\frac{1}{m}\right)} \sim -\delta e^{\frac{-\alpha}{m}}.$$

Integrating both sides, we get

$$\psi \sim \delta m e^{\frac{-\alpha}{m}} + \text{Const.}$$

But $\sigma = -\ln\left(1 - e^{\frac{-\alpha}{m}}\right) \sim e^{\frac{-\alpha}{m}}$, then

$$\psi \sim \delta m \sigma. \tag{5.89}$$

From (5.88) and (5.89), we can see that ψ in regimes 3 and 2 match.

Case 5(ii) :

In this case $c > 0$ and the analysis is very similar to that of Case 2(i).

Case 6 : $0 < S_+ < S_- = 1$
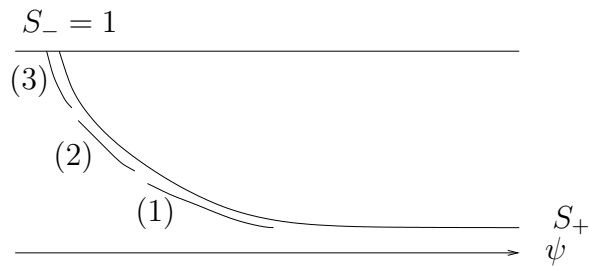
Figure 5.34: This plot shows the three regimes of ψ in case $0 < S_+ < S_- = 1$.

For this case we have $c > 0$, $c = 0$ and $c < 0$. It is exactly like Case 1 when $m \to 0^+$.

5.8 Different Travelling Waves : $m \to 1$

When $m \to 1$, we only consider the case $0 < S_- = S_+ = 1$, Case 1. Case 4, with $0 < 1 - S_+ \to 0$ and Case 6 are expected to be very similar, and are not considered. The other cases appear not to have any interesting limiting m dependence and are not looked at.

Now, when $S_+ = 1$, $0 < S_- < S_+ = 1$, we have a general profile as of Figure 5.9. We have $A = K(S_-) + c\phi S_-$, so that from (5.16), we have

$$\delta D(S)\frac{dS}{d\psi} = A - (K(S) + c\phi S)$$

$$= (K(S_-) + c\phi S_-) - (K(S) + c\phi S)$$

and this should be positive for $S_- < S < S_+ = 1$, which means

$$\delta D(S)\frac{dS}{d\psi} = (K(S_-) + c\phi S_-) - (K(S) + c\phi S) > 0.$$

For this case, we have the sub-cases as in Case 1 (pages 49 - 55) (see Figures 5.7 and 5.4):

The first subcase (Figure 5.7) has

$$A = K(S_-) + c\phi S_- = 1 + c\phi$$

so

$$c = -\frac{1}{\phi}\left(\frac{1 - K(S_-)}{1 - S_-}\right).$$

The second subcase (Figure 5.4) has

$$A = K(S_-) + c\phi S_- > 1 + c\phi$$

so

$$c < -\frac{1}{\phi}\left(\frac{1 - K(S_-)}{1 - S_-}\right).$$

In these cases we notice that the value of c (or its limit) depends on m.

For $m < 1$, $S_- < S_+ = 1$, as can be seen from the graph of Figure 5.35, if S_- is close to 1, c has to be large negative as follows :
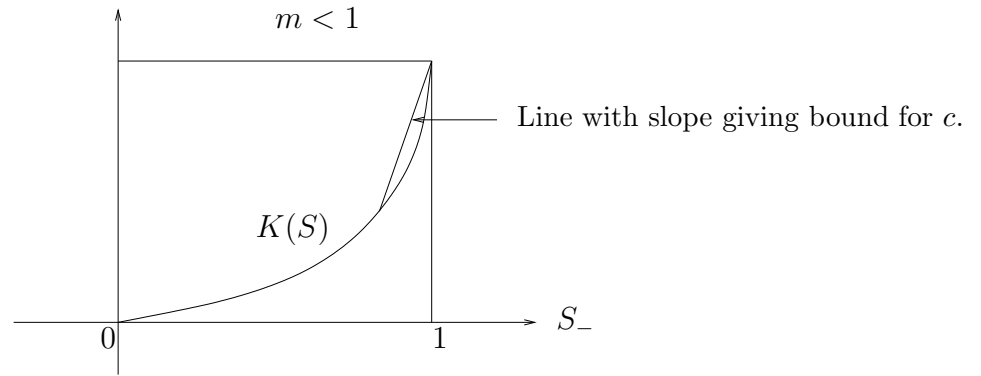
Figure 5.35: This figure shows the plot of function $K(S)$. When S_- is near 1 has to have c a large negative value.

$$-c\phi \geq C_m^* \equiv \frac{1 - K_m(S_-)}{1 - S_-} \quad \rightarrow \quad \infty \quad \text{as} \quad S_- \rightarrow 1^-. \tag{5.90}$$

On the other hand, for $m = 1$, $S_- < S_+ = 1$, the limiting value of c will be given by the much weaker estimate

$$-c\phi \geq C_1^* \equiv \frac{1 - K_1(S_-)}{1 - S_-} = \frac{1 - S_-^{5/2}}{1 - S_-} \quad \rightarrow \quad \frac{5}{2} \quad \text{as} \quad S_- \rightarrow 1^-. \tag{5.91}$$

From (5.90) and (5.91), we have C^* in general is given by :

$$C^*(S_-, m) = \frac{1 - K_m(S_-)}{1 - S_-}. \tag{5.92}$$

The value of the function in (5.92) for $m < 1$ and $m = 1$ will be shown in Figure 5.36.
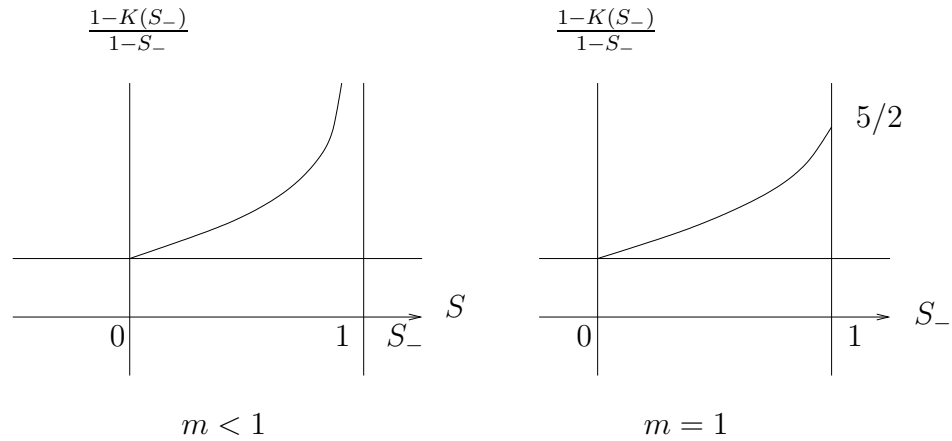
Figure 5.36: The two values of the function $\frac{1-K(S_-)}{1-S_-}$ in case $m < 1$ (left) and $m = 1$ (right).

For $m < 1$, the value of $\mathrm{C}^*(S_-, m)$ is large and increases to ∞ as S_- appraoches 1, but for $m = 1$, it only increases to 5/2. This function for both situations $m < 1$ and $m = 1$ is given by

$$\mathrm{C}^*(S, m) = \begin{cases} \dfrac{1-S^{1/2}\left[1-\left(1-S^{1/m}\right)^m\right]^2}{1-S} & m < 1 \\ \dfrac{1-S^{5/2}}{1-S} & m = 1 \end{cases}.$$

From this equation when $S \to 1$ there is a non-uniformity at $S = 1$, $m = 1$ because $\frac{1-S^{1/2}\left[1-\left(1-S^{1/m}\right)^m\right]^2}{1-S} \to \infty$ as $S \to 1^-$ but $\frac{1-S^{5/2}}{1-S}$ does not. If m is away from 1, there is no problem taking $S \to 1$ and if S is away from 1, there is no problem taking $m \to 1$. The problem is taking $S \to 1$ and $m \to 1$ together.

Let us consider the second sub-case $A = 1 + c\phi$, when $m \to 1$ with fixed S_-, then

$$K_m(S) \to S^{\frac{5}{2}}, \quad c \to -\frac{1}{\phi}\left(\frac{1-S_-^{\frac{5}{2}}}{1-S_-}\right) = c_1$$

so that $S \to S_1$ (S_1 is the solution we get by replacing m by 1).
For this limit $m \to 1$, the functions $D(S)$ and $K(S)$ are simply given by

$$D_1(S) = \frac{S^{\frac{3}{2}}}{1-S}, \tag{5.93}$$

$$K_1(S) = S^{\frac{5}{2}}. \tag{5.94}$$

Here,

$$\delta D_1(S_1)\frac{dS_1}{d\psi} = (K_1(S_-) + c_1\phi S_-) - (K_1(S_1) + c_1\phi S_1).$$

Using (5.93) and (5.94) we have

$$\frac{\delta S_1^{\frac{3}{2}}}{1 - S_1}\frac{dS_1}{d\psi} = (K_1(S_-) + c_1\phi S_-) - \left(S_1^{\frac{5}{2}} + c_1\phi S_1\right). \tag{5.95}$$

When $S_1 \to 1$ then the derivative of the right hand side of (5.95) is going to be a non-zero number. This leads to an exponential approach to $S_1 = 1$ as $\psi \to \infty$.
We observe, however, that, for fixed $m < 1$, from Case 1(ii)** near the start of the chapter, we have $S \to 1$ only algebraically as $\psi \to \infty$.

Now, we fix $m < 1$ and take $S_- \to 1$. We have $K_m = S^{\frac{1}{2}}\left[1 - \left(1 - S^{\frac{1}{m}}\right)^m\right]^2$ and

$$
\begin{aligned}
c &= -\frac{1}{\phi}\left(\frac{1 - K_m(S_-)}{1 - S_-}\right) \\
&= -\frac{1}{\phi}\left(\frac{1 - S_-^{\frac{1}{2}}\left[1 - \left(1 - S_-^{\frac{1}{m}}\right)^m\right]^2}{1 - S_-}\right).
\end{aligned}
$$

If $S_- \to 1$, c goes to $-\infty$. In particular, if we write $S_- = 1 - \sigma$, where $\sigma \to 0$, then

$$
\begin{aligned}
c &\sim -\frac{1}{\phi\sigma}\left(1 - (1 - \sigma)^{\frac{1}{2}}\left[1 - \left(1 - (1 - \sigma)^{\frac{1}{m}}\right)^m\right]^2\right) \\
&\sim -\frac{1}{\phi\sigma}\left(1 - \left(1 - \frac{1}{2}\sigma\ldots\right)\left[1 - \left(1 - \left(1 - \frac{\sigma}{m}\ldots\right)\right)^m\right]^2\right) \\
&\sim -\frac{1}{\phi\sigma}\left(1 - \left(1 - \frac{1}{2}\sigma\ldots\right)\left[1 - \frac{\sigma^m}{m^m}\ldots\right]^2\right) \\
&\sim -\frac{1}{\phi\sigma}\left(1 - \left(1 - \frac{1}{2}\sigma\ldots\right)\left(1 - \frac{2\sigma^m}{m^m}\ldots\right)\right) \\
&\sim -\frac{1}{\phi\sigma}\left(1 - \left(1 - \frac{2\sigma^m}{m^m}\ldots\right)\right) \\
&\sim \frac{-2\sigma^{m-1}}{\phi m^m} \qquad (\sigma \to 0, \quad m < 1) \\
&\sim \frac{-2(1 - S_-)^{-(1-m)}}{\phi m^m} \quad \to \quad -\infty. \tag{5.96}
\end{aligned}
$$

Now take $m \to 1$ and $S_- \to 1$. Still considering for the limiting case, $c = -\frac{1}{\phi}\left(\frac{1-K(S_-)}{1-S_-}\right)$,

$$c = -\frac{1}{\phi}\left(\frac{1 - S_-^{\frac{1}{2}}\left[1 - \left(1 - S_-^{\frac{1}{m}}\right)^m\right]^2}{1 - S_-}\right),$$

$$= -\frac{1}{\phi\sigma}\left\{1 - (1-\sigma)^{\frac{1}{2}}\left[1 - \left(1 - (1-\sigma)^{\frac{1}{m}}\right)^m\right]^2\right\},$$

on writing $S_- = 1 - \sigma$, where we shall let $\sigma \to 0$.

Since $m \to 1$, $\sigma \to 0$, let us take $m = 1 - n$, $n \to 0$, therefore

$$c = -\frac{1}{\phi\sigma}\left\{1 - (1-\sigma)^{\frac{1}{2}}\left[1 - \left(1 - (1-\sigma)^{\frac{1}{1-n}}\right)^{(1-n)}\right]^2\right\}$$

$$\sim -\frac{1}{\phi\sigma}\left\{1 - \left(1 - \frac{1}{2}\sigma\ldots\right)\left[1 - (1 - (1 - \sigma(1 - n\ldots)))^{(1-n)}\right]^2\right\}$$

$$\sim -\frac{1}{\phi\sigma}\left\{1 - \left(1 - \frac{1}{2}\sigma\ldots\right)\left[1 - (\sigma - \sigma n\ldots)^{(1-n)}\right]^2\right\}$$

$$\sim -\frac{1}{\phi\sigma}\left\{1 - \left(1 - \frac{1}{2}\sigma\ldots\right)\left[1 - (\sigma - \sigma n\ldots)\,e^{-n\ln(\sigma-\sigma n\ldots)}\right]^2\right\}$$

$$\sim -\frac{1}{\phi\sigma}\left\{1 - \left(1 - \frac{1}{2}\sigma\ldots\right)\left[1 - (\sigma - \sigma n\ldots)(1 - n\ln\sigma\ldots)\right]^2\right\}$$

$$\sim -\frac{1}{\phi\sigma}\left\{1 - \left(1 - \frac{1}{2}\sigma\ldots\right)\left[1 - \sigma + n\ln\sigma\ldots\right]^2\right\}$$

$$\sim -\frac{1}{\phi\sigma}\left\{1 - \left(1 - \frac{1}{2}\sigma\ldots\right)(1 - 2\sigma + 2n\ln\sigma\ldots)\right\}$$

$$\sim -\frac{1}{\phi\sigma}\left(\frac{5}{2}\sigma - 2n\ln\sigma\ldots\right)$$

$$\sim -\frac{1}{\phi}\left(\frac{5}{2} - \frac{2n\ln\sigma}{\sigma}\right). \tag{5.97}$$

The key balance is when n is of the same size as $\frac{-\ln\sigma}{\sigma}$. So, $n = O\left(\frac{-\ln\sigma}{\sigma}\right)$, i.e. $1 - m$ is the same size as $\frac{-\ln(1-S)}{1-S}$ and this gives the separating behaviour between the two cases, $\phi c = \frac{5}{2}$, got for $n \ll \frac{-\ln\sigma}{\sigma}$, and (5.96), achieved for $n \gg \frac{-\ln\sigma}{\sigma}$.

Now when $A > 1 + c\phi$, we have $c < -\frac{1}{\phi}\left(\frac{1-K_m(S_-)}{1-S_-}\right)$. We have similar results applying to the bounds for $c \to -\infty$ when $S_- \to 1$ and $m < 1$, and $c \leq \frac{-5}{2\phi}$ when

$S_- \to 1$ and $m \to 1$, with an intermediate estimate for $1 - m$ of order $1 - \frac{(1-S)}{\ln(1-S)}$.

5.9   Summary

Frontal travelling wave solutions for the nonlinear convection-diffusion model (5.13) are seen to exist for most cases of limiting saturations S_- and S_+. To be more precise, we have travelling waves for all cases of $0 \le S_- < S_+ \le 1$, but with $0 \le S_+ < S_- \le 1$, they only occur for $0 \le S_+ < S_- = 1$.

Travelling waves with $0 \le S_+ < S_- < 1$ do not exist. With $S_- < 1$, travelling waves move down, under the effect of gravity ($c < 0$, Cases 1 - 4) but with $S_- = 1$ the water can be forced up and we can have waves moving against gravity (c can be non-negative for Cases 5 and 6).

With the model parameter $m \to 0$, the various cases of the travelling waves still applied, but different parts of the wave corresponded to the different regimes giving different approximations for $D(S)$ and $K(S)$. Excluding the asymptotic approach to $S_\pm$ as $\psi \to \pm\infty$, the widest part of the wave, appears, at least for S_- or $S_+ = 1$, to come from the regime 2, where S is $O(m)$ from 1.

In the opposite limit $m \to 1$, little interesting behaviour was observed. However, the limiting critical value of wave speed was seen to have a non-uniform limiting dependence on $m \to 1$ and $S_- \to 1$, at least for Case 1 ($0 < S_- < S_+ = 1$).

The travelling wave in Case 4 can arise as a limiting solution of the problem satisfying the boundary condition (4.2), with $K_0 K(S_+) = Q_{in}$, and initial condition with $S_- = S_{init}$, provided that $S_{init} = S_- < S_+$. This was the situation for our numerical solutions only for $S_{init} = 0.05$ while the other cases which give $S_- > S_+$ belong to Case 8 and do not give rise to travelling waves. Also a travelling wave in Case 3, with $S_- = 0$ and $S_+ = S_{init}$, satisfies (4.3) but unfortunately because $c < 0$ we do not see it (the wave would move into $z < 0$, outside the green roof).

Chapter 6

Self-Similar Solutions

6.1 Introduction

In this chapter, we investigate self-similar solutions for our nonlinear convection-diffusion model (5.13). We particularly seek the solutions for the limiting cases of the saturation S being near 0 and 1.

6.2 Similarity Solutions

This method is a systematic method of change of variables which is sometimes effective in producing solutions to diffusion type equations. The key to this method is that the change of variable may reduce, for instance, a second order PDE to a second order ODE. The change of variables is called a similarity transformation and the resulting solution of the PDE (if it exists) is called a self-similar solution or similarity solution. We want to obtain self-similar solutions of our nonlinear convection-diffusion model given by equation (5.13) by seeking an appropriate similarity solution in the form :

$$S(t,z) = t^\alpha \Phi(\xi); \qquad \xi = zt^\beta, \tag{6.1}$$

where ξ is the similarity variable. Here α and β are some unknown exponents to be determined.
Using (6.1), then (5.13) becomes :

$$\phi t^{\alpha-1}\left(\alpha\Phi(\xi) + \beta\xi\frac{\partial\Phi}{\partial\xi}\right) = \delta\left(\frac{\partial}{\partial\xi}D\left(t^\alpha\Phi(\xi)\right)\frac{\partial\Phi}{\partial\xi}t^{(\alpha+2\beta)} + D\left(t^\alpha\Phi(\xi)\right)t^{(\alpha+2\beta)}\frac{\partial^2\Phi}{\partial\xi^2}\right)$$

$$+ \frac{\partial}{\partial\xi}K(t^\alpha\Phi(\xi))t^\beta. \tag{6.2}$$

Dividing both sides of (6.2) by $t^{\alpha-1}$, we get :

$$\phi\left(\alpha\Phi(\xi) + \beta\xi\frac{\partial\Phi}{\partial\xi}\right) = \delta\left(\frac{\partial}{\partial\xi}D\left(t^\alpha\Phi(\xi)\right)\frac{\partial\Phi}{\partial\xi}t^{(2\beta+1)} + D\left(t^\alpha\Phi(\xi)\right)t^{(2\beta+1)}\frac{\partial^2\Phi}{\partial\xi^2}\right)$$

$$+ \frac{\partial}{\partial\xi}K(t^\alpha\Phi(\xi))t^{(\beta-\alpha+1)}$$

$$= \delta t^{(2\beta+1)}\frac{d}{d\xi}\left(D\left(t^\alpha\Phi(\xi)\right)\frac{d\Phi}{d\xi}\right) + \frac{\partial}{\partial\xi}K(t^\alpha\Phi(\xi))t^{(\beta-\alpha+1)} \tag{6.3}$$

$$= t^{(2\beta+1)}\frac{d}{d\xi}\left(\delta D\left(t^\alpha\Phi(\xi)\right)\frac{d\Phi}{d\xi} + t^{-(\alpha+\beta)}K(t^\alpha\Phi(\xi))\right).$$

This equation is in general dependent on t whatever values constants α and β have. We will investigate the self-similar solutions to equation (6.3) for the two limiting cases when $S \to 0$ and $S \to 1$.

6.2.1   Case 1 : $S \to 0$

In the new variable Φ and for general m, we exactly need $t^\alpha\Phi \to 0$ for $S \to 0$. This could happen with $t \to 0$ if $\alpha > 0$ or $t \to \infty$ if $\alpha < 0$. The functions $D(t^\alpha\Phi)$ and $K(t^\alpha\Phi)$ are approximated, as in (5.1) and (5.2), by :

$$D(t^\alpha\Phi) \sim m^2 t^{\alpha\left(\frac{1}{m}+\frac{1}{2}\right)}\Phi^{\left(\frac{1}{m}+\frac{1}{2}\right)}, \tag{6.4}$$

$$K(t^\alpha\Phi) \sim m^2 t^{\alpha\left(\frac{2}{m}+\frac{1}{2}\right)}\Phi^{\left(\frac{2}{m}+\frac{1}{2}\right)}. \tag{6.5}$$

Then equation (6.3) becomes, approximately,

$$\phi\left(\alpha\Phi + \beta\xi\frac{d\Phi}{d\xi}\right) = m^2\frac{d}{d\xi}\left(\delta t^{\left(2\beta+1+\alpha\left(\frac{1}{m}+\frac{1}{2}\right)\right)}\Phi^{\left(\frac{1}{m}+\frac{1}{2}\right)}\frac{d\Phi}{d\xi} + t^{\left(\beta+1+\alpha\left(\frac{2}{m}-\frac{1}{2}\right)\right)}\Phi^{\left(\frac{2}{m}+\frac{1}{2}\right)}\right). \tag{6.6}$$

Equation (6.6) is independent of t if the exponents $\alpha = \frac{-2m}{6-3m}$ and $\beta = -\frac{2-2m}{6-3m}$. Then equation (6.6) becomes

$$\delta m^2\frac{d}{d\xi}\left(\Phi^{\left(\frac{1}{m}+\frac{1}{2}\right)}\frac{d\Phi}{d\xi}\right) + m^2\frac{d}{d\xi}\Phi^{\left(\frac{2}{m}+\frac{1}{2}\right)} = \frac{-2\phi}{6-3m}\left(m\Phi + (1-m)\xi\frac{d\Phi}{d\xi}\right). \tag{6.7}$$

Now let us introduce the following new variables :

$$\zeta = -\xi, \qquad \vartheta = \Phi^{\left(\frac{1}{m}+\frac{3}{2}\right)}, \qquad \Phi = \vartheta^{\left(1/\left(\frac{1}{m}+\frac{3}{2}\right)\right)}. \tag{6.8}$$

These give

$$\frac{d\vartheta}{d\xi} = \left(\frac{1}{m} + \frac{3}{2}\right)\Phi^{\left(\frac{1}{m}+\frac{1}{2}\right)}\frac{d\Phi}{d\xi}.$$

Hence, equation (6.7) becomes

$$\delta m^2 \frac{d}{d\zeta}\left(\left(\frac{1/m+3/2}{1/m+3/2}\right)\Phi^{\left(\frac{1}{m}+\frac{1}{2}\right)}\frac{d\Phi}{d\xi}\right)$$

$$-\left(2m+\frac{m^2}{2}\right)\Phi^{\left(\frac{2}{m}-\frac{1}{2}\right)}\frac{d\Phi}{d\zeta} = \frac{-2\phi}{6-3m}\left(m\Phi+(1-m)\zeta\frac{d\Phi}{d\zeta}\right),$$

$$\text{or} \quad \left(\frac{2\delta m^3}{2+3m}\right)\frac{d^2\vartheta}{d\zeta^2} = \frac{m^2(4+m)}{2+3m}\vartheta^{\left(\frac{2-2m}{2+3m}\right)}\frac{d\vartheta}{d\zeta} - \frac{2\phi m}{6-3m}\vartheta^{\left(\frac{2m}{2+3m}\right)}$$

$$-\frac{4\phi m(1-m)}{(6-3m)(2+3m)}\zeta\vartheta^{\frac{-(2+m)}{2+3m}}\frac{d\vartheta}{d\zeta},$$

$$\text{so} \quad \frac{d^2\vartheta}{d\zeta^2} = \left(\frac{4+m}{2\delta m}\vartheta^{\left(\frac{2-2m}{2+3m}\right)} - \frac{2\phi(1-m)}{\delta m^2(6-3m)}\zeta\vartheta^{\frac{-(2+m)}{2+3m}}\right)\frac{d\vartheta}{d\zeta} - \frac{(2+3m)\phi}{\delta m^2(6-3m)}\vartheta^{\left(\frac{2m}{2+3m}\right)}, \quad \text{or,}$$

$$\text{finally,} \quad \frac{d^2\vartheta}{d\zeta^2} = \left(c_1\vartheta^{\left(\frac{2-2m}{2+3m}\right)} - c_2\zeta\vartheta^{\frac{-(2+m)}{2+3m}}\right)\frac{d\vartheta}{d\zeta} - c_3\vartheta^{\left(\frac{2m}{2+3m}\right)}, \quad (6.9)$$

where $c_1 = \frac{4+m}{2\delta m}$, $c_2 = \frac{2\phi(1-m)}{\delta m^2(6-3m)}$ and $c_3 = \frac{(2+3m)\phi}{\delta m^2(6-3m)}$ are all positive for $m < 1$.
We now investigate the possible behaviour of solutions of (6.9) satisfying $\vartheta = \vartheta_0$ at $\zeta = 0$, for some arbitrary positive ϑ_0.

$(1)^*$ The solution can blow up

From equation (6.9) we get :

$$\frac{d^2\vartheta}{d\zeta^2} = \left(c_1\vartheta^{\left(\frac{2-2m}{2+3m}\right)} - c_2\zeta\vartheta^{\frac{-(2+m)}{2+3m}}\right)\frac{d\vartheta}{d\zeta} - c_3\vartheta^{\left(\frac{2m}{2+3m}\right)}$$

$$\geq c_1^*\vartheta^{\left(\frac{2-2m}{2+3m}\right)}\frac{d\vartheta}{d\zeta} - c_3\vartheta^{\left(\frac{2m}{2+3m}\right)}, \quad (6.10)$$

in $0 \leq \zeta \leq \zeta_0$ for any given positive $\zeta_0 < (c_1/c_2)\vartheta_0^{\left(\frac{4+3m}{2+3m}\right)}$, taking $0 < c_1^* < c_1 - \zeta_0 c_2\vartheta_0^{-\left(\frac{4+3m}{2+3m}\right)}$, provided that $\vartheta \geq \vartheta_0$.

When $0 \leq m \leq \frac{1}{2}$, then we have : $\frac{2m}{2+3m} \leq \frac{2-2m}{2+3m}$.

In this case, as long as $\frac{d\vartheta}{d\zeta} > \vartheta_1 > 0$ for any given positive ϑ_1, $\vartheta \geq \vartheta_0 > 0$ and

$0 \leq \zeta \leq \zeta_0$, then

$$
\begin{aligned}
\frac{d^2\vartheta}{d\zeta^2} \ \geq \ & c_1^* \vartheta^{\left(\frac{2-2m}{2+3m}\right)} \frac{d\vartheta}{d\zeta} - c_3 \vartheta^{\left(\frac{2m}{2+3m}\right)} \\[2mm]
= \ & \frac{1}{2} c_1^* \vartheta^{\left(\frac{2-2m}{2+3m}\right)} \frac{d\vartheta}{d\zeta} + \left(\frac{1}{2} c_1^* \vartheta^{\left(\frac{2-2m}{2+3m}\right)} \frac{d\vartheta}{d\zeta} - c_3 \vartheta^{\left(\frac{2m}{2+3m}\right)} \right) \\[2mm]
> \ & \frac{1}{2} c_1^* \vartheta^{\left(\frac{2-2m}{2+3m}\right)} \frac{d\vartheta}{d\zeta} + c_3 \vartheta^{\left(\frac{2m}{2+3m}\right)} \left(\vartheta_0^{\left(\frac{4m-2}{2+3m}\right)} \vartheta^{\left(\frac{2-4m}{2+3m}\right)} - 1 \right) \quad \text{taking} \quad \vartheta_1 > \frac{2c_3}{c_1^*} \vartheta_0^{\left(\frac{4m-2}{2+3m}\right)} \\[2mm]
\geq \ & \frac{1}{2} c_1^* \vartheta^{\left(\frac{2-2m}{2+3m}\right)} \frac{d\vartheta}{d\zeta}.
\end{aligned}
$$

Integrating,

$$
\frac{d\vartheta}{d\zeta} \geq \frac{d\vartheta}{d\zeta}(0) + \frac{c_1^*}{2} \left(\frac{2+3m}{4+m} \right) \left(\vartheta^{\left(\frac{4+m}{2+3m}\right)} - \vartheta_0^{\left(\frac{4+m}{2+3m}\right)} \right)
$$

$$
\frac{d\zeta}{d\vartheta} \leq \left[\frac{d\vartheta}{d\zeta}(0) + \frac{c_1^*}{2} \left(\frac{2+3m}{4+m} \right) \left(\vartheta^{\left(\frac{4+m}{2+3m}\right)} - \vartheta_0^{\left(\frac{4+m}{2+3m}\right)} \right) \right]^{-1}. \tag{6.11}
$$

By integrating (6.11), we get :

$$
\zeta \leq \int_{\vartheta_0}^{\vartheta} \left[\frac{d\vartheta}{d\zeta}(0) + \frac{c_1^*}{2} \left(\frac{2+3m}{4+m} \right) \left(\vartheta^{\left(\frac{4+m}{2+3m}\right)} - \vartheta_0^{\left(\frac{4+m}{2+3m}\right)} \right) \right]^{-1} d\vartheta.
$$

In particular, $\quad \zeta \leq \displaystyle\int_{\vartheta_0}^{\infty} \left[\frac{d\vartheta}{d\zeta}(0) + \frac{c_1^*}{2} \left(\frac{2+3m}{4+m} \right) \left(\vartheta^{\left(\frac{4+m}{2+3m}\right)} - \vartheta_0^{\left(\frac{4+m}{2+3m}\right)} \right) \right]^{-1} d\vartheta \leq \zeta_0,$

taking $\frac{d\vartheta}{d\zeta}(0) > \vartheta_1$ large enough. Therefore, $\vartheta \to \infty$ as $\zeta \to \zeta^*$ for some $\zeta^* < \zeta_0$ on choosing such $\frac{d\vartheta}{d\zeta}(0)$.

When $m > \frac{1}{2}$, we cannot proceed as above and we must employ another method to demonstrate blow-up of solutions.

We return to (6.10) which is of the general form

$$
\frac{d^2\vartheta}{d\zeta^2} \geq c_1^* \vartheta^\alpha \frac{d\vartheta}{d\zeta} - c_3 \vartheta^\beta,
$$

with the powers satisfying

$$
0 < \alpha = \frac{2-2m}{2+3m} < \beta = \frac{2m}{2+3m} < \alpha + 1 = \frac{4+m}{2+3m}.
$$

We set $P = \frac{d\vartheta}{d\zeta}$, and

$$
\frac{d^2\vartheta}{d\zeta^2} = \frac{dP}{d\zeta} = \frac{d\vartheta}{d\zeta} \frac{dP}{d\vartheta} = P \frac{dP}{d\vartheta} \geq c_1^* \vartheta^\alpha \frac{d\vartheta}{d\zeta} - c_3 \vartheta^\beta = c_1^* \vartheta^\alpha P - c_3 \vartheta^\beta.
$$

Then

$$\frac{dP}{d\vartheta} \geq c_1^* \vartheta^\alpha - c_3 \vartheta^\beta / P \quad \text{as long as} \quad P \geq \vartheta_1 > 0, \quad \vartheta \geq \vartheta_0 > 0.$$

Supposing that $\quad P > c_3^* \vartheta^{\alpha+1} \quad$ for $\quad \vartheta_0 \leq \vartheta < \vartheta^* \quad$ and some $\quad c_3^* > 0,$

$$\frac{dP}{d\vartheta} > c_1^* \vartheta^\alpha - \frac{c_3}{c_3^*} \vartheta^{\beta-\alpha-1},$$

which gives $\quad P > \vartheta_1 + \dfrac{c_1^*}{\alpha+1}\vartheta^{\alpha+1} - \dfrac{c_3}{c_3^*(\beta-\alpha)}\vartheta^{\beta-\alpha} - \dfrac{c_1^*}{\alpha+1}\vartheta_0^{\alpha+1} + \dfrac{c_3}{c_3^*(\beta-\alpha)}\vartheta_0^{\beta-\alpha},$

$$(6.12)$$

on taking $P = \frac{d\vartheta}{d\zeta} = \vartheta_1 > c_3^* \vartheta_0^{\alpha+1}$ at $\zeta = 0$, where $\vartheta = \vartheta_0$.

We now choose $c_3^* = \frac{c_1^*}{2(\alpha+1)}$, and ϑ_1 large enough, such that

$$\vartheta_1 + \frac{c_1^*}{2(\alpha+1)}\vartheta^{\alpha+1} - \frac{c_3}{c_3^*(\beta-\alpha)}\vartheta^{\beta-\alpha} - \frac{c_1^*}{\alpha+1}\vartheta_0^{\alpha+1} + \frac{c_3}{c_3^*(\beta-\alpha)}\vartheta_0^{\beta-\alpha} > 0 \quad \text{for} \quad \vartheta \geq \vartheta_0,$$

then $\quad \vartheta_1 + \dfrac{c_1^*}{\alpha+1}\vartheta^{\alpha+1} - \dfrac{c_3}{c_3^*(\beta-\alpha)}\vartheta^{\beta-\alpha} - \dfrac{c_1^*}{\alpha+1}\vartheta_0^{\alpha+1} + \dfrac{c_3}{c_3^*(\beta-\alpha)}\vartheta_0^{\beta-\alpha} > \dfrac{c_1^*}{2(\alpha+1)}\vartheta^{\alpha+1}$

$$= c_3^* \vartheta^{\alpha+1}.$$

Assuming some smallest $\vartheta^* > \vartheta_0$ such that $P = c_3^*(\vartheta^*)^{\alpha+1}$, we get a contradiction from (6.12). Therefore,

$$\frac{d\vartheta}{d\zeta} > c_3^* \vartheta^{\alpha+1} \quad \text{for} \quad \vartheta > \vartheta_0.$$

Taking $\frac{d\vartheta}{d\zeta}(0) = \vartheta_1$ large enough then gives blow-up before ζ_0. This would make S no longer small (in contradiction of our original assumptions) as $z \to -t^{-\beta}\zeta^*$.

$(2)^*$ ϑ can fall to zero at some finite value of ζ.

First note that if $\frac{d\vartheta}{d\zeta} = 0$ and $\vartheta > 0$ then $\frac{d^2\vartheta}{d\zeta^2} < 0$. Thus taking $\frac{d\vartheta}{d\zeta}(0) \leq 0$ gives $\frac{d\vartheta}{d\zeta} < 0$ in $\zeta > 0$ as long as $0 < \vartheta < \vartheta_0 = \vartheta(0)$.

Also, from equation (6.9), taking some $\zeta_0 > 0$, as long as $\vartheta > 0$,

$$\frac{d^2\vartheta}{d\zeta^2} \; < \; \left(c_1\vartheta^{\left(\frac{2-2m}{2+3m}\right)} - c_2\zeta\vartheta^{\left(\frac{-2-m}{2+3m}\right)} \right) \frac{d\vartheta}{d\zeta}$$

$$\leq \; \left(c_1\vartheta^{\left(\frac{2-2m}{2+3m}\right)} - c_2\zeta_0\vartheta^{\left(\frac{-2-m}{2+3m}\right)} \right) \frac{d\vartheta}{d\zeta} \quad \text{for} \quad \zeta < \zeta_0 \quad \text{since we have} \quad \frac{d\vartheta}{d\zeta} \leq 0.$$

$$(6.13)$$

Then we get, on integrating,

$$\frac{d\vartheta}{d\zeta} < \frac{d\vartheta}{d\zeta}(0) + c_1\left(\frac{2+3m}{4+m}\right)\vartheta^{\left(\frac{4+m}{2+3m}\right)} - c_1\left(\frac{2+3m}{4+m}\right)\vartheta_0^{\left(\frac{4+m}{2+3m}\right)}$$

$$- c_2\left(\frac{2+3m}{2m}\right)\zeta_0\vartheta^{\left(\frac{2m}{2+3m}\right)} + c_2\left(\frac{2+3m}{2m}\right)\zeta_0\vartheta_0^{\left(\frac{2m}{2+3m}\right)}. \quad (6.14)$$

Therefore,

$$\frac{d\vartheta}{d\zeta} < \frac{d\vartheta}{d\zeta}(0) + c_2\left(\frac{2+3m}{2m}\right)\zeta_0\vartheta_0^{\left(\frac{2m}{2+3m}\right)},$$

so

$$\vartheta < \vartheta_0 + \left(\frac{d\vartheta}{d\zeta}(0) + c_2\left(\frac{2+3m}{2m}\right)\zeta_0\vartheta_0^{\left(\frac{2m}{2+3m}\right)}\right)\zeta = 0,$$

at some $\hat{\zeta} < \zeta_0$, taking $\frac{d\vartheta}{d\zeta}(0)$ large enough negative. In terms of the earlier scaled variables, S falls to zero as $z \to -t^{-\beta}\hat{\zeta}$, see Figure 6.2.

We now have two quite distinct behaviours for ϑ, depending upon its derivative at $\zeta = 0$: $(1)^*$ it can tend to infinity at some finite ζ; $(2)^*$ it can fall to zero at some finite value of ζ_0. Other types of behaviour might be possible for intermediate values of $\frac{d\vartheta}{d\zeta}(0)$ and here we conjecture, because of the contrasting characteristics of $(1)^*$ and $(2)^*$, that some values of $\frac{d\vartheta}{d\zeta}(0)$, for a given $\vartheta_0 = \vartheta(0) > 0$, lead to a solution $\vartheta(\zeta)$ which exists and is positive for all ζ.

To strengthen the evidence for this conjecture, we try to rule out the other sort of solution which can connect the family of solutions of type $(1)^*$ and that of type $(2)^*$, namely assumed solutions which become large at bounded, and bounded away from 0, ζ, and then decrease, see Figure 6.1.
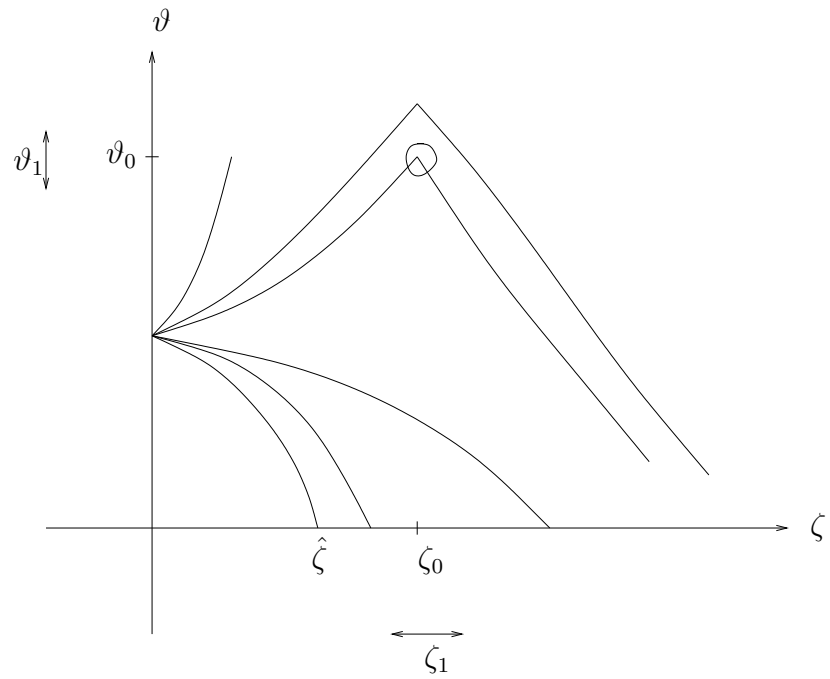
Figure 6.1: Assumed solution having some solutions for (6.9) which are very large at finite values of ζ but then decay.
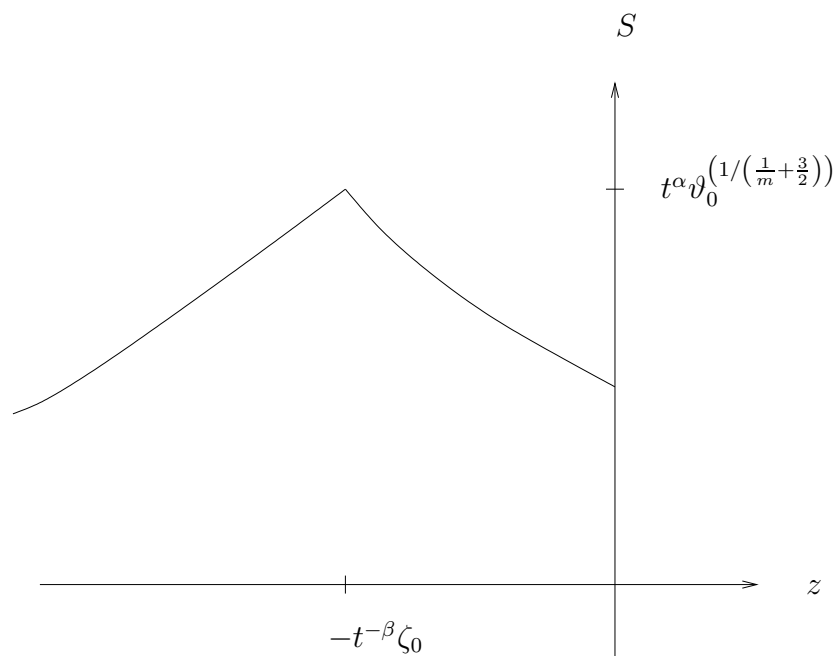
Figure 6.2: The assumed solution, as in Figure 6.1, in terms of the original variables S and z.

First of all, (6.9) can be written as :

$$\frac{d^2\vartheta}{d\zeta^2} = (c_1\vartheta^{\alpha_1} - c_2\zeta\vartheta^{\alpha_2})\frac{d\vartheta}{d\zeta} - c_3\vartheta^{\alpha_3} \tag{6.15}$$

where $\alpha_1 = \left(\frac{2-2m}{2+3m}\right)$, $\alpha_2 = \frac{-(2+m)}{2+3m}$ and $\alpha_3 = \left(\frac{2m}{2+3m}\right)$. Near the maximum of ϑ (circled region in Figure 6.1) we make the following change of variables :

$$\vartheta = \vartheta_0 + \vartheta_1\hat{\vartheta}, \quad \zeta = \zeta_0 + \zeta_1\hat{\zeta} \quad \text{with} \quad \vartheta_0 \gg 1 \quad \text{and} \quad \zeta_0 = O(1).$$

Then substituting the values of ϑ and ζ into (6.15), we have

$$\left(\frac{\vartheta_1}{\zeta_1^2}\right)\frac{d^2\hat{\vartheta}}{d\hat{\zeta}^2} = \left[c_1\left(\vartheta_0 + \vartheta_1\hat{\vartheta}\right)^{\alpha_1} - c_2\left(\zeta_0 + \zeta_1\hat{\zeta}\right)\left(\vartheta_0 + \vartheta_1\hat{\vartheta}\right)^{\alpha_2}\right]\frac{\vartheta_1}{\zeta_1}\frac{d\hat{\vartheta}}{d\hat{\zeta}}$$

$$- \; c_3\left(\vartheta_0 + \vartheta_1\hat{\vartheta}\right)^{\alpha_3},$$

so $\quad \left(\frac{\vartheta_1}{\zeta_1^2}\right)\frac{d^2\hat{\vartheta}}{d\hat{\zeta}^2} \sim \left[c_1\vartheta_0^{\alpha_1} + c_1\alpha_1\vartheta_0^{\alpha_1-1}\vartheta_1\hat{\vartheta} + \cdots - c_2\left(\zeta_0 + \zeta_1\hat{\zeta}\right)\left(\vartheta_0^{\alpha_2} + \alpha_2\vartheta_0^{\alpha_2-1}\vartheta_1\hat{\vartheta} + \cdots\right)\right]$

$$\times \; \frac{\vartheta_1}{\zeta_1}\frac{d\hat{\vartheta}}{d\hat{\zeta}} - c_3\left(\vartheta_0^{\alpha_3} + \alpha_3\vartheta_0^{\alpha_3-1}\vartheta_1\hat{\vartheta} + \cdots\right)$$

$$\sim \; \left(c_1\vartheta_0^{\alpha_1} \cdots - c_2\zeta_0\vartheta_0^{\alpha_2} \cdots\right)\frac{\vartheta_1}{\zeta_1}\frac{d\hat{\vartheta}}{d\hat{\zeta}} - c_3\vartheta_0^{\alpha_3} \cdots .$$

Because α_2 is negative, the term $-c_2\zeta_0\vartheta_0^{\alpha_2}\frac{\vartheta_1}{\zeta_1}\frac{d\hat{\vartheta}}{d\hat{\zeta}}$ can be neglected. Then we get

$$\left(\frac{\vartheta_1}{\zeta_1^2}\right)\frac{d^2\hat{\vartheta}}{d\hat{\zeta}^2} \sim \left(\frac{c_1\vartheta_0^{\alpha_1}\vartheta_1}{\zeta_1}\right)\frac{d\hat{\vartheta}}{d\hat{\zeta}} - c_3\vartheta_0^{\alpha_3}. \tag{6.16}$$

Dividing (6.16) through by $\frac{\vartheta_1}{\zeta_1^2}$, we have

$$\frac{d^2\hat{\vartheta}}{d\hat{\zeta}^2} \sim (c_1\vartheta_0^{\alpha_1}\zeta_1)\frac{d\hat{\vartheta}}{d\hat{\zeta}} - \frac{c_3\vartheta_0^{\alpha_3}\zeta_1^2}{\vartheta_1}.$$

To get a balance in this equation, we must choose ϑ_1 and ζ_1 as follows :

$$\zeta_1 = \frac{1}{c_1\vartheta_0^{\alpha_1}}, \qquad \vartheta_1 = \frac{c_3\vartheta_0^{\alpha_3}}{c_1\vartheta_0^{\alpha_1}}.$$

We have now

$$\frac{d^2\hat{\vartheta}}{d\hat{\zeta}^2} \sim \frac{d\hat{\vartheta}}{d\hat{\zeta}} - 1.$$

The solution in Figure 6.1 must come up linearly and then go exponentially down again (see Figure 6.3). In the earlier regime, where $\hat{\vartheta}$ is behaving linearly, $\hat{\zeta} \to -\infty$, i.e. $\vartheta < \vartheta_0$, the second derivative is negligible.
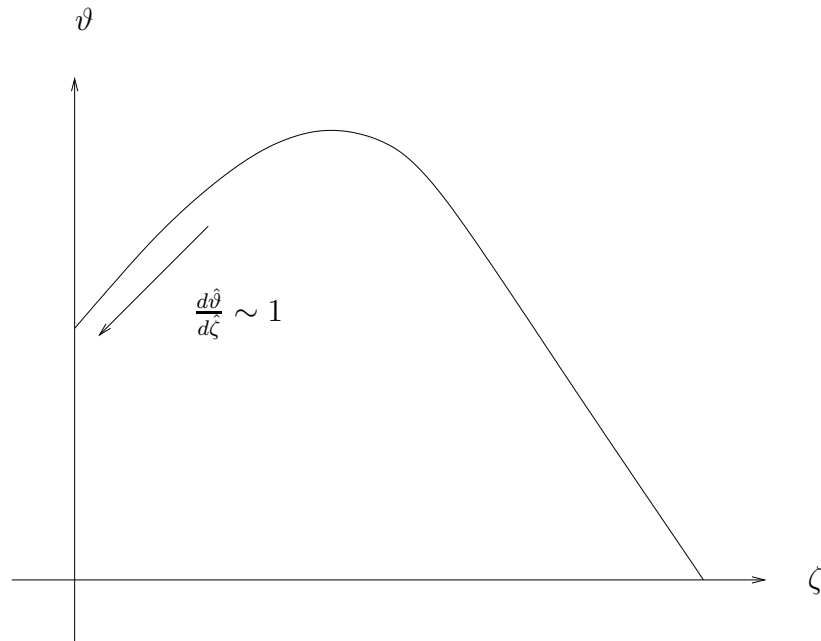
Figure 6.3: Expanded view of the regime near the maximum (circled in Figure 6.1).

We therefore now look at the earlier, $\zeta < \zeta_0$, regime where the second derivative is unimportant where equation (6.15) is approximated by

$$(c_1 \vartheta^{\alpha_1} - c_2 \zeta \vartheta^{\alpha_2}) \frac{d\vartheta}{d\zeta} \sim c_3 \vartheta^{\alpha_3}, \tag{6.17}$$

and we shall want to match with the regime around $\zeta - \zeta_0 = O(\vartheta_0^{-\alpha_1})$, $\vartheta - \vartheta_0 = O(\vartheta_0^{\alpha_3 - \alpha_1})$ just looked at above. For $\vartheta \gg 1$ (large), (6.17) reduces to

$$c_1 \vartheta^{\alpha_1} \frac{d\vartheta}{d\zeta} \sim c_3 \vartheta^{\alpha_3} \quad \text{since} \quad \alpha_2 < 0 < \alpha_1, \tag{6.18}$$

and ζ is bounded. But $\alpha_3 - \alpha_1 < 1$, so (6.18) does not give ϑ becoming large in finite ζ and we do not, after all, approach, let alone match with, the regime previously considered. This suggests strongly we do not get behaviour as in Figure 6.1.

We therefore expect a solution to exist for all $\zeta \geq 0$, and we now look for possible asymptotic behaviour as $\zeta \to \infty$. We expect the highest derivative to be relatively

small so we try to balance terms on the right hand side of equation (6.9) and neglect the $\frac{d^2\vartheta}{d\zeta^2}$ term. The first term on the right is positive while the second and third are negative so we need to balance them.

Then

$$c_1\vartheta^{\left(\frac{2-2m}{2+3m}\right)}\frac{d\vartheta}{d\zeta} \sim c_2\zeta\vartheta^{\frac{-(2+m)}{2+3m}}\frac{d\vartheta}{d\zeta} + c_3\vartheta^{\left(\frac{2m}{2+3m}\right)} \tag{6.19}$$

so

$$c_1\vartheta^{\left(\frac{2-2m}{2+3m}-\frac{2m}{2+3m}\right)}\frac{d\vartheta}{d\zeta} \sim c_2\zeta\vartheta^{\left(\frac{-(2+m)}{2+3m}-\frac{2m}{2+3m}\right)}\frac{d\vartheta}{d\zeta} + c_3,$$

$$\text{i.e.} \quad c_1\vartheta^{\frac{2-4m}{2+3m}}\frac{d\vartheta}{d\zeta} \sim c_2\zeta\vartheta^{-1}\frac{d\vartheta}{d\zeta} + c_3,$$

$$\text{or} \quad \left(c_1\vartheta^{\frac{2-4m}{2+3m}} - c_2\frac{\zeta}{\vartheta}\right)\frac{d\vartheta}{d\zeta} \sim c_3. \tag{6.20}$$

We look for solutions of the form $\vartheta \sim K\zeta^{\frac{2+3m}{4-m}}$. There are two reasons behind this sort of behaviour. The first one is that this balances the first and second terms. The other reason is because such behaviour is also given by balancing the first and third term, which might be just expected initially from what we knew what happened from previous work [2] for the special case of $m = \frac{1}{2}$, when $\vartheta \sim K\zeta$.

Then by substituting this into (6.20), we get

$$c_1K^{\left(\frac{2-4m}{2+3m}+1\right)}\left(\frac{2+3m}{4-m}\right)\zeta^{\left(\frac{2-4m}{4-m}\right)}\zeta^{\left(\frac{-2+4m}{4-m}\right)} - c_2\frac{1}{\zeta^{\left(\frac{-2+4m}{4-m}\right)}}\left(\frac{2+3m}{4-m}\right)\zeta^{\left(\frac{-2+4m}{4-m}\right)} \sim c_3,$$

$$\text{so} \quad c_1\left(\frac{2+3m}{4-m}\right)K^{\left(\frac{4-m}{2+3m}\right)} = c_2\left(\frac{2+3m}{4-m}\right) + c_3,$$

$$K = \left[\frac{\left(\frac{2+3m}{4-m}\right)c_2 + c_3}{\left(\frac{2+3m}{4-m}\right)c_1}\right]^{\frac{2+3m}{4-m}}.$$

Thus

$$K = \left[\frac{nc_2 + c_3}{nc_1}\right]^n, \quad n = \frac{2+3m}{4-m} \quad (n = 1 \quad \text{for} \quad m = \frac{1}{2}). \tag{6.21}$$

From (6.21), we have then :

$$\vartheta \sim \left[\frac{nc_2 + c_3}{nc_1}\right]^n\zeta^n, \quad n = \frac{2+3m}{4-m}. \tag{6.22}$$

From (6.1), (6.8) and (6.22), we can get the self-similar solutions to our model (5.13) when $S \to 0$ as follows :

$$\Phi^{\left(\frac{1}{m}+\frac{3}{2}\right)} \sim \left[\frac{nc_2 + c_3}{nc_1}\right]^n(-\xi)^n,$$

$$\Phi^{\left(\frac{2+3m}{2m}\right)} \sim \left[\frac{nc_2 + c_3}{nc_1}\right]^{\left(\frac{2+3m}{4-m}\right)} (-\xi)^{\left(\frac{2+3m}{4-m}\right)},$$

$$\text{so} \quad \Phi \sim \left[\frac{nc_2 + c_3}{nc_1}\right]^{\left(\frac{2m}{4-m}\right)} (-\xi)^{\left(\frac{2m}{4-m}\right)}.$$

Multiplying by t^α :

$$S(t, z) = t^\alpha \Phi \sim \left[\frac{nc_2 + c_3}{nc_1}\right]^{\left(\frac{2m}{4-m}\right)} t^\alpha (-zt^\beta)^{\left(\frac{2m}{4-m}\right)}.$$

Thus

$$S(t, z) \sim \left[\frac{nc_2 + c_3}{nc_1}\right]^{\left(\frac{2m}{4-m}\right)} t^\alpha (-zt^\beta)^{\left(\frac{2m}{4-m}\right)}$$

$$\sim \left[\frac{nc_2 + c_3}{nc_1}\right]^{\left(\frac{2m}{4-m}\right)} t^{\left(\frac{-2m}{3(2-m)}\right)} (-z)^{\left(\frac{2m}{4-m}\right)} t^{\left(\frac{2m-2}{3(2-m)} \frac{2m}{4-m}\right)}$$

$$\sim \left[\frac{nc_2 + c_3}{nc_1}\right]^{\left(\frac{2m}{4-m}\right)} (-z)^{\left(\frac{2m}{4-m}\right)} t^{\frac{-2m}{3(2-m)}\left(1 + \frac{2(1-m)}{4-m}\right)}$$

$$\sim \left[\frac{nc_2 + c_3}{nc_1}\right]^{\left(\frac{2m}{4-m}\right)} (-z)^{\left(\frac{2m}{4-m}\right)} t^{\left(\frac{-2m}{4-m}\right)}. \tag{6.23}$$

We simply found that the powers of t giving S and the similarity variable are both negative ($\alpha < 0, \beta < 0$). This means that we can say, for fixed z, as $t \to \infty$, $t^\alpha \to 0$, $zt^\beta \to 0$, then $\Phi(zt^\beta) \to \Phi_0$. Therefore, $S \sim t^\alpha \Phi_0 \to 0$ but this is not interesting behaviour as there is no spatial, z, dependence as $\Phi \sim \vartheta_0^{\frac{1}{\left(\frac{1}{m} + \frac{3}{2}\right)}}$.

To get the right asymptotic behaviour of Φ we need $zt^\beta \to -\infty$ (ξ large). For S small, we also need, $t^\alpha \Phi(zt^\beta) = t^\alpha(-zt^\beta)^{\left(\frac{2m}{4-m}\right)} = (-z)^{\left(\frac{2m}{4-m}\right)} t^{\left(\frac{-2m}{4-m}\right)}$ to be small, along with $zt^\beta = zt^{\left(\frac{-2(1-m)}{3(2-m)}\right)}$ to be large.

Taking the $\left(\frac{4-m}{2m}\right)$th power of the former, then we get zt^{-1} small (or tz^{-1} large). Then $z \ll t$.

We also require : $zt^{\left(\frac{-2(1-m)}{3(2-m)}\right)} \gg 1$.

Because $z \ll t$, we then have :

$$t \times t^{\left(\frac{-2(1-m)}{3(2-m)}\right)} = t^{\left(1 - \frac{2(1-m)}{3(2-m)}\right)} = t^{\left(\frac{4-m}{3(2-m)}\right)} \gg zt^{\left(\frac{-2(1-m)}{3(2-m)}\right)} \gg 1.$$

Then $t \gg 1$. Therefore, $t \gg z \gg t^{\left(\frac{2(1-m)}{3(2-m)}\right)} \gg 1$.

Based on t being large then this similarity solution applies, and S is of the form (6.23) and small.

For the special case when $m = 0$, we have :

$$t \gg z \gg t^{\frac{1}{3}} \gg 1.$$

We cannot do $m = 1$ because it gives $\frac{2(1-m)}{3(2-m)} = 0$ making $t^{\left(\frac{2(1-m)}{3(2-m)}\right)} \gg 1$ impossible.

6.2.2   Case 2 : $S \to 1$

In this case, we seek self-similar solutions of equation (5.13) in the form :

$$S(t, z) = 1 - t^\alpha \Phi(\xi), \qquad \xi = zt^\beta, \tag{6.24}$$

where α and β are again some unknown exponents to be determined. By substituting (6.24) in (5.13) we have

$$\phi\left(\alpha\Phi + \beta\xi\frac{d\Phi}{d\xi}\right) = t^{(2\beta+1)}\frac{d}{d\xi}\left\{\delta D(1 - t^\alpha\Phi)\frac{d\Phi}{d\xi} - t^{-(\alpha+\beta)}K(1 - t^\alpha\Phi)\right\}. \tag{6.25}$$

For m fixed, we have the approximations of the functions $D(1 - t^\alpha\Phi)$ and $K(1 - t^\alpha\Phi)$ when $S = 1 - m\sigma \to 1$ (see (5.3) and (5.5)) as follows :

$$D(S) \sim D(1 - m\sigma) \sim \sigma^{-m} \quad \text{for} \quad \sigma \to 0,$$

$$K(S) \sim K(1 - m\sigma) \sim 1 - 2\sigma^m.$$

Therefore, we have

$$D(1 - mt^\alpha\Phi) \sim (t^\alpha\Phi)^{-m} \sim t^{-m\alpha}\Phi^{-m} \quad \text{and} \tag{6.26}$$

$$K(1 - mt^\alpha\Phi) \sim 1 - 2(t^\alpha\Phi)^m \sim 1 - 2t^{\alpha m}\Phi^m. \tag{6.27}$$

By substituting (6.26) and (6.27) into (6.25), we get

$$\begin{aligned}
\phi\left(\alpha\Phi + \beta\xi\frac{d\Phi}{d\xi}\right) &= t^{(2\beta+1)}\frac{d}{d\xi}\left\{\delta t^{-m\alpha}\Phi^{-m}\frac{d\Phi}{d\xi} - t^{-(\alpha+\beta)}\left(1 - 2t^{\alpha m}\Phi^m\right)\right\} \\
&= t^{(2\beta+1-m\alpha)}\frac{d}{d\xi}\left(\delta\Phi^{-m}\frac{d\Phi}{d\xi}\right) - \frac{d}{d\xi}t^{(\beta+1-\alpha)} + 2t^{(\beta+1-\alpha+\alpha m)}\frac{d\Phi^m}{d\xi} \\
&= t^{(2\beta+1-m\alpha)}\frac{d}{d\xi}\left(\delta\Phi^{-m}\frac{d\Phi}{d\xi}\right) + 2t^{(\beta+1-\alpha(1-m))}\frac{d\Phi^m}{d\xi}. \tag{6.28}
\end{aligned}$$

Equation (6.28) is, in general, dependent on t. According to the general theory of self-similar solutions, we have to determine the values of the exponents α and β so that equation (6.28) depends only on the self-similar variable ξ and does not depend

on t. For this, we need

$$2\beta + 1 - m\alpha = 0, \qquad \beta + 1 - (1-m)\alpha = 0. \tag{6.29}$$

From (6.29), the values of α and β can be obtained as

$$\alpha = \frac{-1}{3m-2}, \qquad \beta = \frac{1-2m}{3m-2}.$$

Then (6.28) becomes

$$\phi\left(\left(\frac{-1}{3m-2}\right)\Phi + \left(\frac{1-2m}{3m-2}\right)\xi\frac{d\Phi}{d\xi}\right) = \frac{d}{d\xi}\left(\delta\Phi^{-m}\frac{d\Phi}{d\xi}\right) + 2\frac{d}{d\xi}\Phi^m.$$

Setting

$$\zeta = -\xi, \quad \vartheta = \Phi^{-m+1} \quad \text{gives} \quad \frac{d\vartheta}{d\xi} = (-m+1)\Phi^{-m}\frac{d\Phi}{d\xi}, \quad \Phi = \vartheta^{\left(\frac{1}{-m+1}\right)}.$$

Then we have

$$\delta\frac{d}{d\xi}\frac{(-m+1)}{(-m+1)}\Phi^{-m}\frac{d\Phi}{d\xi} + 2\frac{d}{d\xi}\Phi^m = \frac{-\phi}{(3m-2)}\left(\Phi - (1-2m)\xi\frac{d\Phi}{d\xi}\right),$$

$$\left(\frac{\delta}{-m+1}\right)\frac{d^2\vartheta}{d\zeta^2} = \frac{2m}{-m+1}\vartheta^{\left(\frac{2m-1}{-m+1}\right)}\frac{d\vartheta}{d\zeta} + \frac{\phi(1-2m)}{(3m-2)(-m+1)}\zeta\vartheta^{\left(\frac{m}{-m+1}\right)}\frac{d\vartheta}{d\zeta} - \frac{\phi}{(3m-2)}\vartheta^{\left(\frac{1}{-m+1}\right)},$$

$$\frac{d^2\vartheta}{d\zeta^2} = \frac{2m}{\delta}\vartheta^{\left(\frac{2m-1}{1-m}\right)}\frac{d\vartheta}{d\zeta} + \frac{\phi(1-2m)}{\delta(3m-2)}\zeta\vartheta^{\left(\frac{m}{1-m}\right)}\frac{d\vartheta}{d\zeta} - \frac{\phi(1-m)}{\delta(3m-2)}\vartheta^{\left(\frac{1}{1-m}\right)},$$

$$\frac{d^2\vartheta}{d\zeta^2} = c_1\vartheta^{-\left(\frac{1-2m}{1-m}\right)}\frac{d\vartheta}{d\zeta} + c_2\zeta\vartheta^{\left(\frac{m}{1-m}\right)}\frac{d\vartheta}{d\zeta} - c_3\vartheta^{\left(\frac{1}{1-m}\right)}, \tag{6.30}$$

where $c_1 = \frac{2m}{\delta}$, $c_2 = \frac{\phi(1-2m)}{\delta(3m-2)}$ and $c_3 = \frac{\phi(1-m)}{\delta(3m-2)}$.

Now we will try to deal with this equation to get the self-similar solution in the following three cases of m, $m < \frac{1}{2}$, $\frac{1}{2} < m < \frac{2}{3}$, and when $\frac{2}{3} < m < 1$. Note that the special case of $m = \frac{1}{2}$ has been previously considered [2]. We also do not do the case when $m = \frac{2}{3}$ as no (standard) similarity solution can exist for this value. This can be seen in two ways. First, we can look at our resulting similarity ordinary differential equation, (6.30). Rewriting it, we get

$$(3m-2)\frac{d^2\vartheta}{d\zeta^2} = \frac{2m(3m-2)}{\delta}\vartheta^{-\left(\frac{1-2m}{1-m}\right)}\frac{d\vartheta}{d\zeta} + \frac{\phi(1-2m)}{\delta}\zeta\vartheta^{\left(\frac{m}{1-m}\right)}\frac{d\vartheta}{d\zeta} - \frac{\phi(1-m)}{\delta}\vartheta^{\left(\frac{1}{1-m}\right)} \tag{6.31}$$

with $m = \frac{2}{3}$, (6.31) simplifies to

$$\zeta \vartheta^2 \frac{d\vartheta}{d\zeta} + \vartheta^3 = 0$$

Therefore, we have either $\vartheta = 0$ or $\zeta \frac{d\vartheta}{d\zeta} + \vartheta = 0$. For a non-trivial solution, we want the second one, which gives

$$\vartheta = A\zeta^{-1} = \Phi^{\frac{1}{3}} = A(-\xi)^{-1} \quad \text{so} \quad \Phi = -A\xi^{-3}.$$

This clearly fails badly at $\xi = 0$.

The second, and simpler, reason for failure comes from looking at the similarity exponents α and β for which their expressions give infinite values with $m = \frac{2}{3}$.

Case (i) : $m < \frac{1}{2}$

When $m < \frac{1}{2}$, in equation (6.30), c_1 is positive while c_2 and c_3 are negative so that the first term is positive and second term negative, as long as $\frac{d\vartheta}{d\zeta} > 0$, and the third term is always positive. Then from (6.30), we have

$$\frac{d^2\vartheta}{d\zeta^2} = c_1 \vartheta^{-\left(\frac{1-2m}{1-m}\right)} \frac{d\vartheta}{d\zeta} - \hat{c}_2 \zeta \vartheta^{\left(\frac{m}{1-m}\right)} \frac{d\vartheta}{d\zeta} + \hat{c}_3 \vartheta^{\left(\frac{1}{1-m}\right)}, \tag{6.32}$$

on writing $c_2 = -\hat{c}_2$ and $c_3 = -\hat{c}_3$; $\hat{c}_2$ and $\hat{c}_3$ are both positive.

Assuming we have blow-up at some finite positive value $\zeta^* > 0$, so ζ now is close to a constant value, then

$$\frac{d^2\vartheta}{d\zeta^2} \sim \hat{c}_3 \vartheta^{\left(\frac{1}{1-m}\right)} - \hat{c}_2 \vartheta^{\left(\frac{m}{1-m}\right)} \frac{d\vartheta}{d\zeta}. \tag{6.33}$$

Equation (6.33) is an autonomous (no ζ terms) second order differential equation, so that we can use a phase plane approach here to get qualitative behaviour of the solution.

Equivalently, let us again put $\frac{d\vartheta}{d\zeta} = P$. We get

$$P\frac{dP}{d\vartheta} \sim \hat{c}_3 \vartheta^{\left(\frac{1}{1-m}\right)} - \hat{c}_2 \vartheta^{\left(\frac{m}{1-m}\right)} P,$$

$$\text{so} \quad \frac{dP}{d\vartheta} \sim \frac{\hat{c}_3}{P} \vartheta^{\left(\frac{1}{1-m}\right)} - \hat{c}_2 \vartheta^{\left(\frac{m}{1-m}\right)}. \tag{6.34}$$

The nullcline is obtained from (6.34) as follows :

$$\frac{dP}{d\vartheta} = \vartheta^{\left(\frac{m}{1-m}\right)} \left(\frac{\hat{c}_3 \vartheta}{P} - \hat{c}_2 \right) = 0,$$

so

$$P = \frac{\hat{c}_3}{\hat{c}_2}\vartheta.$$

Therefore, the nullcline is linear.
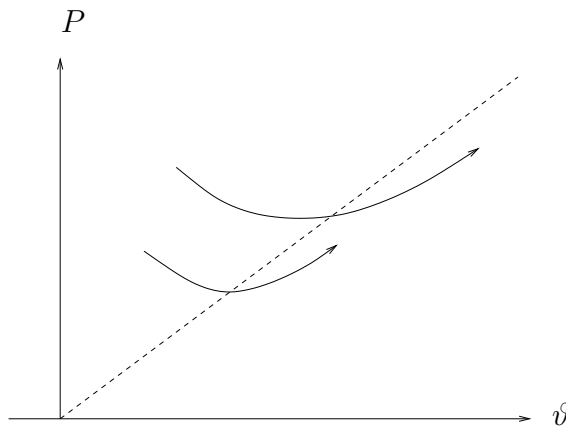
Figure 6.4: Phase plane of (6.34) for ϑ against P. The dotted line represents the nullcline of (6.34).

In (6.34), when $m < 1$, we see that the power $\left(\frac{1}{1-m}\right)$ is bigger than $\left(\frac{m}{1-m}\right)$ so that the term $\frac{\hat{c}_3}{P}\vartheta^{\left(\frac{1}{1-m}\right)}$ increases faster than $\hat{c}_2\vartheta^{\left(\frac{m}{1-m}\right)}$ as a function of ϑ. Therefore, $-\hat{c}_2\vartheta^{\left(\frac{m}{1-m}\right)}$ is coming down and $\frac{\hat{c}_3}{P}\vartheta^{\left(\frac{1}{1-m}\right)}$ is going up. This gives us a phase plane as sketched in Figure 6.4

We see that any solution eventually lies under the straight line $P = \frac{\hat{c}_3}{\hat{c}_2}\vartheta$, i.e. $\frac{d\vartheta}{d\zeta} < \frac{\hat{c}_3}{\hat{c}_2}\vartheta$ for sufficiently large ϑ, which means that there is no blow-up at $\zeta^* > 0$ (see Figure 6.4).

Note from (6.32) that $\frac{d\vartheta}{d\zeta} = 0$ gives $\frac{d^2\vartheta}{d\zeta^2} > 0$.

Hence, taking $\frac{d\vartheta}{d\zeta}(0) \geq 0$, $\frac{d\vartheta}{d\zeta} > 0$ for $\zeta > 0$. As there is no blow-up at finite ζ we deduce that a solution exists and is increasing for all ζ so that $\vartheta \to \infty$ as $\zeta \to \infty$ or $\vartheta \to \vartheta_{\infty-} > 0$ for $\zeta \to \infty$. The latter is impossible because from (6.32) since we see the first and second terms will disappear while the third term is negative. Then we have from (6.32)

$$\vartheta \to \infty \quad \text{as} \quad \zeta \to \infty.$$

We have a solution which exists for all ζ, although it does not appear to be behaving in a suitable way i.e. it does not $\to 0$ as $\zeta \to \infty$. But as we now have evidence of global solutions, we now see what sort of asymptotic behaviour might be possible.

We might also have global decreasing as well as global increasing solutions.

The first and second terms of (6.32) are negative and the third one is positive. According to this, we try to balance terms on the right hand side of this equation and neglect the left hand side as follows

$$-c_1 \vartheta^{\left(\frac{2m-1}{1-m}\right)} \frac{d\vartheta}{d\zeta} \sim -\hat{c}_2 \zeta \vartheta^{\left(\frac{m}{1-m}\right)} \frac{d\vartheta}{d\zeta} + \hat{c}_3 \vartheta^{\left(\frac{1}{1-m}\right)},$$

$$-c_1 \vartheta^{\left(\frac{2m-2}{1-m}\right)} \frac{d\vartheta}{d\zeta} \sim -\hat{c}_2 \zeta \vartheta^{\left(\frac{m-1}{1-m}\right)} \frac{d\vartheta}{d\zeta} + \hat{c}_3,$$

$$\text{so} \quad \left(-c_1 \vartheta^{-2} + \hat{c}_2 \frac{\zeta}{\vartheta}\right) \frac{d\vartheta}{d\zeta} \sim \hat{c}_3. \tag{6.35}$$

Now if we compare the first and third terms, we want $\vartheta \sim K\zeta^{-1}$, then we substitute this into (6.35)

$$c_1 \left(K\zeta^{-1}\right)^{-2} K\zeta^{-2} - \hat{c}_2 \zeta \left(K\zeta^{-1}\right)^{-1} K\zeta^{-2} \sim \hat{c}_3,$$

$$c_1 K^{-1} - \hat{c}_2 \sim \hat{c}_3,$$

and we actually get a balance for all three terms.

Then

$$\vartheta \sim K\zeta^{-1} \quad \text{with} \quad K = \frac{c_1}{\hat{c}_2 + \hat{c}_3}.$$

We now set

$$\zeta = -\xi, \quad \vartheta = \Phi^{-m+1}, \quad \alpha = \frac{-1}{3m-2} > 0, \quad \beta = \frac{1-2m}{3m-2} < 0$$

$$\text{in} \quad S(t, z) = 1 - t^\alpha \Phi(\xi), \quad \xi = zt^\beta.$$

We try to get the self-similar solutions when $S \to 1$ as follows :

$$\Phi^{-m+1} \quad \sim \quad K(-\xi)^{-1}$$

$$\sim \quad \frac{c_1}{\hat{c}_2 + \hat{c}_3}(-\xi)^{-1}.$$

Then

$$\Phi = \left(\frac{c_1}{\hat{c}_2 + \hat{c}_3}\right)^{\left(\frac{1}{1-m}\right)} (-\xi)^{\left(\frac{-1}{1-m}\right)}.$$

Multiply this by $-t^\alpha$, then add 1 to both sides :

$$-t^\alpha \Phi = -\left(\frac{c_1}{\hat{c}_2 + \hat{c}_3}\right)^{\left(\frac{1}{1-m}\right)} \left(-zt^\beta\right)^{\left(\frac{-1}{1-m}\right)} (t^\alpha),$$

$$1 - t^\alpha \Phi = 1 - \left(\frac{c_1}{\hat{c}_2 + \hat{c}_3}\right)^{\left(\frac{1}{1-m}\right)} (t^\alpha) \left(-zt^\beta\right)^{\left(\frac{-1}{1-m}\right)},$$

$$S(t,z) = 1 - \left(\frac{c_1}{\hat{c}_2 + \hat{c}_3}\right)^{\left(\frac{1}{1-m}\right)} \left(t^{\left(\frac{-1}{3m-2}\right)}\right) \left(-zt^{\left(\frac{1-2m}{3m-2}\right)}\right)^{\left(\frac{-1}{1-m}\right)}.$$

To make $S \to 1$ while still having our limit of $|\xi| = |zt^\beta| \to \infty$, we want

$$zt^{\left(\frac{1-2m}{3m-2}\right)} \gg 1 \gg z^{\left(\frac{-1}{1-m}\right)}t^{\frac{-1}{3m-2}\left(1+\frac{1-2m}{1-m}\right)} = z^{\left(\frac{-1}{1-m}\right)}t^{\left(\frac{1}{1-m}\right)}.$$

Then

$$\frac{t}{z} \ll 1 \iff t \ll z,$$

$$\text{while} \quad zt^{\left(-\frac{1-2m}{2-3m}\right)} \gg 1 \iff z \gg t^{\left(\frac{1-2m}{2-3m}\right)}.$$

We compare powers of t here : $\frac{1-2m}{2-3m} - 1 = \frac{m-1}{2-3m} < 0$, so $1 > \frac{1-2m}{2-3m} > 0$. Therefore,

$$z \gg \max\left\{t, t^{\left(\frac{1-2m}{2-3m}\right)}\right\} = \begin{cases} t & \text{for } t \gg 1 \\ t^{\left(\frac{1-2m}{2-3m}\right)} & \text{for } t \ll 1 \end{cases}$$

The similarity solution will then work for z large (t is fixed of order one) and for t small (z is fixed of order one).

Case (ii) : $\frac{1}{2} < m < \frac{2}{3}$

(1) For $\frac{1}{2} < m < \frac{2}{3}$, we see from equation (6.30) that c_1 and c_2 are both positive but c_3 is negative.

Take an initial value $\vartheta(0) = \vartheta_0 > 0$. This means $\frac{d\vartheta}{d\zeta} \geq 0$ at $\zeta = 0$, then $\frac{d\vartheta}{d\zeta} \geq 0$ as long as the solution exists in $\zeta \geq 0$ giving $\vartheta(\zeta) \geq \vartheta_0 > 0$ for $\zeta \geq 0$.

From (6.30), we have :

$$\frac{d^2\vartheta}{d\zeta^2} \geq c_2\zeta\vartheta^{\left(\frac{m}{1-m}\right)}\frac{d\vartheta}{d\zeta} - c_3\vartheta^{\left(\frac{1}{1-m}\right)}$$

$$> c_2\zeta\vartheta^{\left(\frac{m}{1-m}\right)}\frac{d\vartheta}{d\zeta} \geq 0 \quad \text{because} \quad c_3 < 0.$$

Assuming no blow-up, ϑ exists at $\zeta = \zeta_1$ for some $\zeta_1 > 0$.
Then for $\zeta \geq \zeta_1$,

$$\frac{d^2\vartheta}{d\zeta^2} > c_2\zeta_1\vartheta^{\left(\frac{m}{1-m}\right)}\frac{d\vartheta}{d\zeta}.$$

Integrating,

$$\frac{d\vartheta}{d\zeta}(\zeta) \geq \frac{d\vartheta}{d\zeta}(\zeta_1) + c_2\zeta_1(1-m)\vartheta^{\left(\frac{1}{1-m}\right)} - c_2\zeta_1(1-m)\vartheta(\zeta_1)^{\left(\frac{1}{1-m}\right)} \quad \text{for} \quad \zeta \geq \zeta_1,$$

where $\frac{d\vartheta}{d\zeta}(\zeta_1) > \frac{d\vartheta}{d\zeta}(0)$.

Hence $\quad \dfrac{d\vartheta}{d\zeta}(\zeta) \geq \dfrac{d\vartheta}{d\zeta}(0) + c_2\zeta_1(1-m)\left(\vartheta^{\left(\frac{1}{1-m}\right)} - \vartheta(\zeta_1)^{\left(\frac{1}{1-m}\right)}\right).$

Integrating again, we get

$$\zeta - \zeta_1 \;\leq\; \int_{\vartheta(\zeta_1)}^{\vartheta}\left(\dfrac{d\vartheta}{d\zeta}(0) + c_2\zeta_1(1-m)\left(\vartheta^{\left(\frac{1}{1-m}\right)} - \vartheta(\zeta_1)^{\left(\frac{1}{1-m}\right)}\right)\right)^{-1} d\vartheta$$

$$<\;\; \zeta^*,$$

where $\quad \zeta^* = \displaystyle\int_{\vartheta(\zeta_1)}^{\infty}\left(\dfrac{d\vartheta}{d\zeta}(0) + c_2\zeta_1(1-m)\left(\vartheta^{\left(\frac{1}{1-m}\right)} - \vartheta(\zeta_1)^{\left(\frac{1}{1-m}\right)}\right)\right)^{-1} d\vartheta < \infty.$

Then $\zeta \leq \zeta_1 + \zeta^*$ and we have blow-up before $\zeta_1 + \zeta^*$.

(2) Now, we want ϑ to fall to zero at finite ζ if $\frac{d\vartheta}{d\zeta}(0)$ is large negative enough. Taking $\frac{d\vartheta}{d\zeta}(0) < 0$, then there must be some interval $[0, \zeta_0]$ such that $\frac{d\vartheta}{d\zeta} < 0$ for $0 \leq \zeta < \zeta_0$ and hence $\vartheta < \vartheta_0$ for $\zeta \in [0, \zeta_0]$. Hence

$$\dfrac{d^2\vartheta}{d\zeta^2} \;<\; c_1\vartheta^{-\left(\frac{1-2m}{1-m}\right)}\dfrac{d\vartheta}{d\zeta} + c_3^*\vartheta^{\left(\frac{1}{1-m}\right)} \quad \text{where} \quad c_3^* = -c_3,$$

$$<\; c_1\vartheta^{-\left(\frac{1-2m}{1-m}\right)}\dfrac{d\vartheta}{d\zeta} + c_3^*\vartheta_0^{\left(\frac{1}{1-m}\right)} \quad \text{for} \quad 0 < \zeta < \zeta_0.$$

Integrating,

$$\dfrac{d\vartheta}{d\zeta} \;<\; \dfrac{d\vartheta}{d\zeta}(0) + \dfrac{c_1(1-m)}{m}\left(\vartheta^{\left(\frac{m}{1-m}\right)} - \vartheta_0^{\left(\frac{m}{1-m}\right)}\right) + c_3^*\vartheta_0^{\left(\frac{1}{1-m}\right)}\zeta$$

$$<\; \dfrac{d\vartheta}{d\zeta}(0) + c_3^*\vartheta_0^{\left(\frac{1}{1-m}\right)}\zeta \leq 0 \quad \text{for} \quad \zeta \leq \zeta_0, \tag{6.36}$$

and

$$\dfrac{d\vartheta}{d\zeta} < 0 \quad \text{for} \quad \zeta \leq \zeta_0 \quad \text{on taking} \quad \zeta_0 = -\dfrac{d\vartheta}{d\zeta}(0)\Big/\left(c_3^*\vartheta_0^{\left(\frac{1}{1-m}\right)}\right),$$

as long as ϑ remains positive.

Now take $\frac{d\vartheta}{d\zeta}(0)$ large negative to integrate (6.36) and get :

$$\vartheta < \vartheta_0 + \left(\dfrac{d\vartheta}{d\zeta}(0) + c_3^*\vartheta_0^{\left(\frac{1}{1-m}\right)}\dfrac{\zeta}{2}\right)\zeta = 0$$

before $\zeta = \zeta_0$. As for the other cases, some solutions blow-up and some of them go to 0. We now conjecture that there will be some solutions which exist for all $\zeta > 0$. To get the large ζ behaviour, in a similar approach to the previous case (i), we will

try to balance terms on the right hand side of (6.30). For this, we have

$$- \left(c_1 \vartheta^{-2} + c_2 \zeta \vartheta^{-1}\right) \frac{d\vartheta}{d\zeta} \sim -c_3. \tag{6.37}$$

Similarly to the previous case, we will substitute the same assumption $\vartheta \sim K\zeta^{-1}$ into (6.37) to get :

$$K = \frac{-c_1}{c_2 + c_3} \quad \Rightarrow \quad \vartheta \sim K\zeta^{-1}.$$

Hence,

$$S(t,z) = 1 - \left(\frac{-c_1}{c_2 + c_3}\right)^{\left(\frac{1}{1-m}\right)} \left(t^{\left(\frac{-1}{3m-2}\right)}\right) \left(-zt^{\left(\frac{1-2m}{3m-2}\right)}\right)^{\left(\frac{-1}{1-m}\right)}.$$

Because $\frac{1}{2} < m < \frac{2}{3}$, we now want

$$zt^{\left(\frac{2m-1}{2-3m}\right)} \gg 1 \gg z^{\left(\frac{-1}{1-m}\right)} t^{\left(\frac{1}{2-3m} - \frac{1}{1-m}\left(\frac{2m-1}{2-3m}\right)\right)} = z^{\left(\frac{-1}{1-m}\right)} t^{\frac{-1}{2-3m}\left(\frac{2m-1}{1-m} - 1\right)} = z^{\left(\frac{-1}{1-m}\right)} t^{\left(\frac{1}{1-m}\right)}$$

to simultaneously get $t^\alpha \Phi$ small and $|zt^\beta|$ large.

$$\text{Now} \quad zt^{\left(\frac{2m-1}{2-3m}\right)} \gg 1, \quad \frac{t}{z} \ll 1, \text{the latter meaning} \quad t \ll z$$

$$\text{so} \quad z^{\left(\frac{1-m}{2-3m}\right)} = zz^{\left(\frac{2m-1}{2-3m}\right)} \gg zt^{\left(\frac{2m-1}{2-3m}\right)} \gg 1.$$

$$\text{Then} \quad z \gg 1$$

$$\text{with} \quad t \ll z \quad \text{and} \quad t^{\left(\frac{2m-1}{2-3m}\right)} \gg z^{-1} \quad \text{i.e.} \quad t \gg z^{-\left(\frac{2-3m}{2m-1}\right)}.$$

Therefore, z has to be large and t must not to be too large or too small. So, in particular, this case works for z large with t of order 1.

Case (iii) : $\frac{2}{3} < m < 1$

As with the other ranges of m, the aim here is to try to find the qualitative behaviour of solutions of the ODE, and then say how a similarity solution might behave locally. In this case, from equation (6.30) we have that c_1 and c_3 are positive but c_2 is negative.

We first note all eventualities (no matter how unlikely) for solutions :

1) A solution ϑ exists for all ζ (this is what we want);

2) A solution ϑ falls to 0 at some finite ζ;

3) The solution blows-up at a finite value of ζ.

(1) can be broken down according to whether it decays to zero, 1(*a*), is bounded and bounded away from 0, 1(*b*), or tends to infinity as $\zeta \to \infty$, 1(*c*). Finally, 1(*b*) can

be subdivided further according to whether it tends monotonically decreasing towards some ϑ_∞, $0 < \vartheta_\infty < \infty$, $1(b)i$, it increases towards some ϑ_∞, $0 < \vartheta_\infty < \infty$, $1(b)ii$, or continues to oscillate, not necessarily approaching any limit as $\zeta \to \infty$, $1(b)iii$. Figure 6.5 indicates all possibilities.
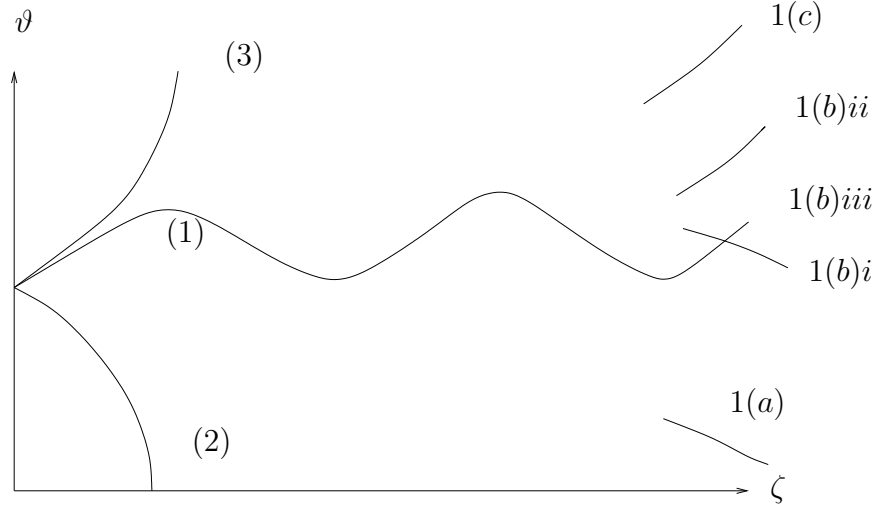
Figure 6.5: The three main possibilities of the types of behaviour of solutions of the ODE. Type 1, it might be oscillating or monotonic : 1(a) ϑ tends to zero, 1(b) ϑ tends to something positive but finite or oscillates or 1(c) ϑ tends to ∞. Type 2 : ϑ falls to zero at finite ζ. Type 3 : becomes infinite as $\zeta \to \zeta_\infty < \infty$.

We first note that when $\frac{2}{3} < m < 1$, the solution cannot oscillate. This is seen immediately from equation (6.30). Where ϑ is positive, it can have a maximum but not a minimum. $1(b)iii$ is ruled out.

Also, $\vartheta \to \infty$ as $\zeta \to \zeta_\infty < \infty$ is not possible because it turns out that ϑ is bounded as will be shown now. First note that because ϑ cannot have a local minimum, if it was to be unbounded then $\frac{d\vartheta}{d\zeta} > 0$ for all $\zeta \geq 0$.
From (6.30), we have the inequality

$$\frac{d^2\vartheta}{d\zeta^2} \; < \; c_1 \vartheta^{\left(\frac{2m-1}{1-m}\right)} \frac{d\vartheta}{d\zeta} + c_2 \zeta \vartheta^{\left(\frac{m}{1-m}\right)} \frac{d\vartheta}{d\zeta}$$

$$\leq \; c_1 \vartheta^{\left(\frac{2m-1}{1-m}\right)} \frac{d\vartheta}{d\zeta} + c_2 \zeta_1 \vartheta^{\left(\frac{m}{1-m}\right)} \frac{d\vartheta}{d\zeta} \quad \text{for} \quad \zeta \geq \zeta_1 > 0, \quad \text{as long as} \quad \frac{d\vartheta}{d\zeta} \geq 0.$$

Then, by integrating this inequality, we have

$$\frac{d\vartheta}{d\zeta}(\zeta) - \frac{d\vartheta}{d\zeta}(\zeta_1) \le c_1 \left(\frac{1-m}{m}\right) \left[\vartheta^{\left(\frac{m}{1-m}\right)} - \vartheta_1^{\left(\frac{m}{1-m}\right)}\right] + c_2\zeta_1(1-m)\left[\vartheta^{\left(\frac{1}{1-m}\right)} - \vartheta_1^{\left(\frac{1}{1-m}\right)}\right],$$

so

$$\frac{d\vartheta}{d\zeta}(\zeta) < \text{Const.} \quad + \quad C_1\vartheta^{\left(\frac{m}{1-m}\right)} - C_2\vartheta^{\left(\frac{1}{1-m}\right)} \quad \text{with} \quad C_1 > 0, C_2 = -c_2\zeta_1(1-m) > 0$$

$$\equiv \quad F(\vartheta).$$

Because the third, negative, term grows faster than the second, positive, one in F there exists some ϑ_1 such that $F(\vartheta) \le 0$ for $\vartheta \ge \vartheta_1$.

Hence $\frac{d\vartheta}{d\zeta}$ must becomes 0 before ϑ reaches ϑ_1. Therefore $\vartheta < \vartheta_1$ for all $\zeta \ge \zeta_1$ while ϑ is also bounded in the range $0 \le \zeta \le \zeta_1$. This then rules out $\vartheta \to \infty$ as $\zeta \to \zeta_\infty \le \infty$. We have now also eliminated $1(c)$ and (3).

Next, we look at the possibility of ϑ tending to a nonnegative finite value. Assuming ϑ tends to some finite value, then

$$(1-m)\vartheta^{\left(\frac{1}{1-m}\right)} \quad \text{and} \quad \left(\frac{1-m}{m}\right)\vartheta^{\left(\frac{m}{1-m}\right)} \quad \text{also tend to finite values} \quad \text{as} \quad \zeta \to \infty.$$

It follows that $\vartheta^{\left(\frac{2m-1}{1-m}\right)}\frac{d\vartheta}{d\zeta}$ and $\vartheta^{\left(\frac{m}{1-m}\right)}\frac{d\vartheta}{d\zeta}$ are both integrable. Therefore, they decay faster than $\frac{1}{\zeta}$ which is not integrable. (Recall that they are single-signed for large enough ζ as ϑ cannot oscillate).

Integrating equation (6.30) under our assumption of this behaviour (so that $\frac{d\vartheta}{d\zeta} \to 0$ and $\vartheta \to \vartheta_\infty$, $0 \le \vartheta_\infty < \infty$, as $\zeta \to \infty$), we have

$$\text{Const.} \sim \text{Const.} + c_2 \int_0^\infty \zeta\vartheta^{\left(\frac{m}{1-m}\right)}\frac{d\vartheta}{d\zeta}d\zeta - c_3 \int_0^\infty \vartheta^{\left(\frac{1}{1-m}\right)}d\zeta \quad \text{for} \quad \zeta \to \infty. \quad (6.38)$$

For $\vartheta_\infty > 0$ which is case 1(b), the last term behaves like $-c_3\vartheta_\infty^{\left(\frac{1}{1-m}\right)}\zeta$, if $\vartheta_\infty > 0$, while the second last term is $O(\zeta)$ because $\zeta\vartheta^{\left(\frac{m}{1-m}\right)}\frac{d\vartheta}{d\zeta} \to 0$ as $\zeta \to \infty$.

Therefore, we have got a contradiction because no other term in (6.38) can balance the last one. We have now ruled out $1(b)i$ and $1(b)ii$ as well.

We are left, if ϑ is not to become zero at a finite ζ (possibility (2)), with $\vartheta \to 0^+$ as $\zeta \to \infty$, which is behaviour $1(a)$.

Now we will try to see if there is suitable limiting behaviour. To do this let us try

$\vartheta \sim A\zeta^{-\gamma}$ where $\gamma > 0$ and $A > 0$. Substituting this into (6.30), we get

$$\gamma(\gamma+1)A\zeta^{-(\gamma+2)} \sim -c_1\gamma A^{\left(\frac{m}{1-m}\right)}\zeta^{\left(\frac{-m\gamma}{1-m}-1\right)} - c_2\gamma A^{\left(\frac{1}{1-m}\right)}\zeta^{\left(\frac{-\gamma}{1-m}\right)}$$

$$- c_3 A^{\left(\frac{1}{1-m}\right)}\zeta^{\left(\frac{-\gamma}{1-m}\right)}.$$

(6.39)

Now we want to find a balance between at least two of the four terms in equation (6.39), observing immediately that the third and fourth terms are automatically the same size.

First, we try balancing the second, third and fourth terms as follows :
For $\zeta^{-\left(\frac{m\gamma}{1-m}+1\right)} = \zeta^{\left(\frac{-\gamma}{1-m}\right)}$,

$$\text{we need} \quad m\gamma + 1 - m = \gamma \quad \text{so} \quad \gamma = 1.$$

When $m > \frac{2}{3}$, we now have

$$\frac{\gamma}{1-m} = \frac{1}{1-m} > \frac{1}{1-\frac{2}{3}} = 3 = \gamma + 2,$$

which makes, for ζ large, the first term much larger than the others, contradicting our choice of terms to balance.

Second, we try balancing the first, third and fourth terms :
For $\zeta^{-(\gamma+2)} = \zeta^{\left(\frac{-\gamma}{1-m}\right)}$,

$$\text{we need} \quad \gamma + 2 = \frac{\gamma}{1-m} \quad \text{which gives} \quad \gamma = \frac{2}{m} - 2 > 0.$$

Then we have
$$\frac{m\gamma}{1-m} + 1 = 3 > \frac{2}{m}, \quad \text{again since} \quad m > \frac{2}{3},$$
so that the second term now becomes much smaller than the others for $\zeta \to \infty$.
In this case powers work.

Third, the first and second terms are balanced to give

$$\gamma + 2 = \frac{m\gamma + 1 - m}{1-m} \quad \text{and so} \quad \gamma = \frac{1-m}{2m-1}.$$

Then when $m > \frac{2}{3}$ we get

$$\frac{m\gamma}{1-m} + 1 = \frac{m}{2m-1} + 1 = \frac{3m-1}{2m-1} > \frac{1}{2m-1} = \frac{\gamma}{1-m}.$$

This, like the first we tried, is no good because the size of the neglected third and

fourth terms are in fact much larger than the first and second ones for $\zeta \gg 1$.

The final and fourth possibility is when the third and fourth terms are bigger than the first and second ones. This gives,

$$0 = \left(-c_2\gamma A^{\left(\frac{1}{1-m}\right)} - c_3 A^{\left(\frac{1}{1-m}\right)}\right)\zeta^{\left(\frac{-\gamma}{1-m}\right)}. \tag{6.40}$$

This fourth possibility, is rather different, in that we still have to fix the power, γ. From (6.40), we have $\gamma = \frac{c_3}{-c_2} = \frac{1-m}{2m-1}$. Now we check the powers of ζ in the other terms of (6.39) as follows :
The power of the first term of (6.39) is

$$\gamma + 2 = \frac{1-m}{2m-1} + 2 = \frac{3m-1}{2m-1}.$$

For the second term we have :

$$\frac{m\gamma}{1-m} + 1 = \frac{m}{2m-1} + 1 = \frac{3m-1}{2m-1},$$

so that first two terms are the same size.
For the third and fourth terms, the power is

$$\frac{\gamma}{1-m} = \frac{1}{2m-1}.$$

Then we compare the first term with the third and fourth ones, we note that

$$3m-1 > 1 \quad \text{since} \quad \frac{2}{3} < m < 1.$$

Thus the first and second terms are small, compared with the third and fourth. For the final case, A is undetermined. For these two possible asymptotic behaviours, A is fixed in the first one and in the second one is not.

We now consider the two working possibilities, the second and fourth, to be more specific regarding their behaviours. With the second possibility, with the value of $\gamma = \frac{2}{m} - 2$ got when we compared the first, third and fourth terms, from (6.39),

$$\begin{aligned}\gamma(\gamma+1)A &= \left(\frac{\phi(2m-1)}{\delta(3m-2)}\gamma - \frac{\phi(1-m)}{\delta(3m-2)}\right)A^{\left(\frac{1}{1-m}\right)} \\ &= \frac{\phi(1-m)}{\delta m(3m-2)}(2(2m-1)-m)A^{\left(\frac{1}{1-m}\right)} \\ &= \frac{\phi(1-m)}{\delta m}A^{\left(\frac{1}{1-m}\right)}.\end{aligned}$$

$$\text{Thus} \quad A^{\left(\frac{m}{1-m}\right)} = \frac{\gamma(\gamma+1)m\delta}{\phi(1-m)},$$

where

$$\gamma(\gamma+1) = \frac{2(1-m)}{m}\left(\frac{2(1-m)}{m}+1\right) = \frac{2}{m^2}(1-m)(2-m).$$

Hence,

$$A^{\left(\frac{m}{1-m}\right)} = \frac{2(2-m)\delta}{m\phi}.$$

For limiting cases we have $A = \left(\frac{2(2-m)\delta}{m\phi}\right)^{\frac{1-m}{m}} \to \infty$ as $m \to 0$ while $A \to 1$ for $m \to 1$. There is a limiting value for $m = 1$ but not for $m = 0$.

The similarity solution for S close to 1, we are trying to find is $S \sim 1 - t^\alpha \Phi(zt^\beta)$ where $\alpha = -\frac{1}{3m-2}$ and $\beta = -\frac{(2m-1)}{3m-2}$. When z is big or t is small, there would be an interesting behaviour as sketched in Figure 6.6.

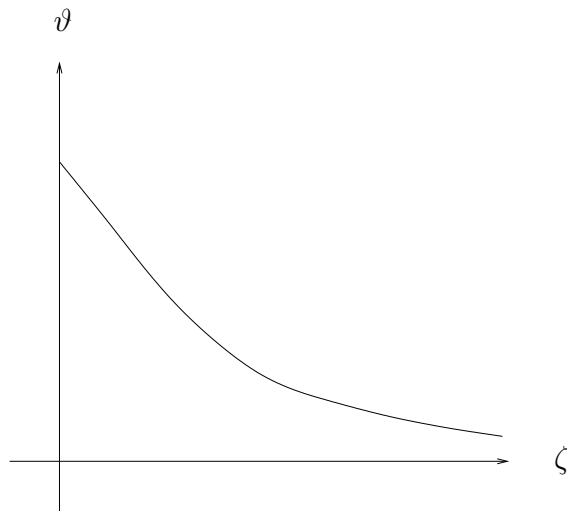

Figure 6.6: The behaviour of the similarity solution for $z \gg 1$ (applying for a problem on a half line rather than on the original, green roof, interval of $0 \le z \le 1$) or $t \ll 1$.

Based on our asymptotic behaviour of the ODE (6.39), we now want, for an interesting similarity solution,

$$\mid zt^\beta \mid = \mid zt^{-\left(\frac{2m-1}{3m-2}\right)} \mid \quad \text{to be large,}$$

and

$$| t^\alpha \Phi | \sim A \mid z \mid^{-\gamma} t^{\left(\gamma\left(\frac{2m-1}{3m-2}\right)-\frac{1}{3m-2}\right)} \sim A \mid z \mid^{-\gamma} t^{\left(\frac{\gamma(2m-1)-1}{3m-2}\right)} \quad \text{to be small.}$$

For the case of $\gamma = \frac{2(1-m)}{m}$, we have

$$\frac{\gamma(2m-1)-1}{3m-2} = \frac{2(1-m)(2m-1)-m}{m(3m-2)} = \frac{5m-4m^2-2}{m(3m-2)} < 0. \tag{6.41}$$

Therefore, we need $\mid z \mid t^{-\left(\frac{2m-1}{3m-2}\right)} \gg 1$ and $\mid z \mid^{-\left(\frac{2(1-m)}{m}\right)} t^{\left(\frac{-4m^2+5m-2}{m(3m-2)}\right)} \ll 1$, which are satisfied, with $\frac{2}{3} < m < 1$, for $\mid z \mid$ large and t order 1 (but not for z order one, and t either large or small).

For the case of $\gamma = \frac{1-m}{2m-1}$,

$$\frac{\gamma(2m-1)-1}{3m-2} = \frac{(1-m)(2m-1)-(2m-1)}{(2m-1)(3m-2)} = \frac{-m}{3m-2}, \quad m > \frac{2}{3}. \tag{6.42}$$

We need $\mid z \mid t^{-\left(\frac{2m-1}{3m-2}\right)} \gg 1$ and $\mid z \mid^{-\left(\frac{1-m}{2m-1}\right)} t^{\left(\frac{-m}{3m-2}\right)} \ll 1$, which also are satisfied with $\frac{2}{3} < m < 1$, and (6.42) for $\mid z \mid$ large and t order 1.
So the two cases work much the same as each other.

6.3   Summary

As an extension of what has been done in Chapter 6, we looked at the possibility of the existence of other asymptotic solutions, namely self-similar solutions, for the nonlinear convection-diffusion model (5.13) for the limiting cases when the saturation S is close to 0 and 1.

For the first case in subsection 7.2.1, when the saturation is low, so that we are near a dry region, we investigated the asymptotic behaviour of solutions. A limiting self-similar solution appears to exist. For the second case in subsection 7.2.2, when the saturation is near 1 so that we are near a saturated region, limiting similarity solutions again appear to exist but the forms vary according to the three cases, $m < \frac{1}{2}$, $\frac{1}{2} < m < \frac{2}{3}$ and $\frac{2}{3} < m < 1$.

Always looking at limiting cases S near 0 and 1 so never had cases linking two finite positive values of S as ξ changed from 0 to $\pm\infty$. To be specific the boundary condition (4.2) corresponds to giving a finite, non-zero, non-unity value of S on $\xi = 0$, while the initial condition, $S = S_{init}$, fixes $0 < S < 1$ at $\xi = -\infty$; unfortunately such conditions do not fit with our analysis in this chapter. Likewise, although having $\Phi(0) = 0$ could satisfy the boundary condition (4.3), the initial condition $0 < \Phi(\infty) = S_{init} < 1$ does

not fit with the analysis. The saturation in Chapter 4 was not close to $S = 1$ and not really close to $S = 0$ so we do not have z^γ or $(1 - z)^\gamma$ local behaviour.

Chapter 7

Discussion

In this chapter we review the main outcomes of this thesis. This thesis is divided into two parts:

In the first part we focused on the numerical solutions of the non-linear PDEs (the Allen-Cahn equation and the RCD equation) using the exponential integrator schemes ETDs and the semi-implicit Euler method.

In the second part, we studied a green roof model, in particular the unsaturated region (5.13). For this model we applied the ETD method to get the solution numerically. In addition, we looked for travelling wave solutions and we tried to get the asymptotic behaviour of the solutions of equation (5.13) for limiting cases of the saturation S being close to 0 and 1. In order to do the latter, we looked at travelling wave and similarity solutions.

In Chapter 3, for the Allen-Cahn equation, we found out that the order of convergence at the final time for all methods ETD, ETD with Krylov subspace technique and the semi-implicit Euler is the first order, $O(\Delta t)$. However, the semi-implicit Euler method is less costly than the other schemes, the ETD and ETD with the Krylov subspace technique. We also looked for the order of convergence for fixed time step and varying spatial steps for only the ETD and the semi-implicit Euler methods. The order of convergence in space found is the second order $O(\Delta x^2)$ for both schemes. For this case, the ETD gave a great improvement, through the order of convergence in space step, over the semi-implicit, however, the numerical error constants were very similar for both methods.

Regarding the one-dimensional constant coefficients reaction-convection-diffusion equation, we add the real fast Léja points technique when applying the ETD to this equation as well as the three previous methods : the standard ETD, ETD with Krylov subspace technique, and the semi-implicit Euler method. We concluded that the ETD, ETD with Krylov and real fast Léja points techniques are more accurate than

the semi-implicit Euler scheme. All schemes are of the first order convergence in time, though. Moreover, the semi-implicit Euler method appears to be faster than the other methods.

In Chapter 4, the green roof model, the one-dimensional Richards' equation without the sink term (5.13), was solved numerically using the finite difference and ETD methods for three different initial values of the saturation S. We found that the results looked very similar to those in paper [1] where S_{bottom} reached 1 for only the two initial saturations 0.1 and 0.15 whereas for the initial saturation 0.05, even for $t = 100$, S_{bottom} did not reach 1 . Unfortunately, our values of S_{top} did not approach the same value as those in [1]. Instead, they depended upon the initial saturation S_{init} as well as on the prescribed flux at the boundary, νQ.

In Chapters 5 and 6, the asymptotic behaviour of solutions of the non-linear convection-diffusion (green roof) model (5.13) were investigated, using travelling wave and self-similar solutions. Those solutions were particularly looked at for the saturation close to 0 and 1. Most possible cases were investigated when the value of m for the expanded-clay soil is fixed and near 0 and 1. The travelling wave, when m is fixed, exists for several cases, given by relative sizes of the limiting saturations $S_{\pm}$. For the limiting case, $m \to 0^+$, we were able to get asymptotic solutions for the travelling wave profiles for all the cases for which travelling waves exist. When $m \to 1$, we got a different behaviour of the travelling wave solution from m fixed in only Case 1, Case 4 and Case 6.
We were able to find limiting similarity solutions both for $S \to 0$ and for $S \to 1$. For the latter, the behaviour differed according to whether $0 \leq m \leq \frac{1}{2}$, $\frac{1}{2} < m < \frac{2}{3}$ or $\frac{2}{3} < m < 1$, with limiting behaviour being subtly different for each range of m.

For future study, our work in Chapter 3 can be extended to investigate the convergence results in time and space for two-dimensional problems. For the green roof model we might work on the full model with the sink term. We also could investigate the numerical solution of the convection-diffusion model using the ETD with Krylov subspace and real fast Léja points techniques to be compared with current results. It would be also worth working on the saturated region for the green roof model using ETD schemes. It also might be interesting and worthwhile to work on the green roof model for two dimensions.

Bibliography

[1] C. C. Adley, M. Cooker, G. L. Fay, I. Hewitt, A. A. Lacey, N. Mellgren, M. Robinson, and M. Vynnycky. A mathematical model of the rainwater flows in a green roof. *Mathematics in industry case studies*, 6:1–21, 2014.

[2] A. Alzahrani. *Local Travelling Wave Solutions and Self-Similar Solutions for a Green Roof Model*. PhD thesis, Heriot-Watt University, 2014.

[3] J. Baglama, D. Calvetti, and L. Reichel. Fast Léja points. *ETNA. Electronic Transactions on Numerical Analysis [electronic only]*, 7:124–140, 1998.

[4] G. Barenblatt. *Scaling, Self-similarity, and Intermediate Asymptotics: Dimensional Analysis and Intermediate Asymptotics*. Cambridge Texts in Applied Mathematics. Cambridge University Press, 1996.

[5] J. Bear. *Dynamics of Fluids in Porous Media*. Dover Civil and Mechanical Engineering Series. Dover, 1988.

[6] L. Bergamaschi, M. Caliari, A. Martinez, and M. Vianello. Comparing Léja and Krylov approximations of large scale matrix exponentials. Volume 3994 of *Lecture Notes in Computer Science*, pages 685–692. Springer, 2006.

[7] H. Berland, B. Skaflestad, and W. M. Wright. Expint - a Matlab package for exponential integrators. *ACM Trans. Math. Softw.*, 33(1):4, 2007.

[8] R. Burden and J. Faires. *Numerical Analysis*. Prindle, Weber & Schmidt, 1985.

[9] M. Caliari. Accurate evaluation of divided differences for polynomial interpolation of exponential propagators. *Computing*, 80(2):189–201, 2007.

[10] M. Caliari, M. Vianello, and L. Bergamaschi. Interpolating discrete advection-diffusion propagators at Léja sequences. *J. Comput. Appl. Math.*, 172(1):79–99, 2004.

[11] M. Caliari, M. Vianello, and L. Bergamaschi. The LEM exponential integrator for advection-diffusion-reaction equations. *J. Comput. Appl. Math.*, 210(1–2):56–63, 2007.

[12] J. G. Caputo and Y. A. Stepanyants. Front solutions of Richards' equation. *Transp. Porous Media*, 74(1):1–20, 2008.

[13] E. Carr, T. Moroney, and I. Turner. Efficient simulation of unsaturated flow using exponential time integration. *Applied Mathematics and Computation*, 217(14):6587 – 6596, 2011.

[14] J. Certaine. *The Solution of Ordinary Differential Equations with Large Time Constants*. Wiley, 1960.

[15] S. M. Cox and P. C. Matthews. Exponential time differencing for stiff systems. *J. Comput. Phys.*, 176(2):430–455, 2002.

[16] E. Cumberbatch and A. Fitt. *Mathematical Modeling: Case Studies from Industry*. Cambridge University Press, 2001.

[17] D. Etter. *Introduction to MATLAB*. Pearson, 2011.

[18] B. Gilding and R. Kersner. *Travelling Waves in Nonlinear Diffusion-Convection Reaction*. Progress in Nonlinear Differential Equations and Their Applications. Birkhäuser, 2004.

[19] G. G. Golub and C. F. V. Loan. *Matrix Computations*. The Johns Hopkins University Press, 3rd edition, 1996.

[20] M. Guedda. Self-similar solutions to a convection-diffusion processes. *Electron. J. Qual. Theory Differ. Equ., (electronic)*, pages 1–18, 2000.

[21] I. Hewitt, A. A. Lacey, N. Mellgren, M. Vynnycky, M. Robinson, and M. Cooker. Designing a green roof for Ireland. *MIIS Eprints Archive report*, 2009.

[22] D. J. Higham and N. J. Higham. *MATLAB Guide*. Society for Industrial and Applied Mathematics, 2000.

[23] N. J. Higham. *Functions of Matrices: Theory and Computation*. Society for Industrial and Applied Mathematics, 2008.

[24] M. Hochbruck and C. Lubich. On Krylov subspace approximations to the matrix exponential operator. *SIAM J. Numer. Anal.*, 34(5):1911–1925, 1997.

[25] M. Hochbruck and A. Ostermann. Exponential integrators. *Acta Numerica*, 19:209–286, 2010.

[26] W. Hundsdorfer and J. Verwer. *Numerical Solution of Time-Dependent Advection-Diffusion-Reaction Equations*. Springer Series in Computational Mathematics. Springer, 2003.

[27] M. Köhler. Long-term vegetation research on two extensive green roofs in Berlin. *Urban Habitats*, 4(1):3–25, 2006.

[28] R. LeVeque. *Numerical Methods for Conservation Laws.* Lectures in Mathematics ETH Zürich, Department of Mathematics Research Institute of Mathematics. Springer, 1992.

[29] J. D. Logan. *An Introduction to Nonlinear Partial Differential Equations.* Pure and Applied Mathematics. Wiley, 1994.

[30] A. Martinez, L. Bergamaschi, M. Caliari, and M. Vianello. A massively parallel exponential integrator for advection-diffusion models. *J. Computational Applied Mathematics*, 231(1):82–91, 2009.

[31] B. V. Minchev and W. M. Wright. A review of exponential integrators for first order semi-linear problems. *Technical Report 2/05, The Norwegian University of Science and Technology, Available online at http://www.math.ntnu.no/preprint/,* 2005.

[32] C. Moler and C. V. Loan. Nineteen dubious ways to compute the exponential of a matrix. *SIAM Review,* 20:801–836, 1978.

[33] J. Niesen and W. M. Wright. A Krylov subspace algorithm for evaluating the phi-functions appearing in exponential integrators. *Technical Report arXiv : 0907. 4631,* 2009.

[34] J. Niesen and W. M. Wright. Algorithm 919: A Krylov subspace algorithm for evaluating the phi-functions appearing in exponential integrators. *ACM Trans. Math. Softw.,* 38(3):22:1–22:19, 2012.

[35] P. J. Philip. *Theory of Infiltration.* In Advances in Hydroscience, Academic Press, 1969.

[36] L. A. Richards. Capillary conduction of liquids through porous mediums. *Physics,* 1(5):318–333, 1931.

[37] T. Roose and A. Fowler. A model for water uptake by plant roots. *Journal of Theoretical Biology,* 228(2):155 – 171, 2004.

[38] Y. Saad. Analysis of some Krylov subspace approximations to the matrix exponential operator. *SIAM J. Numer. Anal,* 29:209–228, 1992.

[39] R. B. Sidje. Expokit: A software package for computing matrix exponentials. *ACM Trans. Math. Softw.,* 24(1):130–156, 1998.

[40] A. Tambue, G. Lord, and S. Geiger. An exponential integrator for advection-dominated reactive transport in heterogeneous porous media. *Journal of Computational Physics*, 229(10):3957–3969, 2010.

[41] J. Thomas. *Numerical Partial Differential Equations: Finite Difference Methods.* In Graduate Texts in Mathematics. Springer, 1995.

[42] C. G. Wark and W. W. Wark. Green roof specifications and standards. *The Construction Editor*, 56(8), 2003.